Simulations of K-Ras GTPase Mutagenesis

Dujmović, Viktorija

University of Split
Faculty of Science

Simulations of K-Ras GTPase Mutagenesis

Master thesis

Viktorija Dujmović

Split, August 2024

Temeljna dokumentacijska kartica

Sveučilište u Splitu
Prirodoslovno–matematički fakultet
Odjel za fiziku
Ruđera Boškovića 33, 21000 Split, Hrvatska

Diplomski rad

Simulacije mutageneze K-Ras GTPaze

Viktorija Dujmović

Sveučilišni diplomski studij Fizika; smjer: Biofizika

Sažetak:

K-Ras (eng. *Kirsten rat sarcoma*) protein je signalna GTPaza koja igra važnu ulogu u radu signalnog puta mitogenom-aktiviranih proteinskih kinaza (MAPK). U ovom radu ćemo koristeći molekulsko-dinamičke (MD) simulacije istražiti mogući utjecaj specifične mutageneze K-Ras proteina na njegova signalna svojstva. Promatrana je mutacija G12C koja je predominantna kod ljudi. K-Ras je u aktivnom stanju kad veže molekulu GTP-a te tada signalizira aktivaciju MAPK signalnog puta čija funkcija je među ostalim proliferacija i rast stanica. Hidrolizom GTP-a do molekule GDP-a K-Ras pada u neaktivno stanje. Pokazano je da poremećaji u signaliranju K-Ras proteinom dovode do razvoja karcinoma. Stoga su simulacije njegove mutageneze relevantne da bi se pokazali točni mehanizmi vezanja molekula GTP-a/GDP-a. U ovom radu izračunali smo slobodne energije primjenjujući metodu termodinamičke integracije na MD simulacijama i napravili analizu trajektorija istog skupa simulacija. Istraživanje je pokazalo da se afinitet vezanja molekule GTP-a/GDP-a mijenja ovisno o tome veže li se na protein divljeg tipa ili na njegovu mutaciju. Simulacije su pokazale nedosljednost u rezultatima između identičnih replika sustava i histerezu među simulacijama istog sustava perturbiranog u suprotnim smjerovima. Ove nedosljednosti opravdane su ekstenzivnom analizom trajektorija. Pokazano je da nereproducibilnost replika proizlazi iz nepouzdanog stvaranja vodikove veze između cisteina i molekule GTP-a, dok je histereza posljedica konformacijskih promjena tzv. Switch– petlji K-Ras proteina. Kao glavni rezultat izdvaja se izračun slobodnih energija koji pokazuje da je vezanje molekule GTP-a preferirano stanje mutiranog proteina. Drugim riječima, mutirani protein preferira aktivno stanje čime utječe na aktivnost cijeloga MAPK signalnog puta te dovodi do razvoja karcinoma.

Ključne riječi: K-Ras, MD simulacije, Slobodna energija, Termodinamička integracija

Rad sadrži: 57 stranica, 33 slike, 14 tablica, 36 literaturnih navoda. Izvornik je na engleskom jeziku.

Mentor: Naslovni doc. dr. sc. Dražen Petrov

Neposredni voditelj: Dr. rer. nat. Mislav Cvitković

Ocjenjivači: Naslovni doc. dr. sc. Dražen Petrov
Dr. rer. nat. Mislav Cvitković
Izv. prof. dr. sc. Larisa Zoranić
Prof. dr. sc. Ante Bilušić
Doc. dr. sc. Lucija Krce

Rad prihvaćen: 28. kolovoza 2024.

Rad je pohranjen u Knjižnici Prirodoslovno–matematičkog fakulteta, Sveučilišta u Splitu.

Basic documentation card

University of Split
Faculty of Science
Department of Physics
Ruđera Boškovića 33, 21000 Split, Croatia

Master thesis

Simulations of K-Ras GTPase Mutagenesis

Viktorija Dujmović

University graduate study Physics, specialization in Biophysics

Abstract:

Kirsten rat sarcoma (K-Ras) protein is a signaling GTPase which has an important role in the Mitogen-activated protein kinase (MAPK) pathway. Using the methods of molecular dynamics (MD) simulations, in this thesis we will investigate if and how does the specific mutagenesis of K-Ras protein affect its signaling properties. The mutation studied here is G12C, as it is predominant in humans. K-Ras exists in an active state when it binds to a GTP molecule, and then it signals the activation of MAPK pathway, whose functions include proliferation and growth of cells. By a hydrolysis GTP to GDP molecule, K-Ras gets into an inactive state. As it is observed that irregularities in K-Ras signaling lead to development of cancer, simulations of its mutagenesis become more relevant to show the exact mechanisms of binding GTP/GDP molecules. In this thesis we have calculated the free energy using the method of thermodynamic integration on MD simulations and performed the analysis of the trajectories from the same set of simulations. The results reveal that the binding affinity of GTP/GDP molecule changes depending on whether it binds to the wild type or mutated protein. Apparent inconsistencies in results between identical replicas, as well as a prominent hysteresis between different directions in simulations of the same perturbation system is discussed. In order to understand these inconsistencies, a thorough analysis of simulation trajectories is exploited. It is shown that such a lack of the full reproducibility of the simulation replicas emerges from the inconsistencies in the formation of h-bond between cysteine and GTP molecule, whereas the hysteresis is a consequence of the conformational changes in the Switch loops of K-Ras protein. In other words, a mutated protein favours the active state, which directly influences the activity of the MAPK pathway, which in turn leads to a cancer development.

Keywords: K-Ras, MD simulations, Free energy, Termodynamic integration

Thesis consists of: 57 pages, 33 figures, 14 tables, 36 references. Original language: English.

Supervisor: Titular Assist. Prof. Dr. Dražen Petrov

Leader: Dr. Rer. Nat. Mislav Cvitković

Reviewers: Titular Assist. Prof. Dr. Dražen Petrov
Dr. Rer. Nat. Mislav Cvitković
Assoc. Prof. Dr. Larisa Zoranić
Prof. Dr. Ante Bilušić
Assist. Prof. Dr. Lucija Krce

Thesis accepted: August 28, 2024

Thesis is deposited in the library of the Faculty of Science, University of Split.

In following lines, I would like to express my gratitude to people and institutions which have been supporting me through my studies and life.

First of all, I would like to thank Assist. Prof. Dr. Dražen Petrov for introducing me to the world of scientific work by letting me join him for my ERASMUS+ internship at the BOKU University in Vienna. I will always be thankful for the way he teaches, as he hasn't only once served me with an answer, but has also been pushing me to come to conclusions myself, supporting me on the way. His commitment to improvement is truly contagious and it was a true honour to work with him.

I would also like to thank the whole Molecular Modeling and Simulations group at BOKU University and Christian Doppler Laboratory for Molecular Informatics in the Biosciences Department for a constant support in my research presented in this thesis. I would like to specially thank Prof. Dr. Chris Oostenbrink and Dr. Edgar Galicia Andrés for all the suggestions and encouragement when things didn't go as planned and my results were all over the place. I also have to mention Barbara, Natalia and Tea who made my days in the office and Vienna much more enjoyable and listened to my complaints. To them I owe many beautiful memories I will cherish forever.

Special thanks go to my thesis leader, Dr. Rer. Nat. Mislav Cvitković. From the first day we met he has been feeding my ambition, making me wish to take a step forward, to do better, to do more. He has guided me throughout my studies professionally, but also has offered a friendly ear whenever I needed an advice or wasn't sure what the next step was. I have never felt anything but pure support and approval from him. Of course, this thesis would not exist in this state and shape without his extensive comments and suggestions, which I greatly appreciate.

I want to express my gratitude to all professors and assistants at the Faculty of Science in Split for all the knowledge I have obtained throughout my studies. Special thanks go to the head of the Biophysics section, Assoc. Prof. Dr. Larisa Zoranić for being like a mother to all of us. She was always full of care and compassion, but also fair and strict when needed. I want to thank her for she has always believed in me, even when I was in the worst shape, and for connecting Dražen and me to work on this thesis.

Big thanks to my study colleagues Anamarija, Anđela, Dubravko, Frane, Grgur, Ivor, Jana, Karla, Maja, Marko, Roko, Stjepan, Vjeko, Žana for all the amazing memories of my student days that I will carry in my heart forever. And I have to thank some of them for dealing with my nervous breakdowns (these will recognize themselves).

Lastly, but most importantly, I want to say a most cordial thank you to my family, my parents and my brothers. I owe them being a person I am today. To my parents: Majko, Ćaća, fala van za svu jubav i podršku, fala van šta ste me napravili čovikon i šta ste mi dali najboje od sebe — znatiželju i dišpet.

And to everyone not mentioned above, thank you for being a part of my journey.

Contents

1 Introduction

The fast advance in computational systems and algorithm development lead to a vast use of computational methods in many scientific fields. A need to simulate fundamental physical processes in large biological systems, such as membranes and membrane-embedded proteins, caused a whole new branch within biophysics to emerge. Molecular dynamics (MD) simulations have made it possible to explore biological systems at smaller scales than the experiments provided.

This research is based on utilizing the MD simulations, specifically free energy calculations through the method of thermodynamic integration, on a G12C mutation of the Kirsten rat sarcoma (K-Ras) protein. This specific mutation and its mechanisms became crucial since it is known that this protein's mutations lead to cancer development in humans [1, 2, 3]. It is known that the cause of cancerous cell development lies in the over-activation of the Mitogen-activated protein kinase (MAPK) pathway, in which K-Ras plays a prominent role [1, 3, 4]. The preferable binding of GTP Pγ oxygen to the sulfate on a mutated cysteine leads to excessive amount of phosphorilations [1, 3, 4]. To inspect how the process of activation and over-activation plays out on a molecular level, binding of GTP and GDP molecules to a wild type and a mutated protein were simulated using the method of thermodynamic integration.

In the second chapter of the thesis, a theoretical overview is given on K-Ras protein, its mutations and involvement in MAPK pathway. Additionally, there is a short review of the basis of MD simulations and free energy calculations as used in this work.

The third chapter exposes the methods used in this research, specifically how the system was prepared, which were the simulation settings and how were the energies calculated. Programs and algorithms that have been used are described in a more detail.

In the final chapter, results of the research are presented and discussed. Results of the free energy calculations are revealed, and possible problems within the system and its perturbations are explained, as well as the question how they might relate to apparent energy differences between the same system simulation replicas. Finally, trajectories are directly analysed to show how system conformations affected final results and if there are additional aspects of the system that are important to consider.

Overall, the main goal of this thesis is to show that binding free energies, calculated using MD simulations, can be used to explain the over-activation of a mutated K-Ras protein in MAPK pathway and therefore to explain the molecular mechanism behind the cancer development in these proteins by cystein-GTP binding.

2 Theoretical overview

In this chapter, the significance of K-Ras protein is discussed, as well as the effects of its mutagenesis to cancer development. Secondly, the theoretical overview of the MD simulations is presented, together with the evaluation of free energies using the method of thermodynamic integration.

2.1 K-Ras in MAPK pathway

K-Ras protein is a signaling GTPase which regulates cell proliferation, playing a key role in the mitogen-activated protein kinase (MAPK) pathway [1, 2]. K-Ras protein cycles between an active GTP-bound and an inactive GDP-bound state which are regulated by the presence of guanine nucleotide exchange factors (GEFs). GEFs promote the exchange from GDP to GTP and GTPase-activating proteins (GAPs) which mediate GTP hydrolysis [3].

K-Ras protein is a part of the Ras superfamily which contains 36 proteins in humans. Within the family, H-Ras and N-Ras are phylogenetically close to K-Ras protein that is studied in this thesis [2]. K-Ras is found in two alternative splice variants, K-Ras4a and K-Ras4b, with the change in fourth exons which encode the C-terminal helix $\alpha 5$ of the G-domain (residues 1-166, non-conserved residues being 151, 153, 165, and 166) and the hypervariable region (HVR, residues 167-189/188 of K-Ras4a and K-Ras4b, respectively) involved in the membrane attachment [5].

The structure and sequence of K-Ras4b isoform is shown in Figure 1. The crystal structure shows that GDP molecule binds to the magnesium ion with its PO_3 group, which connects it to the Switch-I loop. The pocket into which the GDP slides is formed by another two loops: Switch-II and P-loop. Switch loops aditionally form binding interfaces for Ras regulators, GAPs and GEFs [1]. Loop definitions throughout the literature are quite arbitrary, which means that shown depiction might be expanded by a few residues. This is a result of protein's high intrisic flexibility, especially taking into consideration the P-loop which can be extended up to residue number 17 [1, 6].

MAPK is a pathway of signal transduction activated downstream of protein kinases with highly conserved regions that play a significant role in signal transduction in eukaryotic cells, specifically being characterised as a part of the extracellular signal-regulated kinase (ERK) family in mammalian cells [7]. Being composed of serine/threonine and tyrosine kinases, most notably Ras, Raf, Mitogen-activated protein kinase kinase (MAPKK or MEK) and ERK, MAPK pathway gets activated by the stimulation of membrane tyrosine kinase receptors [8].

The central role of ERK signaling in mammalian cells came to light from the studies of the Ras proteins, first identified as the oncogenic proteins that cause sarcomas in rats [1, 2, 7, 8].

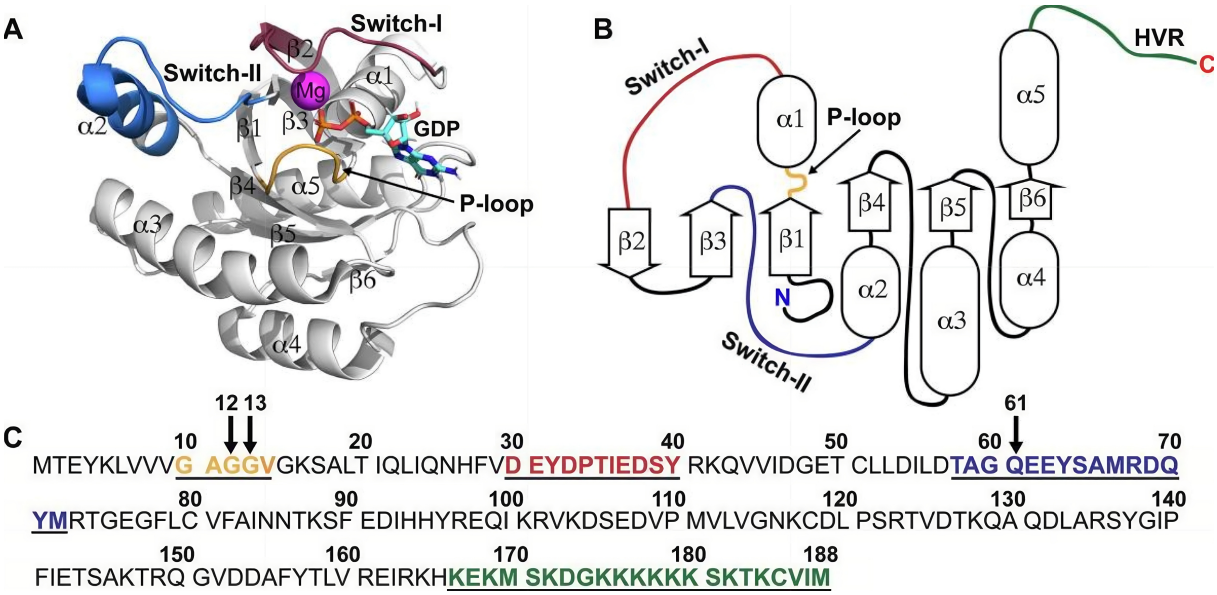

Figure 1: *Structure and sequence of K-Ras4b protein. All relevant loops are marked. (A) Wild type crystal structure with magnesium ion and bound GDP molecule. Protein is presented without HVR region. (B) 2D depiction of secondary structure. (C) K-Ras4b sequence with colored loop residues (analog to A and B). Arrows point to most common mutation hotspots. Figure taken from [1].*

The first research that connected mutations to cancerous cell growth was made in 1982 [9]. In 1993 the first conclusions on how Ras protein is activated by epidermal growth factor (EGF) tyrosine kinase receptors were made [10].

As it is shown in the MAPK pathway scheme in Figure 2, GEFs bind to the phosphorylated site of the receptor, which enables the exchange of GDP to GTP in membrane-bound Ras and its activation [8]. This activation leads to fixation, dimerization and phosphorylation of Raf, activating MEK by phosphorylation on serines 218 and 222, which finaly activates ERK phosphorylating threonine 202 and tyrosine 204 in ERK1 isoform or threonine 185 and tyrosine 187 in ERK2 isoform [7, 8]. Once activated, ERK then phosphorylates a variety of target proteins, and a fraction of them translocates to the cell nucleus, regulating transcription factors [7].

The mutagenesis of MAPK effectors affects the functionality and signaling of the cascade, which leads to development of cancer [11]. Therefore, in the next subsection, the focus will be on the mutagenesis of Ras proteins, specifically K-Ras, and the way they can affect human health.

2.1.1 K-Ras mutagenesis

Concerning MAPK pathway, the majority of tumors are caused by mutations of Raf and Ras families of proteins [1, 2, 3, 11]. Namely, Ras mutations are found in 15-29% cases of melanoma, 5-20% colorectal, and 12-30% lung cancer; Raf mutations are observed in 50-60%

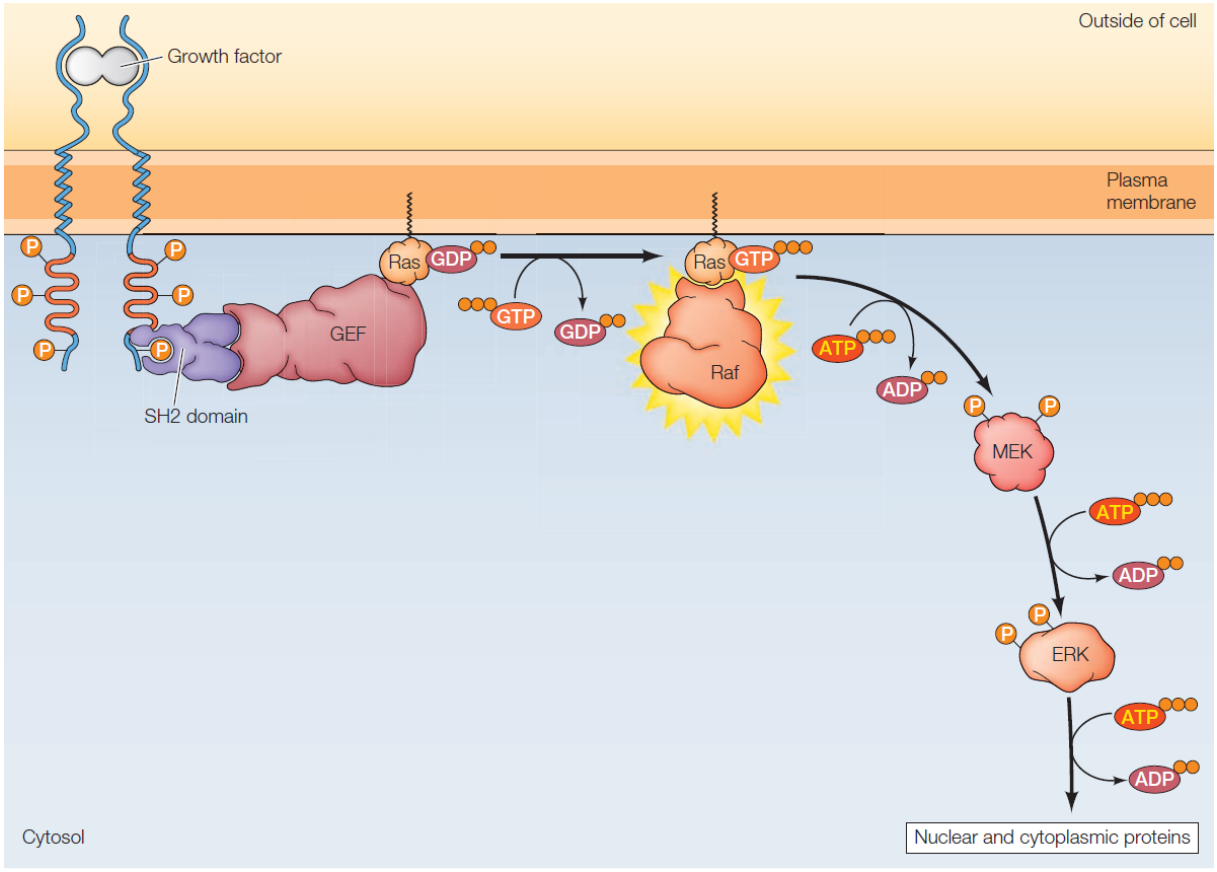

Figure 2: *Scheme of MAPK pathway. Activation of Ras, Raf and ERK downstream of receptor tyrosine kinases. Figure taken from [7].*

melanoma, 5-20% colorectal, 4% lung cancer cases; mutations in MEK and ERK are found in only 3-8% melanoma and 3% colorectal cases [11]. Specific mutation occurances in human cancers are shown in Results and discussion chapter.

2.2 Molecular dynamics simulations

Molecular dynamics (MD) simulations are utilized to show the differences between molecular mechanisms of the wild type and mutated protein. They allow one to analyse basic interactions between molecules and solvent described through classical mechanics and thermodynamics, as well as to calculate the physical parameters of the system [15, 16].

First molecular simulations were introduced in 1949 by Metropolis et al., which proposed a probabilistic approach to approximate properties of a set of particles [17]. This inspired molecular simulations by Alder and Wainwright in 1959 that introduced assigned initial velocities and positions of individual atoms [18]. First simulations of molecules were presented by Rahman and Stillinger in 1971 [19]. These were also first simulations of liquid water. In 1976, Warshel and Levitt integrated quantum mechanics into molecular simulations exchanging classical atom charge with quantum mechanics equations [20]. An enormous

advancement occured in 1977 when molecular simulations were used to study proteins by setting constraints to reach longer simulation times. This study by Karplus et al. led to the Nobel Prize in Chemistry in 2013 awarded to Warshel, Levitt and Karplus for the development of multiscale models for complex chemical systems [20, 21]. In 1985, Car and Parrinello combined molecular dynamics with density-functional theory [22]. Further advances in technology led to higher computer performance, which meant that MD simulations could be more widely used and performed on larger systems for longer simulation times [16].

The importance of MD simulations in protein research is in the ability to look into dynamic features which are essential for protein function, and can not be observed through available experimental methods [16]. In MD simulations, time evolution of interacting particles motion in given as a solution of Newton's equations:

$$\mathbf{F}_i = m_i \frac{\mathrm{d}^2 \mathbf{r}_i(t)}{\mathrm{d}t^2}, \tag{2.1}$$

where $\mathbf{F}_i$ is the force acting upon ith particle, m_i the mass of the particle, and $\mathbf{r}_i(t) = (x_i(t), y_i(t), z_i(t))$ is the position vector at time t [23]. Positions $\mathbf{r}_i$ and velocities $\mathbf{v}_i$ define particle trajectories and determine kinetic energy and temperature of the system. To solve equation 2.1 numerically in MD simulations, the Verlet algorithm is most commonly used:

$$\mathbf{r}_i(t + \Delta t) \cong 2\mathbf{r}_i(t) - \mathbf{r}_i(t - \Delta t) + \frac{\mathbf{F}_i(t)}{m_i} \Delta t^2, \tag{2.2}$$

expression being accurate to the forth power of Δt [23].

To solve former equations, one needs to evaluate the force $\mathbf{F}_i$ on each particle, and for that force fields are used. Force field is a set of mathematical expressions and parameters that describes all the intramolecular and intermolecular forces on each particle of the system [16]. A typical force field expression looks like this:

$$\begin{aligned} U = &\sum_{\text{bonds}} \frac{1}{2} k_{\text{b}} (r - r_0)^2 + \sum_{angles} \frac{1}{2} k_{\text{a}} (\theta - \theta_0)^2 + \sum_{\text{torsions}} \frac{V_n}{2} [1 + \cos(n\phi - \delta)] + \\ &+ \sum_{\text{improper}} V_{\text{imp}} + \sum_{\text{LJ}} 4\epsilon_{ij} \left(\frac{\sigma_{ij}^{12}}{r_{ij}^{12}} - \frac{\sigma_{ij}^{6}}{r_{ij}^{6}} \right) + \sum_{\text{elec}} \frac{q_i q_j}{r_{ij}}, \end{aligned} \tag{2.3}$$

where first four terms present intramolecular contributions in the form of bond stretching, angle bending, dihedral and improper torsion, while the last two describe Van der Waals interactions, specifically Lennard-Jones and Coulombic interactions [24]. From this expression, calculating the force $\mathbf{F}_i$ is trivial, using well known expression $\mathbf{F} = -\nabla U$.

All the simulations in this thesis were performed in the GROMOS Software using GROMOS force fields, specifically 54A8, which is an atomistic force field with exception of CH_n hydrogens modelled as united-atoms [25, 26].

Instead of previously proposed Verlet algorithm (eq 2.2), GROMOS uses leapfrog scheme:

$$\mathbf{r}_i(t+\Delta t) \cong \mathbf{r}_i(t) + \mathbf{v}_i(t)\Delta t + \frac{1}{2}\mathbf{a}_i(t)\Delta t^2, \tag{2.4a}$$

$$\mathbf{v}_i(t+\Delta t) \cong \mathbf{v}_i(t) + \frac{1}{2}(\mathbf{a}_i(t) + \mathbf{a}_i(t+\Delta t))\Delta t, \tag{2.4b}$$

and the MD algorithm runs in 13 steps [25]:

a) saving positions and velocities for later analysis;

b) removing center of mass motion;

c) calculating energies, forces, and virial contribution;

d) enforcing any given position restraints by setting forces and velocities of constrained atoms to zero;

e) updating velocities using leapfrog scheme (eq 2.4b)

f) scaling velocities to apply temperature coupling;

g) updating positions based on leapfrog scheme (eq 2.4a);

h) enforcing distance constraints (using SHAKE) and calculating corresponding forces and virials;

i) calculating kinetic energy and temperature;

j) calculating pressure;

k) applying pressure scaling by scaling positions;

l) updating coupling parameter λ for free energy simulations involving λ changes

m) calculating total energies, averages and fluctuations.

These steps are then repeated for the duration of a simulation.

2.3 Free energy calculations

The estimation of free energy changes is relevant in understanding biomolecular processes. The calculation of conformational free energies aims at evaluating the relative free energies of relevant conformational states, while alchemical free energies calculation aims at evaluating the relative free energies of different molecules [27, 28]. Whether the free energies or free enthalpies are calculated depends on the constraints given to the system: the relative (Helmholtz) free energy ΔF is calculated under isochoric-isothermic conditions (NVT), while the relative (Gibbs) free enthalpy ΔG is calculated under isobaric-isothermic conditions (NpT) [27]. Some of the computational methods used to estimate free energy are Thermodynamic Integration (TI), Umbrella Sampling, and Enveloping Distribution Sampling (EDS). In this thesis, TI is a method of choice.

2.3.1 Thermodynamic integration

Thermodynamic integration is a method in which the λ parameter is set in a way that $\lambda_{\mathrm{A}} = 0$ indicates state A and $\lambda_{\mathrm{B}} = 1$ indicates state B. System is then perturbed between states A and B with user set λ step change, and free energy difference ΔG_{BA} is given by:

$$\Delta G_{\mathrm{BA}} = G(\lambda_{\mathrm{B}}) - G(\lambda_{\mathrm{A}}) = \int_{\lambda_{\mathrm{A}}}^{\lambda_{\mathrm{B}}} \left\langle \frac{\partial H(\lambda)}{\partial \lambda} \right\rangle_{\lambda} \mathrm{d}\lambda, \tag{2.5}$$

where $H(\lambda)$ in the ensemble average of the system [27]. Given long simulation times and enough λ points sampled, this expression converges.

Once configuration sets have been sampled, various approaches could be used to estimate free energy changes. Besides TI calculations, one can use Bennett Acceptance Ratio (BAR) to estimate free energy differences. BAR formula states that:

$$\Delta G_{\mathrm{A,B}}^{(n)} - C = \ln \frac{\langle f[H_{\mathrm{A}}(x) - H_{\mathrm{B}}(x) - C]\rangle_{\mathrm{B}}}{\langle f[H_{\mathrm{B}}(x) - H_{\mathrm{A}}(x) - C]\rangle_{\mathrm{A}}}, \tag{2.6}$$

where $f(x) = 1/(1 + \mathrm{e}^{x})$ is the Fermi function and $C \approx \Delta G_{\mathrm{A,B}}$ is iteratively determined [29, 30]. This expression can be expanded in case of multiple states to calculate MBAR values [28].

3 Methods

After describing the theoretical concepts of the problem, here the methods used in the research will be displayed. All the used programs will be listed, as well as all the simulation settings.

Simulations were done in GROMOS software [25] and analysis was performed using GROMOS built-in programs, customized Python scripts and GROMACS built-in programs [31].

3.1 Preparing the system

Before setting up simulations, starting structures have to be prepared. To check how the mutation G12C in K-Ras protein affects GTP/GDP binding, one wants to prepare structured containing wild type protein or mutated protein, both with either GTP or GTP, or in total 4 structures. Besides those, structures of sole wild type (wt) / mutated protein and sole GTP/GDP molecules are needed.

To obtain those structures, the protein data bank (PDB) should be firstly searched for possible available crystal structures. Thereby, one structure that suits this research can be found. Under

the PDB ID 8afc one can find the mutated K-Ras4b protein with mutation G12C in complex with the compound 12 obtained through x-ray diffraction with resolution of 2.41 Å [32].

Compound 12 is 2-azanyl-4,4-dimethyl-6,7-dihydro-5~H-1-benzothiophene-3-carbonitrile, or LXK ligand for short. Besides K-Ras with G12C mutation and LXK ligand, PDB file contains one magnesium ion, one sulfate ion, guanosine-5'-diphosphate (GDP) and 26 water molecules.

Simulations in this research were performed after removing LXK, sulfate ion and water molecules. It was decided not to make all the structures initially, but to start with G12C-GDP combination and make rest of the structures from the final ones of each perturbation within a thermodynamic cycle. Still, to represent G12C-GDP→G12C-GTP, there are additional four atoms to include in the final structure, and one to be removed. This means that the input PDB file needs to contain both the atoms included and atoms excluded from the final structure.

To resolve this problem, PyMOL molecular graphics system program was used [33]. To add or remove the phosphate group, PyMOL *Builder* option was used. Both GTP and GDP conformations are saved as PDB files, and the H3Pβ hydrogen is added to the PDB file, so that it contains three phosphate groups in the end, together with the said hydrogen so GDP molecule can be built. Here one can also change the mutated residues. While mutating cysteine to glycine consists of removing the thiol group, which can be done manually by deleting atoms one by one, if the original file contains glycine, thiol group has to be built from scratch to mutate it to cysteine. This can hardly be done by simply adding atoms manually, as it is troublesome to direct their positions. PyMOL wizard *Mutagenesis* makes this process much easier than building individual atoms, as it allows user to select a residue and simply choose to which residue they want to mutate it to.

Besides getting the PDB files, topologies had to be made. To do this, GROMOS program *make_top* was used, giving the protein sequence of K-Ras. Topologies were made for wt and G12C K-Ras, and also for GTP and GDP molecule and magnesium ion. To get topologies of full systems, GROMOS program *com_top* was used, to combine previously prepared topologies.

Previously made structures have to be translated from PDB format to .cnf file format. This may be done using GROMOS *pdb2g96* program. Sometimes atom names in pdb files do not correspond to atom names in GROMOS topologies, which requires additionally stating those cases and how to resolve them. To check the .cnf file content in PyMOL at any step, GROMOS program *frameout* writes out a pdb file from the .cnf file using given topology file.

Before creating simulation box and filling it out with solvent, a minimisation of the system is done using the steepest-descent algorithm in vacuum for 2500 steps with 0.002 dt. Constraints are imposed by SHAKE algorithm. All of those simulation parameters, as well as some not mentioned, are stated in the .imd file, which is given with topology and .cnf files to the GROMOS *md* program which performs minimisation based on those parameters and gives

back a minimized .cnf file.

This file is then given to the *sim_box* GROMOS program. The simulation box is set to the rectangular box with the minimal solute-wall distance of 0.8, and the minimal solute-solvent distance of 0.23. This step places the protein into the solvent withing a box preparing it for further simulation steps. To relax this new soluted system, minimisation has to be performed, this time with positional restraints on the solute. This is performed by making two additional files with extensions .por and .rpr by copying .cnf file and making some small changes manually. In .por file POSITION keyword at the beginning of the atom coordinate block has to be exchanged to POSRESSPEC. All the solvent atoms have to also be removed from this file. Similarly, in .rpr file the keyword in the begining of the block should read REFPOSITION. Now minimisation is performed the same way as before. Changes in the .imd file include setting the number of solvent molecules and changing it from being performed in vacuum to being performed in solvent. POSITIONRES block is added, specifying that position restraints should be taken into account. Simulations were done without any ion atoms in the solvent, which means that systems are now prepared for further equilibration which will be explained in further subsections.

3.1.1 Thermodynamic cycle

Figure 3 shows a scheme of a thermodynamic cycle which is followed in simulations which shall be presented. The starting point is in upper left corner, or specifically mutated K-Ras protein with GDP molecule bound to it. From there, arrows lead in both the direction of G12C-GTP and WT-GDP perturbations. Simulations are performed in a way that the beginning structure of each new simulation is obtained by taking the final structure of the previous simulation and, if needed, adding or subtracting atoms. This is done until the cycle is closed, in both directions.

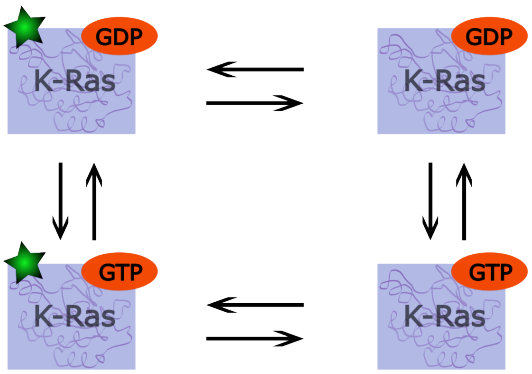

Figure 3: *Scheme of a thermodynamic cycle of K-Ras mutation and GTP/GDP binding. The presence of a G12C mutation is represented by a green star.*

3.1.2 Creating replicas

To get a better statistical representation, system is simulated in three replicas. Replicas are systems constructed of same number of atoms with a slight change in conformations. This results from using a different random number generator seed in the .imd file in equilibration step, which is to be described. MD simulations are reproducible, meaning that by using the same starting point (all the initial input files) and the same seed and other simulation parameters, one should get the same simulation results, or same trajectories. By changing the seed, the input parameters stay the same, while the initialized velocities are shifted which results in different conformations of atoms.

To set the equilibration steps, a few changes have to be made in the .imd file compared to the minimisation step. Firstly, in INITIALISE block NTIVEL value is set to 1, which means that the velocities were assigned randomly according to Maxwell-Boltzmann distribution. In the same box, IG is the seed value. Also, equilibration is run for a longer simulation time of 10000 steps. As the system is now placed in a box, periodic boundary conditions have to be set in a BOUNDCOND block by setting NTB to 1. Finally, MULBITATH, COMTRANSROT, WRITETRAJ and some other blocks are added to make sure the system remains on the same temperature, without centre of mass motion, and trajectory write out in a file. Most importantly, POSITIONRES block is added, which keeps the volume constant throughout simulation.

To perform equilibration at the temperature of 300 K by slowly incrementing it from 60 K in five steps, GROMOS program *mk_script* is used. This program takes a joblist as an input, where all imput parameters that are changed throughout are stated, and as an output gives .imd files and .run files for each equilibration step.

This way, three replicas of the beginning system may be produced. Besides them, equilibration step might be repeated when moving from one simulation to another as number of atoms in the system differs.

3.2 Setting simulations

In contrast to the equilibration step, in the MD sampling simulation, POSITIONRES block is removed and PRESSURESCALE block is added to the .imd file. This means that the system is going from NVT to NpT ensemble. To include thermodynamic integration into MD simulation, PERTURBATION block is also needed. There one can specify whether free energy calculations are performed and set Lennard-Jones and Coulomb soft-core parameters. Those are usually set to 0.5 each. This block controls how the system changes through each λ point.

To reestablish, changing the system from one state to another, it gets slowly perturbed by λ points from 0 to 1 in a way that λ points describe the percentage in which the interactions of

perturbed atoms are perceived by the remaining atoms. To state which atoms are exchanged, besides a regular topology file, there should be a perturbation topology file .ptp that states the exact atoms from topology. There is said which atom goes from *dummy* to *real* atom, and vice versa.

In the initial cycle, all the simulations are set to 21 λ points simulated for 2 ns with 0.002 time step. Before each new lambda point, there is 0.2 ns equilibration run that is excluded from free energy calculations. The other interchangeable thing in those simulations are atom numbers of solute and the whole system. Those range from 1774 to 1779 for solute and 24442 to 24447 for the whole system.

To get the free energy changes in binding of GTP/GDP to G12C/WT, free energies of sole perturbations from GTP to GDP and G12C to WT had to be performed. For that, systems were prepared in the same way as before, and simulated again for 2 ns for 21 λ points. Free energy values taken from here are in the end subtracted from the one of originally set perturbations to get the difference in binding free energies that are of the interest in this research.

3.3 Extended thermodynamic integration

One of the common problems using the method of thermodynamic integration is that the curve that represents the free energies is sometimes too steep between two lambda points, which makes the integration estimate unreliable. For this reason, to make the integration smoother, as shown in Figure 4, the extended thermodynamic integration method is used [34].

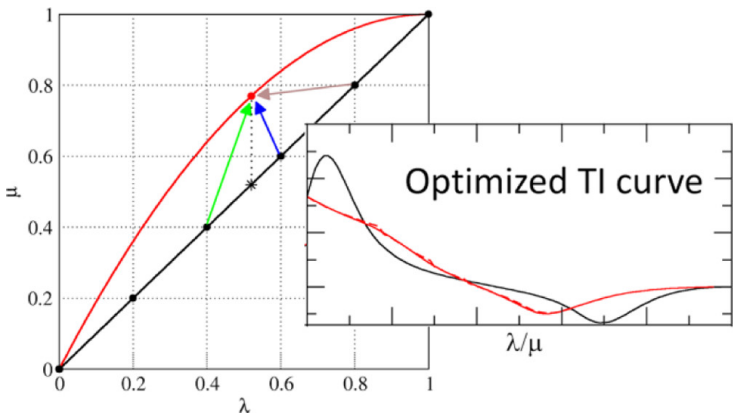

Figure 4: *Extended TI. Graph shows an optimization of the TI curve after performing extended simulations on additional lambda points. Figure taken from [34].*

Extended TI includes prolongation of simulations of selected λ points and inclusion of new λ points in between the existing ones. Also, if some of the λ points do not need to be prolonged, they are excluded from further simulations.

Calculations to determine which λ points are prolonged and for how long can be done in multiple ways, and the convergence conditions can be set freely. In this research, preexisting

Python script written by Assist. Prof. Dr. Dražen Petrov was used. To generate .run and .imd files for new λ points, Python script was written which can be found in Appendix B. The script used SMArt environment [35].

Ideally, after some number of cycle repeats, the free energy results would converge, and there would be no more λ points to simulate. In chapter 4 it is explained how, with this system, that outcome was not reachable and the decision to stop simulating was based on the MBAR and BAR value errors.

3.4 Free energy calculations

As mentioned previously, free energy calculations were performed using a preexisting Python script. Additional ways of estimating free energies from simulations by the thermodynamic integration method are described in section 2.3.1, specifically equations 2.5 and 2.6.

There are many algorithms available that calculate BAR and MBAR values, and the TI values could be calculated using GROMOS. The problem with BAR calculations is to optimise calculation time because of the recursion that is calculated. This makes BAR value slow to calculate, but at the same time more precise.

The above mentioned script was used not only to calculate the free energies, but to estimate which λ points to simulate. Reading all the simulation output trajectories and energies and estimating TI and BAR values, based on set of parameters to estimate convergence of a particular region, a new set of λ points is given to the user, together with new simulation times based on the total time of the full cycle that is given by the user.

3.5 Data analysis

Besides energy calculations, a detailed analysis was performed on obtained trajectories. In the following chapters will the motivation for performing these exact analysis become transparent.

As the simulations performed in total were at most in tenths of microseconds and there was a lot of noise, root-mean-square deviation (RMSD) calculations were performed using GROMOS program *rmsd* on these systems compared to the clusters obtained from simulations provided by Dr. Edgar Galicia Andrés, which had much longer simulation times. RMSD was performed on the first two (highest) clusters for Switch-I and Switch-II loop.

Secondly, it was relevant to look into hydrogen bonds forming between GTP Pγ oxygen and sulfate in mutated cysteine, as this bond is crucial in K-Ras activation. This was done using GROMOS program *hbond*.

Finally, to look more deeply into the role of magnesium ion, and interaction of GTP/GDP with

specific loops, GROMOS files were translated into GROMACS format. This way GROMACS program *mdmat* could be used to get all the distances between residues.

4 Results and discussion

4.1 K-Ras mutations occurance in human cancers

Looking into Ras protein family, K-Ras isoform has the highest occurrence of human cancers related to its mutations, as it is shown in Table 1. It is notable that K-Ras seems to show a mutual exclusivity with both H-Ras and N-Ras, while H-Ras and N-Ras show co-occurrence tendencies on this specific data set [12, 13, 14].

As it is shown in the further analysis of cancer cases possibly affected by K-Ras mutations shown in Table 2, cancer type is not consistent with a specific mutation, neither is one mutation limited to the specific cancer type. That being said, mutations with high cancer comorbidities and fatalities are G12A, G12C, G12D, G12R, G12S, G12V, G13C, G13D, Q61H, and A146T. Full data can be found in the Appendix A.

All the data used in the work that follows is obtained from cBioPortal database for cancer genomics [12, 13, 14], specifically TCGA PanCancer Atlas Studies (as of August 2nd 2024) and sorted for the purpose of this thesis. The mutation that is specifically investigated in this thesis is G12C, which has been shown to have a significant effect in lung cancer development with high fatality rates.

4.2 Obtained free energies

As mentioned before, free energies were calculated using a Python script. Results for individual replicas and combined results are shown in tables 3, 4, and 5. Results for perturbation from GDP to GTP, WT to G12C, and other ways around, are shown in Table 6. Error values in Table 6 are as high because only 2 ns per λ point was performed, or just the zero-th TI cycle, without extension.

To evaluate binding energies, as discussed before, energies (MBAR) from Table 6 are subtracted from Total MBAR values in Table 4. This gives results shown in Figure 5. First obvious thing is that there are double values in GDP/GTP perturbations in mutated type. This is due to the fact that energies in the first cycle compared to ones in second and third are off (or, as will be deduced and explained later, the other way around). For this reason, the total binding energy is shown in red, while the one taking only the first cycle into account is shown in green.

There is slight hysteresis in results going from mutated to wild type (-3.05 kJ/mol for GDP

Table 1: *Frequency of mutations in Ras isoforms in human cancers. Data were compiled from cBioPortal database for cancer genomics, TCGA PanCancer Atlas Studies (as of August 2nd 2024) [12, 13, 14].*

Cancer type (c stands for cancer)	Ras mutation frequency	Sample size	K-Ras mut. frequency	H-Ras mut. frequency	N-Ras mut. frequency
Pancreatic c.	65.36%	179	**65.36%**	0.56%	0%
Colorectal c.	46.82%	534	**40.82%**	0.75%	6.18%
Melanoma	31.82%	440	2.27%	2.05%	**28.41%**
Seminoma	26.98%	63	**19.05%**	0%	7.94%
Endometrial c.	22.13%	574	**18.47%**	1.39%	3.83%
Non-small cell lung c.	18.38%	1050	**16.67%**	0.95%	0.95%
Leukemia	13%	200	5%	0%	**8%**
Thyroid c.	12.04%	490	0.82%	3.27%	**7.96%**
Pheochromocytoma	11.56%	147	0%	**11.56%**	0%
Thymic epithelial tumor	11.38%	123	0.81%	**8.13%**	2.44%
Bladder c.	10%	410	3.66%	4.39%	1.95%
Cholangiocarcinoma	8.33%	36	**5.56%**	0%	2.78%
Esophagogastric c.	7.61%	618	**6.8%**	0.16%	0.81%
Head and neck c.	6.41%	515	0.19%	**6.02%**	0.19%
Cervical c.	6.19%	291	**5.15%**	0.34%	1.03%
Mature B-cell neoplasms	4.88%	41	**4.88%**	0%	0%
Miscellaneous neuroepithelial tumor	3.23%	31	0%	**3.23%**	0%
Hepatobiliary c.	2.73%	366	1.37%	0%	1.37%

Table 2: *Frequency of K-Ras mutations in human cancers with fatalities. Data corresponds to Table 1, while numbers presented are number of cancer cases with the specific mutation / number of fatalities / ratio of fatalities in all cases with said mutation. Only cancer types highly impacted by K-Ras mutations from Table 1 are shown. Data were compiled from cBioPortal database for cancer genomics, TCGA PanCancer Atlas Studies (as of August 2nd 2024) [12, 13, 14].*

	G12A	G12C	G12D	G12R	G12S
Cervical c.	- / - / -	2/ 1/ 0.5	4/ 1/ 0.25	- / - / -	- / - / -
Colorectal c.	**10/ 3/ 0.3**	**15/ 3/ 0.2**	**58/ 9/ 0.16**	2/ 1/ 0.50	8/ 1/ 0.13
Endometrial c.	9/ 2/ 0.22	7/ 2/ 0.29	**34/ 2/ 0.06**	- / - / -	3/ - / 0
Esophagogastric c.	- / - / -	2/ - / 0	12/ - / 0	- / - / -	4/ 1/ 0.25
Non-smallcell lung c.	**18/ 3/ 0.17**	**70/ 15/ 0.21**	**20/ 3/ 0.15**	- / - / -	5/ - / 0
Pancreatic c.	1/ 1/ 1	1/ - / 0	**49/ 25/ 0.51**	**25/ 9/ 0.36**	1/ - / 0
Seminoma	1/ - / 0	- / - / -	- / - / -	2/ - / 0	1/ - / 0
	G12V	G13C	G13D	Q61H	A146T
Cervical c.	2/ 1/ 0.5	- / - / -	4/ 3/ 0.75	- / - / -	2/ - / 0
Colorectal c.	**49/ 5/ 0.1**	2/ - / 0	**37/ 4/ 0.11**	4/ - / 0	**16/ 2/ 0.13**
Endometrial c.	**22/ 1/ 0.05**	3/ - / 0	11/ - / 0	4/ - / 0	1/ - / 0
Esophagogastric c.	3/ 1/ 0.33	- / - / -	11/ - / 0	2/ - / 0	3/ - / 0
Non-smallcell lung c.	**41/ 8/ 0.2**	8/ 3/ 0.38	3/ 1/ 0.33	2/ - / 0	- / - / -
Pancreatic c.	**33/ 17/ 0.52**	1/ 1/ 1	- / - / -	6/ 3/ 0.5	- / - / -
Seminoma	3/ 1/ 0.33	- / - / -	- / - / -	- / - / -	- / - / -

Table 3: *Free energy BAR values. All values are expressed in kJ/mol.*

	1st Replica	2nd Replica	3rd Replica	Total	Error
G12C-GDP→WT-GDP	7.66	5.09	4.97	7.25	0.05
WT-GDP→G12C-GDP	-4.36	-11.33	-9.75	-6.2	0.1
WT-GDP→WT-GTP	-10.16	-3.85	-0.68	-5.4	0.2
WT-GTP→WT-GDP	38.41	38.91	32.35	38.9	0.2
WT-GTP→G12C-GTP	-18.48	-14.76	-9.36	-15.4	0.1
G12C-GTP→WT-GTP	20.94	13.08	13.91	15.24	0.09
G12C-GTP→G12C-GDP	60.22	14.00	13.64	26.6	0.2
G12C-GDP→G12C-GTP	-67.91	-21.12	-7.47	-41.4	0.2

Table 4: *Free energy MBAR values. All values are expressed in kJ/mol.*

	1st Replica	2nd Replica	3rd Replica	Total	Error
G12C-GDP→WT-GDP	6.71	5.09	3.68	6.43	0.05
WT-GDP→G12C-GDP	-3.04	-10.84	-9.62	-6.96	0.09
WT-GDP→WT-GTP	-10.27	-2.84	-1.91	-5.8	0.2
WT-GTP→WT-GDP	38.80	38.16	31.31	38.4	0.2
WT-GTP→G12C-GTP	-18.30	-14.39	-9.45	-15.1	0.1
G12C-GTP→WT-GTP	20.30	12.51	13.92	15.03	0.07
G12C-GTP→G12C-GDP	60.36	13.09	13.55	27.0	0.2
G12C-GDP→G12C-GTP	-66.98	-20.95	-7.08	-37.2	0.2

Table 5: *Free energy TI values. All values are expressed in kJ/mol.*

	1st Replica	2nd Replica	3rd Replica	Total
G12C-GDP→WT-GDP	8.39	4.78	4.71	7.19
WT-GDP→G12C-GDP	-4.28	-12.04	-8.34	-7.86
WT-GDP→WT-GTP	-9.33	-3.81	1.52	-4.74
WT-GTP→WT-GDP	36.04	40.22	33.04	37.10
WT-GTP→G12C-GTP	-17.16	-15.05	-9.98	-14.75
G12C-GTP→WT-GTP	21.22	12.62	13.86	14.99
G12C-GTP→G12C-GDP	58.83	14.17	13.54	29.04
G12C-GDP→G12C-GTP	-68.49	-20.78	-5.98	-42.44

and 5.54 kJ/mol for GTP) and the other way around (3.25 kJ/mol for GDP and -4.91 kJ/mol for GTP), but the specific differences are not considered to be significant. On the other hand, there is significant hysteresis (for an order of magnitude) in GDP/GTP perturbations (-26.87 kJ/mol and 19.80 kJ/mol for the mutated protein), especially in the wild type protein (34.28 kJ/mol and -2.14 kJ/mol).

Taking into account results that are consistent, they show a biological relevance. Specifically, they show that the preferable state in case of the wild type is GDP binding, and in the case of mutated type GTP binding. This goes together with the assumption that GTP over-binding in mutated type is the main cause of cancer development [1, 3, 4].

Table 6: *Free energy values for ligand and protein perturbations in water. All values are expressed in kJ/mol.*

	1st Replica	2nd Replica	3rd Replica	Total	Error
G12C→WT BAR	7.90	7.23	12.77	9.3	0.2
G12C→WT MBAR	7.91	7.34	13.30	9.5	0.2
G12C→WT TI	7.87	6.88	12.94	9.23	-
WT→G12C BAR	-8.79	-9.02	-12.54	-10.1	0.2
WT→G12C MBAR	-8.81	-9.02	-12.85	-10.2	0.2
WT→G12C TI	-9.15	-9.32	-12.59	-10.36	-
GDP→GTP BAR	-40.19	-41.25	-39.41	-40.3	0.5
GDP→GTP MBAR	-39.93	-41.05	-39.13	-40.1	0.5
GDP→GTP TI	-40.19	-41.63	-39.32	-40.38	-
GTP→GDP BAR	41.16	40.17	40.92	40.8	0.5
GTP→GDP MBAR	41.01	40.06	40.59	40.6	0.5
GTP→GDP TI	40.98	40.96	41.65	41.19	-

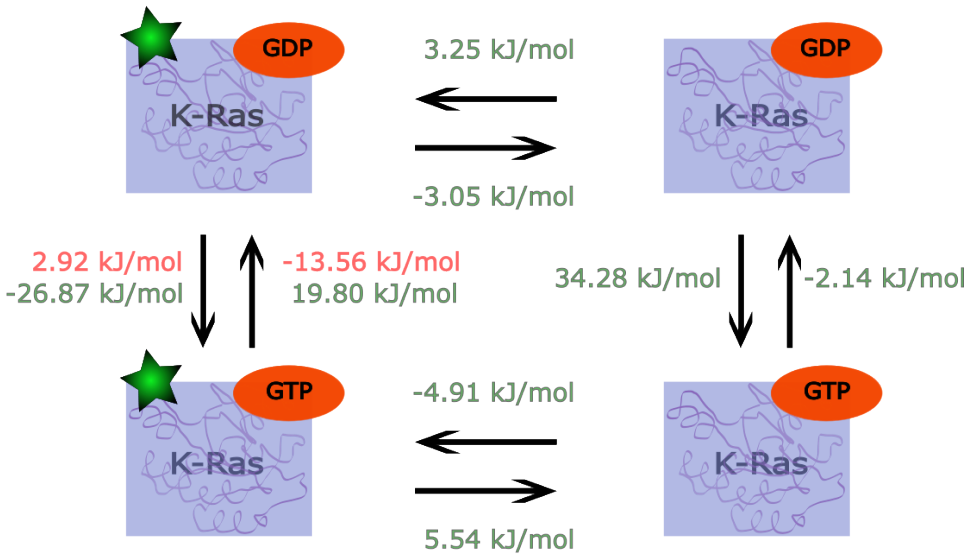

Figure 5: *Free energies in thermodynamic cycle. Energies in red inconsistent with biological implications.*

4.2.1 MBAR-BAR differences

First thing to realize from this data is that there is a significant difference from BAR to MBAR data. While it is not common to be so, because of the slight algorithm difference, it is possible when the data is not nicely converging. As this is the case with K-Ras system, the difference in BAR and MBAR data is somewhat justified, even though still highly unwanted.

Another thing to look at is the comparison to TI data. The difference here is more prominent, and one specific result to show so is the WT-GDP→WT-GTP perturbation, replica 3, where the

energy value becomes positive, which, compared to other results and biological background, is clearly the consequence of the algorithm inadequacies.

4.2.2 λ-point evaluation

To show the convergence of individual λ points, unconverged (or simulated) λ points are shown in green, newly converged in pink and previously converged in yellow in figures 6-13. Left side numbers indicate λ points with the step of 0.025, or 41 λ points in total. The numbers on the top represent the number of cycle performed, zeroth being the starting TI cycle, and one and higher repeats for the extended TI. Blue colour represents full convergence.

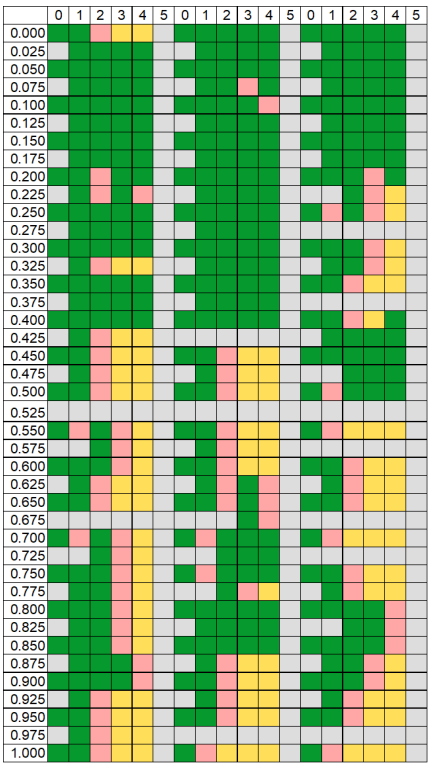

Figure 6: *Convergence regions of G12C-GDP→WT-GDP perturbation, replicas 1-3.*

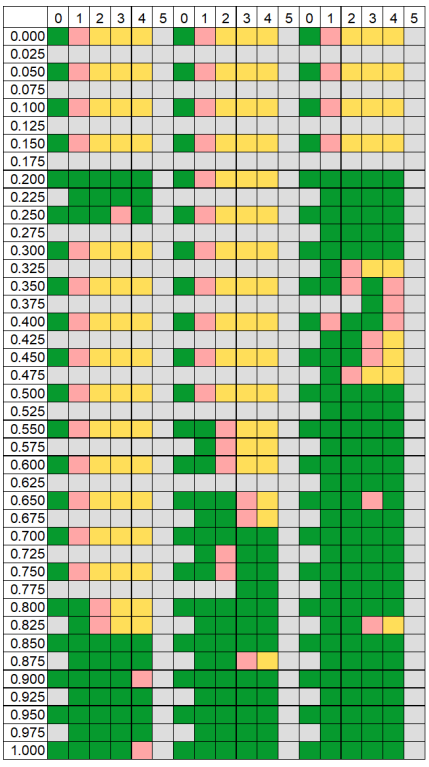

Figure 7: *Convergence regions of WT-GDP→G12C-GDP perturbation, replicas 1-3.*

As one can realize from the figures above, some perturbations converged to some point, while the others hardly at all. The only successful convergence is shown in Figure 11 for the first replica. It is also noTable that convergence moves on more smoothly for WT to G12C and G12C to WT perturbation than for GTP and GDP molecule ones.

The difference in convergence patterns may also justify energy differences between replicas, while the difference in convergence patterns between same perturbations in different directions might explain hysteresis in results between those.

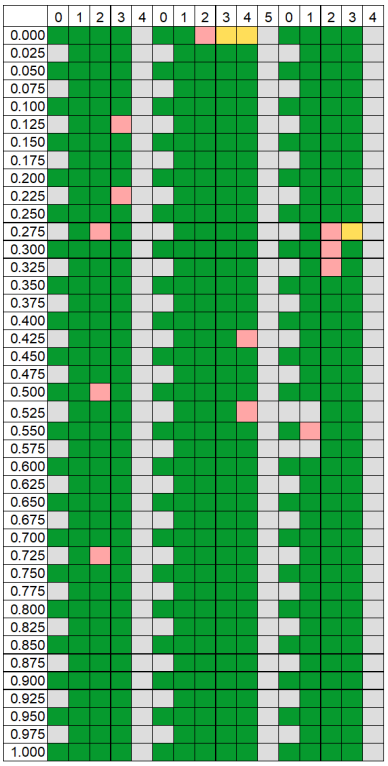

Figure 8: *Convergence regions of WT-GDP→WT-GTP perturbation, replicas 1-3.*

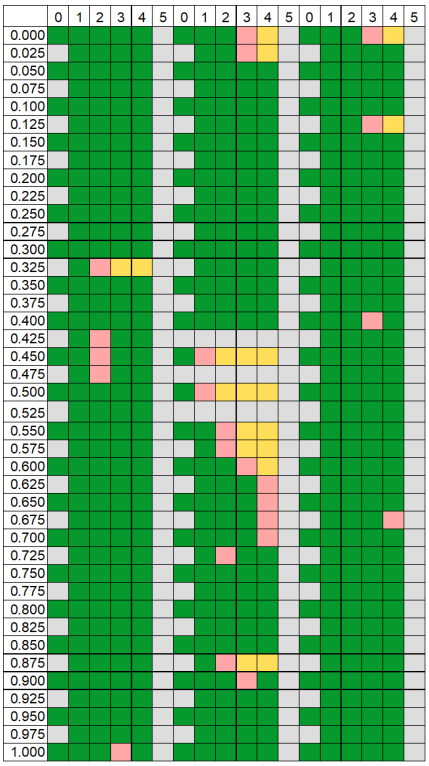

Figure 9: *Convergence regions of WT-GTP→WT-GDP perturbation, replicas 1-3.*

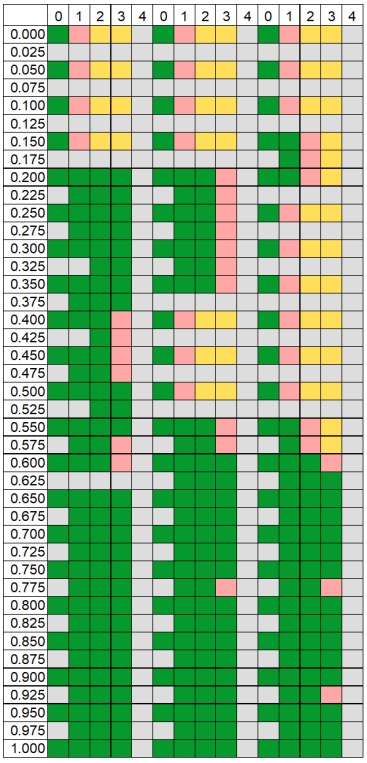

Figure 10: *Convergence regions of WT-GTP→G12C-GTP perturbation, replicas 1-3.*

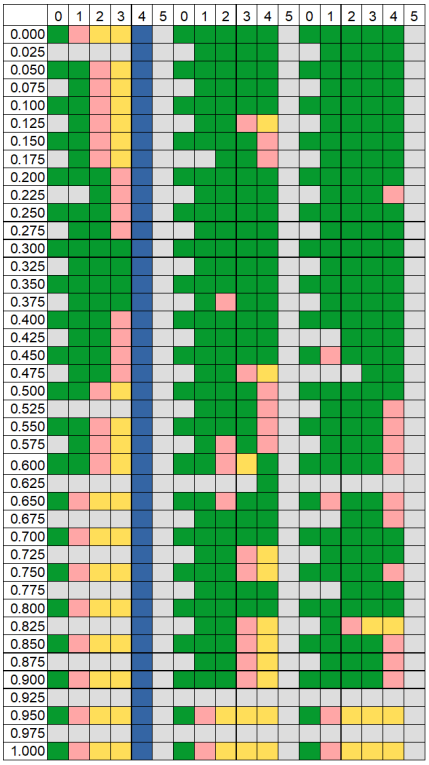

Figure 11: *Convergence regions of G12C-GTP→WT-GTP perturbation, replicas 1-3.*

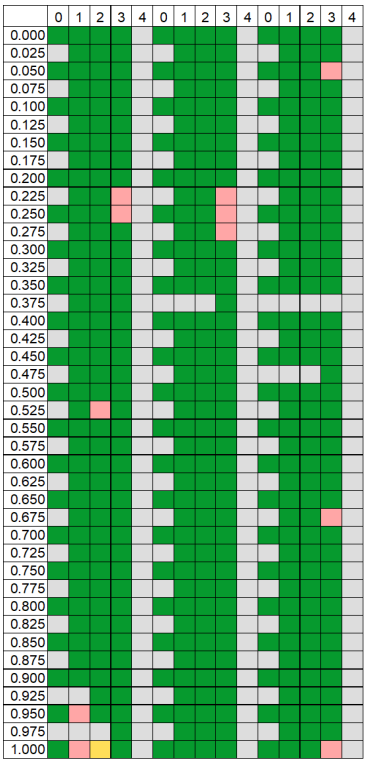

Figure 12: *Convergence regions of G12C-GTP→G12C-GDP perturbation, replicas 1-3.*

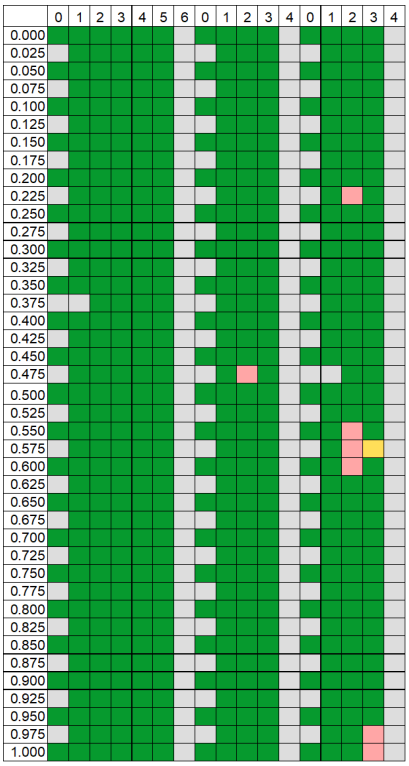

Figure 13: *Convergence regions of G12C-GDP→G12C-GTP perturbation, replicas 1-3.*

4.2.3 Problems with perturbations

As observeded, there is an obvious difference in convergence between simulations where protein is perturbed and where GDP or GTP is perturbed. This is due to the charge change while going from one molecule to another. PO_3 group has a triple negative charge. Such a change in the protein pocket leads to highly disturbed system that takes a while to converge.

Besides the charge change, there is also a question of size of the binding molecule, but this change is not as prominent as the one mentioned before. To solve this, one could go for longer simulation times, but looking into convergence figures, there was no sign of it converging at some short distance point.

Another reason not to proceed with simulations were BAR and MBAR error values and value changes between the two cycles. As those errors and changes were small enough, simulations were stopped at that point to save resources, as it was not sure if simulating for double the time would make a change.

It is important to mention that even the glycine perturbation is problematic. It is shown that perturbations to and from glycine yield high degree hysteresis due to poor sampling of dihedral angles [36]. This basically means that any change from glycine to another aminoacid might take a while to settle as glycine is too flexible, or that other way around glycine doesn't get to

be as flexible as it would be. This might also influence results in WT protein going from GDP to GTP and vice versa, where a huge hysteresis is seen in tables 4-6. Due to the flexibility of glycine and its poor binding to GDP/GTP, there might be some influence on final values.

Another obvious problem is a difference in energies between replicas. While slight differences are expected and contribute to final result statistics, perturbations of GTP and GDP in G12C mutated protein show by far different results in the first replica compared to the second and the third. To have a better look into why it is like that, it was an imperative to look into trajectory files and look for answers there.

4.3 Trajectory analysis

In an attempt to explain the hysteresis observed between pairs of simulations going in different directions as well as the difference in energies between replicas in GTP/GDP perturbations in mutated type, trajectories were thoroughly analyzed.

4.3.1 Root mean square distance analysis

First analysis performed on trajectories were RMSD calculations. Structures from simulations performed by Dr. Edgar Galicia Andrés were taken as reference structures. This is because doing clustering on simulations as short as these would not be effective, and the ones used for reference were simulated for around 1 microsecond or more. These simulations were clustered based on the movement of Switch-I and Switch-II loops.

As those loops are quite flexible, results from these RMSD calculations, taking into account only the movement of those loops, gave some interesting results. RMSD for the Switch-II loop was performed on the first two clusters, while for the Switch-I loop it was performed on the first three clusters. Results are shown in tables 7-11. Average values are colored based on the value.

From the Switch-II tables 7 and 8 it is seen that the system stayed in cluster 2 for most of the simulation time. This means it was not in the most preferable state detected by Dr. Galicia's simulations. Besides that, RMSD values seem consistent between simulations.

Switch-I RMSD results are more versatile, showing a major difference in RMSD values between same system simulations in different directions for all the clusters and replicas. As simulations in the one direction take the previous state as a starting point, this could mean that an initial perturbation already experiences a huge shift in the structure. With regard to the free energy calculations, this might explain the hysteresis between same system perturbations, as the Switch-I loop is not in the same state in both directions. Its proximity to both the magnesium ion and the GTP/GDP molecule means that changes in the RMSD influence the free energy values.

Table 7: *RMSD values for Switch-II loop, cluster 01. All the values are in nm.*

		min	max	avg	dev
1st Replica	G12C-GDP→WT-GDP	0.14	0.35	0.28	0.03
	WT-GDP→G12C-GDP	0.19	0.33	0.27	0.03
	WT-GDP→WT-GTP	0.15	0.31	0.23	0.02
	WT-GTP→WT-GDP	0.15	0.34	0.27	0.03
	WT-GTP→G12C-GTP	0.12	0.25	0.18	0.02
	G12C-GTP→WT-GTP	0.20	0.33	0.26	0.02
	G12C-GTP→G12C-GDP	0.12	0.21	0.16	0.02
	G12C-GDP→G12C-GTP	0.16	0.40	0.29	0.04
2nd Replica	G12C-GDP→WT-GDP	0.13	0.31	0.20	0.03
	WT-GDP→G12C-GDP	0.15	0.24	0.20	0.01
	WT-GDP→WT-GTP	0.13	0.24	0.18	0.02
	WT-GTP→WT-GDP	0.14	0.25	0.19	0.02
	WT-GTP→G12C-GTP	0.12	0.22	0.16	0.02
	G12C-GTP→WT-GTP	0.13	0.25	0.18	0.02
	G12C-GTP→G12C-GDP	0.11	0.20	0.16	0.01
	G12C-GDP→G12C-GTP	0.16	0.35	0.24	0.04
3rd Replica	G12C-GDP→WT-GDP	0.18	0.33	0.26	0.02
	WT-GDP→G12C-GDP	0.07	0.25	0.19	0.03
	WT-GDP→WT-GTP	0.18	0.32	0.25	0.02
	WT-GTP→WT-GDP	0.11	0.26	0.18	0.02
	WT-GTP→G12C-GTP	0.16	0.28	0.22	0.02
	G12C-GTP→WT-GTP	0.14	0.31	0.24	0.03
	G12C-GTP→G12C-GDP	0.13	0.30	0.23	0.03
	G12C-GDP→G12C-GTP	0.14	0.32	0.26	0.02

Table 8: *RMSD values for Switch-II loop, cluster 02. All the values are in nm.*

		min	max	avg	dev
1st Replica	G12C-GDP→WT-GDP	0.07	0.22	0.14	0.02
	WT-GDP→G12C-GDP	0.08	0.19	0.13	0.02
	WT-GDP→WT-GTP	0.05	0.18	0.12	0.02
	WT-GTP→WT-GDP	0.07	0.23	0.14	0.03
	WT-GTP→G12C-GTP	0.04	0.20	0.09	0.02
	G12C-GTP→WT-GTP	0.06	0.20	0.12	0.03
	G12C-GTP→G12C-GDP	0.06	0.18	0.11	0.02
	G12C-GDP→G12C-GTP	0.06	0.29	0.17	0.04
2nd Replica	G12C-GDP→WT-GDP	0.06	0.22	0.12	0.02
	WT-GDP→G12C-GDP	0.06	0.13	0.09	0.01
	WT-GDP→WT-GTP	0.05	0.18	0.10	0.02
	WT-GTP→WT-GDP	0.05	0.16	0.09	0.02
	WT-GTP→G12C-GTP	0.07	0.22	0.13	0.03
	G12C-GTP→WT-GTP	0.05	0.15	0.09	0.02
	G12C-GTP→G12C-GDP	0.05	0.18	0.11	0.02
	G12C-GDP→G12C-GTP	0.06	0.24	0.12	0.03
3rd Replica	G12C-GDP→WT-GDP	0.07	0.19	0.12	0.02
	WT-GDP→G12C-GDP	0.05	0.25	0.12	0.04
	WT-GDP→WT-GTP	0.06	0.21	0.12	0.03
	WT-GTP→WT-GDP	0.06	0.23	0.12	0.03
	WT-GTP→G12C-GTP	0.06	0.21	0.14	0.03
	G12C-GTP→WT-GTP	0.07	0.22	0.13	0.02
	G12C-GTP→G12C-GDP	0.07	0.25	0.13	0.02
	G12C-GDP→G12C-GTP	0.07	0.21	0.13	0.02

Table 9: *RMSD values for Switch-I loop, cluster 01. All the values are in nm.*

		min	max	avg	dev
1st Replica	G12C-GDP→WT-GDP	0.07	0.22	0.13	0.02
	WT-GDP→G12C-GDP	0.09	0.17	0.13	0.01
	WT-GDP→WT-GTP	0.09	0.19	0.14	0.02
	WT-GTP→WT-GDP	0.08	0.18	0.14	0.02
	WT-GTP→G12C-GTP	0.12	0.24	0.17	0.02
	G12C-GTP→WT-GTP	0.13	0.21	0.16	0.01
	G12C-GTP→G12C-GDP	0.10	0.29	0.16	0.02
	G12C-GDP→G12C-GTP	0.07	0.24	0.15	0.03
2nd Replica	G12C-GDP→WT-GDP	0.08	0.19	0.13	0.02
	WT-GDP→G12C-GDP	0.15	0.29	0.21	0.02
	WT-GDP→WT-GTP	0.07	0.22	0.14	0.03
	WT-GTP→WT-GDP	0.17	0.26	0.21	0.01
	WT-GTP→G12C-GTP	0.09	0.20	0.14	0.02
	G12C-GTP→WT-GTP	0.17	0.26	0.21	0.01
	G12C-GTP→G12C-GDP	0.07	0.21	0.13	0.02
	G12C-GDP→G12C-GTP	0.07	0.24	0.16	0.04
3rd Replica	G12C-GDP→WT-GDP	0.09	0.28	0.14	0.03
	WT-GDP→G12C-GDP	0.11	0.22	0.17	0.02
	WT-GDP→WT-GTP	0.07	0.26	0.16	0.03
	WT-GTP→WT-GDP	0.09	0.20	0.15	0.02
	WT-GTP→G12C-GTP	0.12	0.35	0.18	0.02
	G12C-GTP→WT-GTP	0.08	0.21	0.14	0.02
	G12C-GTP→G12C-GDP	0.11	0.23	0.18	0.01
	G12C-GDP→G12C-GTP	0.08	0.20	0.13	0.02

Table 10: *RMSD values for Switch-I loop, cluster 02. All the values are in nm.*

		min	max	avg	dev
1st Replica	G12C-GDP→WT-GDP	0.11	0.24	0.17	0.02
	WT-GDP→G12C-GDP	0.13	0.23	0.18	0.02
	WT-GDP→WT-GTP	0.11	0.27	0.16	0.02
	WT-GTP→WT-GDP	0.11	0.22	0.18	0.02
	WT-GTP→G12C-GTP	0.17	0.31	0.23	0.02
	G12C-GTP→WT-GTP	0.14	0.23	0.19	0.02
	G12C-GTP→G12C-GDP	0.17	0.37	0.23	0.03
	G12C-GDP→G12C-GTP	0.10	0.29	0.17	0.02
2nd Replica	G12C-GDP→WT-GDP	0.09	0.24	0.16	0.03
	WT-GDP→G12C-GDP	0.16	0.30	0.21	0.03
	WT-GDP→WT-GTP	0.07	0.23	0.14	0.03
	WT-GTP→WT-GDP	0.16	0.23	0.20	0.01
	WT-GTP→G12C-GTP	0.08	0.24	0.13	0.02
	G12C-GTP→WT-GTP	0.15	0.23	0.19	0.01
	G12C-GTP→G12C-GDP	0.07	0.24	0.13	0.02
	G12C-GDP→G12C-GTP	0.11	0.23	0.17	0.02
3rd Replica	G12C-GDP→WT-GDP	0.13	0.34	0.19	0.03
	WT-GDP→G12C-GDP	0.08	0.21	0.16	0.02
	WT-GDP→WT-GTP	0.10	0.33	0.20	0.03
	WT-GTP→WT-GDP	0.08	0.22	0.16	0.02
	WT-GTP→G12C-GTP	0.16	0.39	0.23	0.02
	G12C-GTP→WT-GTP	0.10	0.25	0.17	0.02
	G12C-GTP→G12C-GDP	0.15	0.30	0.24	0.02
	G12C-GDP→G12C-GTP	0.14	0.25	0.18	0.02

Table 11: *RMSD values for Switch-I loop, cluster 03. All the values are in nm.*

		min	max	avg	dev
1st Replica	G12C-GDP→WT-GDP	0.09	0.25	0.14	0.03
	WT-GDP→G12C-GDP	0.09	0.18	0.13	0.02
	WT-GDP→WT-GTP	0.10	0.22	0.16	0.02
	WT-GTP→WT-GDP	0.07	0.19	0.13	0.03
	WT-GTP→G12C-GTP	0.09	0.25	0.16	0.02
	G12C-GTP→WT-GTP	0.13	0.23	0.17	0.02
	G12C-GTP→G12C-GDP	0.10	0.26	0.15	0.02
	G12C-GDP→G12C-GTP	0.08	0.29	0.16	0.04
2nd Replica	G12C-GDP→WT-GDP	0.06	0.24	0.14	0.03
	WT-GDP→G12C-GDP	0.19	0.31	0.24	0.02
	WT-GDP→WT-GTP	0.09	0.24	0.16	0.03
	WT-GTP→WT-GDP	0.19	0.29	0.24	0.02
	WT-GTP→G12C-GTP	0.10	0.25	0.18	0.02
	G12C-GTP→WT-GTP	0.19	0.29	0.24	0.02
	G12C-GTP→G12C-GDP	0.09	0.26	0.17	0.03
	G12C-GDP→G12C-GTP	0.09	0.28	0.18	0.04
3rd Replica	G12C-GDP→WT-GDP	0.09	0.32	0.14	0.04
	WT-GDP→G12C-GDP	0.12	0.25	0.20	0.02
	WT-GDP→WT-GTP	0.10	0.29	0.17	0.03
	WT-GTP→WT-GDP	0.11	0.24	0.18	0.02
	WT-GTP→G12C-GTP	0.14	0.40	0.19	0.03
	G12C-GTP→WT-GTP	0.08	0.23	0.16	0.03
	G12C-GTP→G12C-GDP	0.12	0.26	0.18	0.02
	G12C-GDP→G12C-GTP	0.07	0.24	0.14	0.03

4.3.2 Analysis of h-bonds

To look more into the problem of energy differences between replicas in the GTP/GDP perturbations in mutated type protein, analysis of h-bonds between protein residues and GTP/GDP molecule was performed. Results for those simulations in the P-loop region are shown in figures 14 and 15. Additionally, all the h-bonds for all of the simulations can be found in the Appendix C.

Res	DONO	Res	ACC	Atom	D	A	OCCUR	%	Res	DONO	Res	ACC	Atom	D	A	OCCUR	%	Res	DONO	Res	ACC	Atom	D	A	OCCUR	%
12	CYSH	1	GTP	110	SG	O1PG	72	13.46	12	CYSH	1	GTP	110	SG	O1PG	52	8.51	12	CYSH	1	GTP	110	SG	O1PB	32	5.32
12	CYSH	1	GTP	110	SG	O3PG	6	1.12	12	CYSH	1	GTP	110	SG	O2PG	39	6.38	12	CYSH	1	GTP	110	SG	O3PB	1	0.17
13	GLY	1	GTP	114	N	O3PA	2	0.37	13	GLY	1	GTP	114	N	O3PA	15	2.45	12	CYSH	1	GTP	110	SG	O1PG	15	2.5
13	GLY	1	GTP	114	N	O1PB	29	5.42	13	GLY	1	GTP	114	N	O1PB	3	0.49	13	GLY	1	GTP	114	N	O3PA	20	3.33
13	GLY	1	GTP	114	N	O3PB	279	52.15	13	GLY	1	GTP	114	N	O3PB	396	64.81	13	GLY	1	GTP	114	N	O1PB	456	75.87
13	GLY	1	GTP	114	N	O1PG	41	7.66	13	GLY	1	GTP	114	N	O1PG	36	5.89	13	GLY	1	GTP	114	N	O3PB	69	11.48
13	GLY	1	GTP	114	N	O2PG	5	0.93	13	GLY	1	GTP	114	N	O2PG	46	7.53	13	GLY	1	GTP	114	N	O1PG	6	1
13	GLY	1	GTP	114	N	O3PG	25	4.67	13	GLY	1	GTP	114	N	O3PG	34	5.56	13	GLY	1	GTP	114	N	O2PG	3	0.5
14	VAL	1	GTP	119	N	O3PA	1	0.19	14	VAL	1	GTP	119	N	O1PB	107	17.51	14	VAL	1	GTP	119	N	O1PB	44	7.32
14	VAL	1	GTP	119	N	O1PB	231	43.18	14	VAL	1	GTP	119	N	O1PG	8	1.31	15	GLY	1	GTP	127	N	O2*	3	0.5
14	VAL	1	GTP	119	N	O1PG	1	0.19	14	VAL	1	GTP	119	N	O2PG	2	0.33	15	GLY	1	GTP	127	N	O3*	57	9.48
15	GLY	1	GTP	127	N	O4*	1	0.19	14	VAL	1	GTP	119	N	O3PG	1	0.16	16	LYSH	1	GTP	132	N	O1PB	1	0.17

Figure 14: *Occurrence of h-bonds in G12C-GTP→G12C-GDP perturbation P-loop. Colored in yellow is P-loop, and in orange the h-bond between sulfur in cysteine and Pγ/Pβ oxygen. Three colours represent three different replicas, numerated from left to right.*

Comparing the occurrence of h-bonds between cysteine sulfur and Pγ oxygen in replicas 1-3, it can be concluded that in replica 1 h-bond is present for a significant amount of time, while in replicas 2-3, it is not seen. One must take into account that only for a certain time of the simulation are Pγ oxygens visible to the full or close to full extent to the sulfur atom, as

Res	DONO	Res	ACC	Atom	D	A	OCCUR	%	Res	DONO	Res	ACC	Atom	D	A	OCCUR	%	Res	DONO	Res	ACC	Atom	D	A	OCCUR	%
12	CYSH	1	GTP	110	SG	O3PB	1	0.09	12	CYSH	1	GTP	110	SG	O1PB	36	6.81	12	CYSH	1	GTP	110	SG	O1PG	1	0.19
12	CYSH	1	GTP	110	SG	O1PG	220	20.39	12	CYSH	1	GTP	110	SG	O1PG	14	2.65	12	CYSH	1	GTP	110	SG	O2PG	6	1.13
12	CYSH	1	GTP	110	SG	O3PG	2	0.19	12	CYSH	1	GTP	110	SG	O2PG	3	0.57	12	CYSH	1	GTP	110	SG	O3PG	1	0.19
13	GLY	1	GTP	114	N	O3PA	10	0.93	12	CYSH	1	GTP	110	SG	O3PG	4	0.76	13	GLY	1	GTP	114	N	O3PB	41	7.72
13	GLY	1	GTP	114	N	O1PB	34	3.15	13	GLY	1	GTP	114	N	O1PA	3	0.57	13	GLY	1	GTP	114	N	O1PG	26	4.9
13	GLY	1	GTP	114	N	O3PB	459	42.54	13	GLY	1	GTP	114	N	O3PA	20	3.78	13	GLY	1	GTP	114	N	O2PG	152	28.63
13	GLY	1	GTP	114	N	O1PG	146	13.53	13	GLY	1	GTP	114	N	O1PB	179	33.84	13	GLY	1	GTP	114	N	O3PG	168	31.64
13	GLY	1	GTP	114	N	O2PG	74	6.86	13	GLY	1	GTP	114	N	O3PB	14	2.65	14	VAL	1	GTP	119	N	O1PB	12	2.26
13	GLY	1	GTP	114	N	O3PG	172	15.94	13	GLY	1	GTP	114	N	O1PG	23	4.35	14	VAL	1	GTP	119	N	O1PG	141	26.55
14	VAL	1	GTP	119	N	O1PB	112	10.38	13	GLY	1	GTP	114	N	O2PG	21	3.97	14	VAL	1	GTP	119	N	O2PG	6	1.13
14	VAL	1	GTP	119	N	O1PG	20	1.85	13	GLY	1	GTP	114	N	O3PG	11	2.08	14	VAL	1	GTP	119	N	O3PG	2	0.38
14	VAL	1	GTP	119	N	O2PG	9	0.83	14	VAL	1	GTP	119	N	O1PA	15	2.84	15	GLY	1	GTP	127	N	O3PA	15	2.82
14	VAL	1	GTP	119	N	O3PG	12	1.11	14	VAL	1	GTP	119	N	O2PA	1	0.19	15	GLY	1	GTP	127	N	O1PB	240	45.2
15	GLY	1	GTP	127	N	O1PA	3	0.28	14	VAL	1	GTP	119	N	O1PB	4	0.76	15	GLY	1	GTP	127	N	O1PG	136	25.61
15	GLY	1	GTP	127	N	O3PA	78	7.23	14	VAL	1	GTP	119	N	O3PG	2	0.38	15	GLY	1	GTP	127	N	O3PG	7	1.32

Figure 15: *Occurrence of h-bonds in G12C-GDP→G12C-GTP perturbation P-loop. Colored in yellow is P-loop, and in orange the h-bond between sulfur in cysteine and Pγ/Pβ oxygen. Three colours represent three different replicas, numerated from left to right.*

perturbation moves on through λ points.

4.3.3 Atom-atom distance analysis

As RMSD hinted that there is a significant difference in how Switch-I loop moves, more analysis was done in that direction. The position of the Switch-I loop can be observed in Figure 1. There one can see that it interacts with GTP/GDP molecule through bound magnesium ion. For this reason, atom-atom distance analysis of magnesium ion and GTP/GDP molecule was performed. Figures 16-23 show once again an inconsistency in binding between the two directions.

In Figures 21 and 22, distances of the C12 residue, as well as surrounding residues, are a bit smaller compared to the distances with G12 present or with the GDP molecule involved. The distance of the magnesium ion from P-loop residues is consistent regardless of the perturbation or mutation.

There is also a consistency in magnesium ion binding to D57 and T58 residues of the Switch-II loop. Its interaction with the GTP/GDP molecule also relies on interactions with G60, Q61 and R68 residues. Looking into Tables 12-14 in Appendix A, those are other possible mutation hotspots.

The problematic Switch-I loop does not have a clear binding scheme as the Switch-I loop, but it can be seen in Figures 16-23 that the GTP/GDP interacts with different aminoacid residues based on the perturbation and replica. Residues with the highest interaction rate (lowest distance from the GTP/GDP molecule) are F28, D30, E31, Y32, D33, P34, I36, and Y40. A lack of the pattern in presented pictures confirms that the Switch-I loop lacks consistency within different perturbations and replicas, which leads to inconsistent binding free energy results.

Differences between replicas for the beginning to the end of a simulation can also be observed. Distances of specific residues of the P-loop and Switch-II loop seem consistent throughout, which is shown as light colored squares. In Figures 24-25 it is seen once more that the Switch-I loop is the most flexible one. The distance change within singe simulation is prominent in Switch-I region, difference being the most prominent in the exact residues that

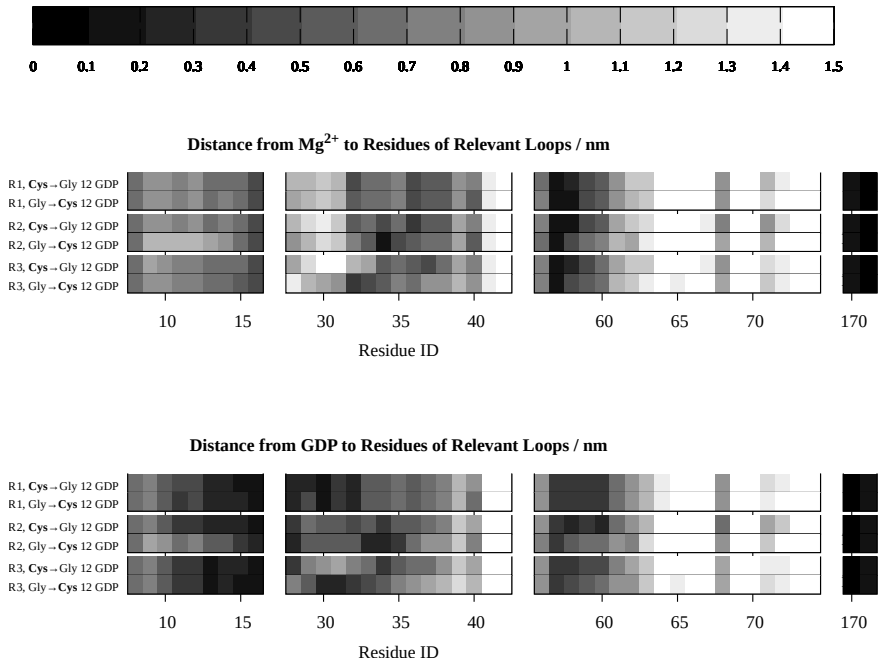

Figure 16: *Distance between residues in G12C-GDP→WT-GDP perturbation at λ=0 and WT-GDP→G12C-GDP perturbation at λ=1. Residue number 170 is GTP/GDP molecule and 171 is magnesium ion.*

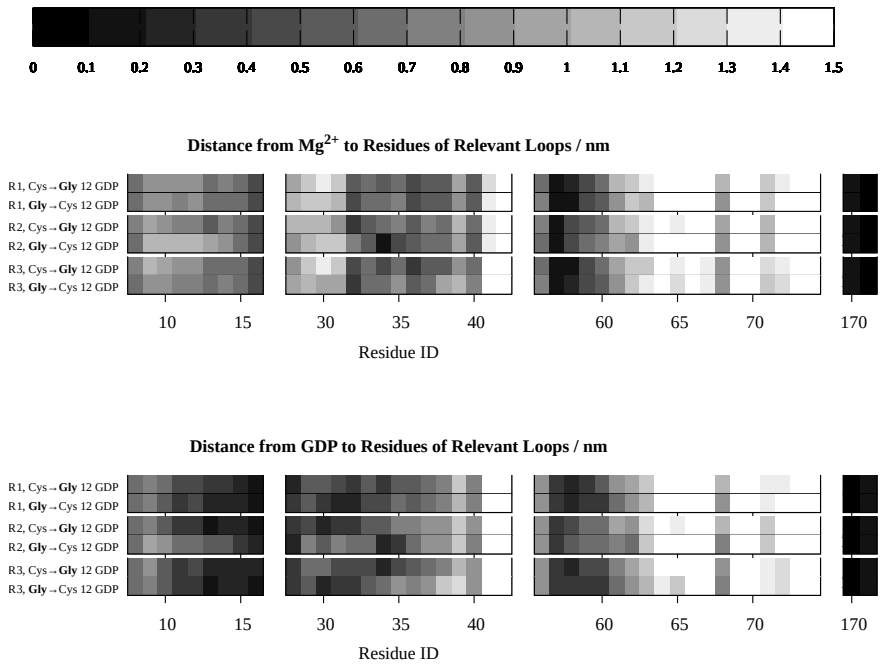

Figure 17: *Distance between residues in G12C-GDP→WT-GDP perturbation at λ=1 and WT-GDP→G12C-GDP perturbation at λ=0. Residue number 170 is GTP/GDP molecule and 171 is magnesium ion.*

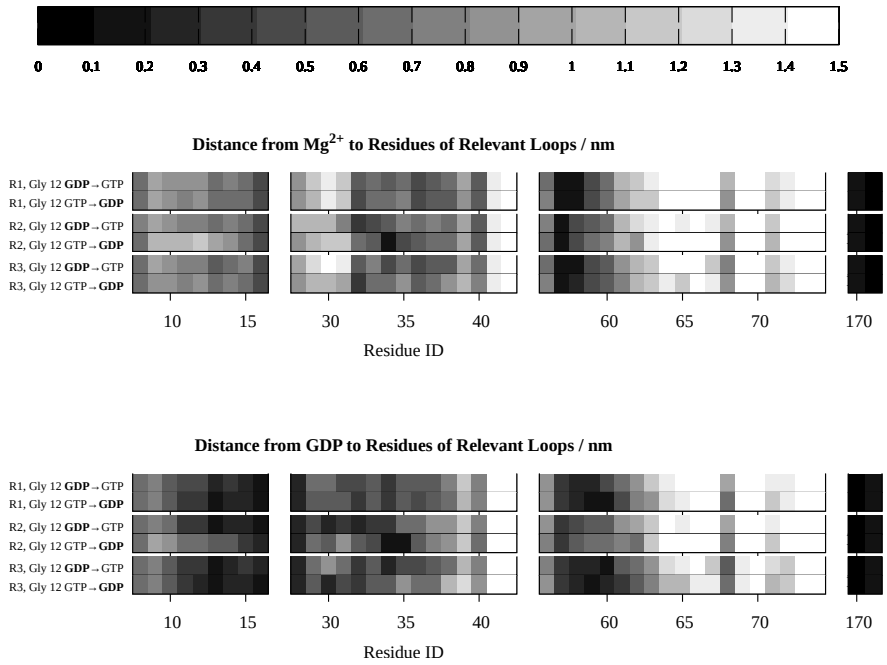

Figure 18: *Distance between residues in WT-GDP→WT-GTP perturbation at λ=0 and WT-GTP→WT-GDP perturbation at λ=1. Residue number 170 is GTP/GDP molecule and 171 is magnesium ion.*

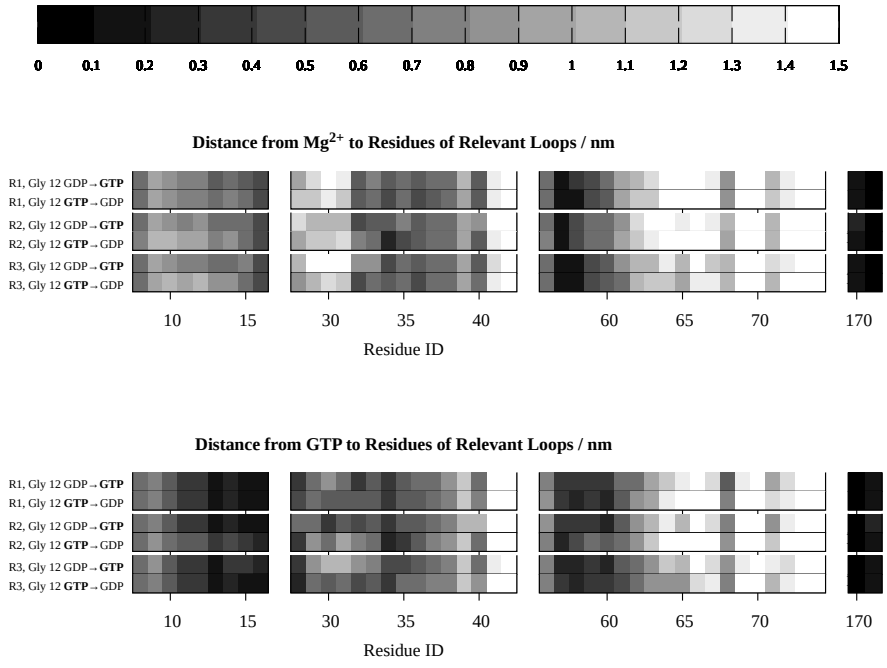

Figure 19: *Distance between residues in WT-GDP→WT-GTP perturbation at λ=1 and WT-GTP→WT-GDP perturbation at λ=0. Residue number 170 is GTP/GDP molecule and 171 is magnesium ion.*

are interacting the most with the GTP/GDP molecule based on Figures 16-23.

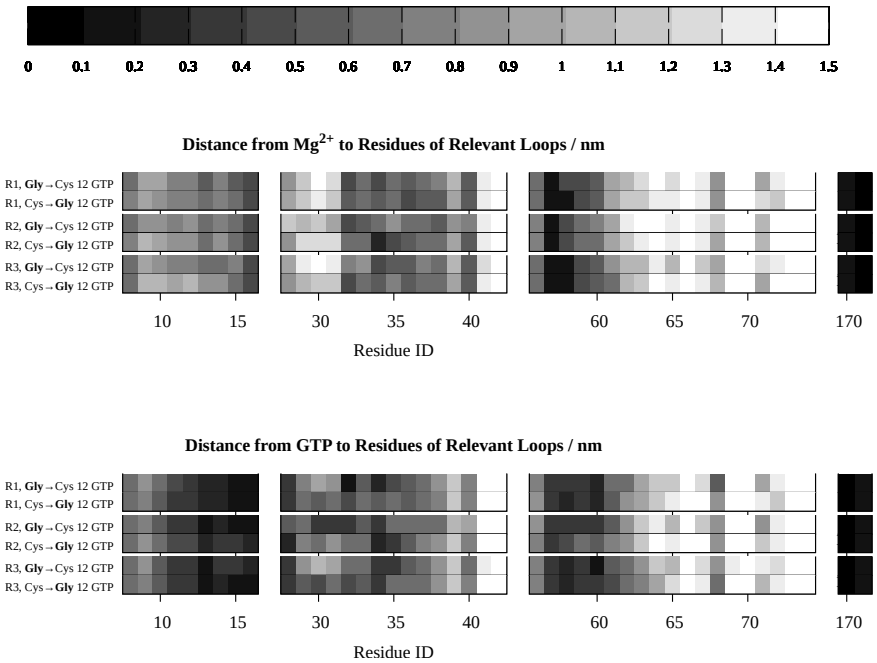

Figure 20: *Distance between residues in WT-GTP→G12C-GTP perturbation at λ=0 and G12C-GTP→WT-GTP perturbation at λ=1. Residue number 170 is GTP/GDP molecule and 171 is magnesium ion.*

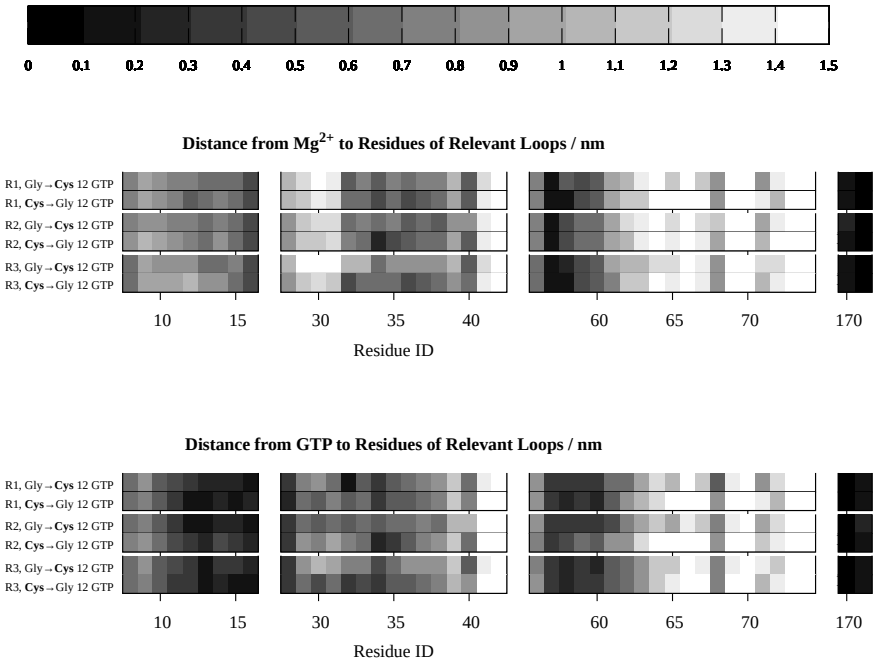

Figure 21: *Distance between residues in WT-GTP→G12C-GTP perturbation at λ=1 and G12C-GTP→WT-GTP perturbation at λ=0. Residue number 170 is GTP/GDP molecule and 171 is magnesium ion.*

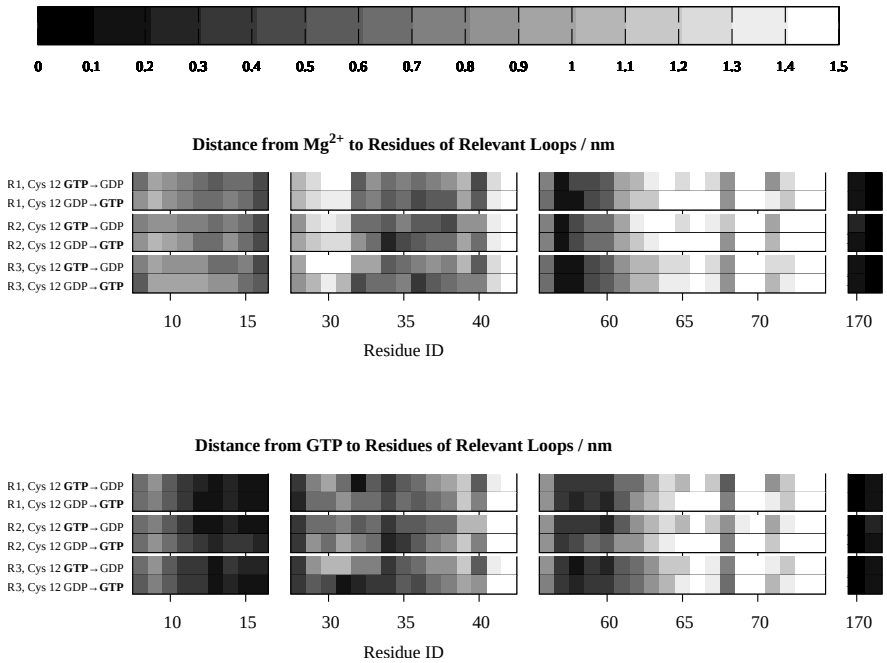

Figure 22: *Distance between residues in G12C-GTP→G12C-GDP perturbation at λ=0 and G12C-GDP→G12C-GTP perturbation at λ=1. Residue number 170 is GTP/GDP molecule and 171 is magnesium ion.*

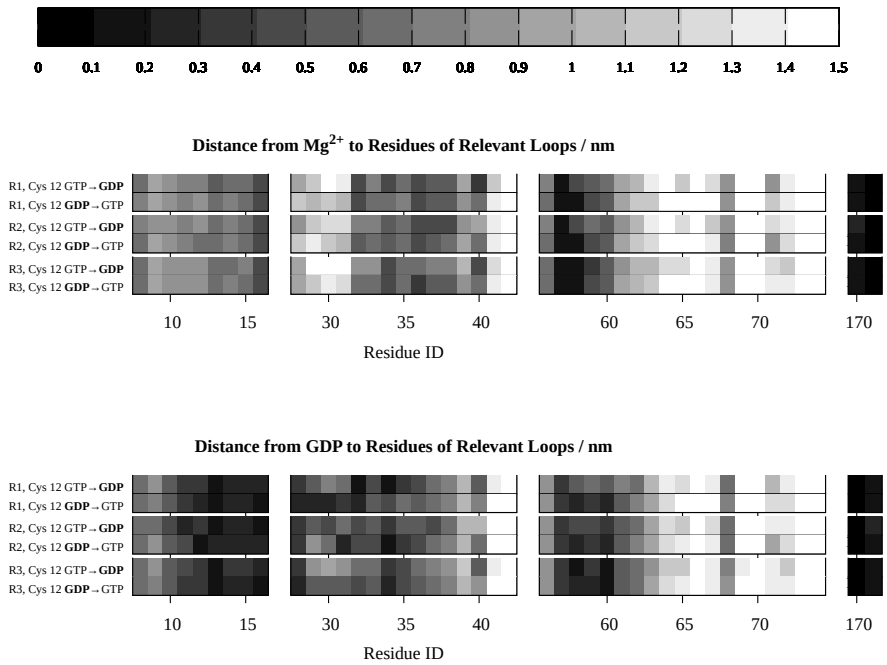

Figure 23: *Distance between residues in G12C-GTP→G12C-GDP perturbation at λ=1 and G12C-GDP→G12C-GTP perturbation at λ=0. Residue number 170 is GTP/GDP molecule and 171 is magnesium ion.*

Looking into a pattern on Figures 24 and 25, it can also be seen that the distance changes more in one of the simulation directions. This is best observed in Figure 25, third set of perturbations, but is also quite visible in the same set of simulations in Figure 24. Looking into results in Figure 5, there is no significant hysteresis there, but energy values are also quite low. More of the inconsistency in the pattern is seen in the first and fourth block, which correlates with the prominent hysteresis and the differences in replica's energies shown in Figure 5, respectively.

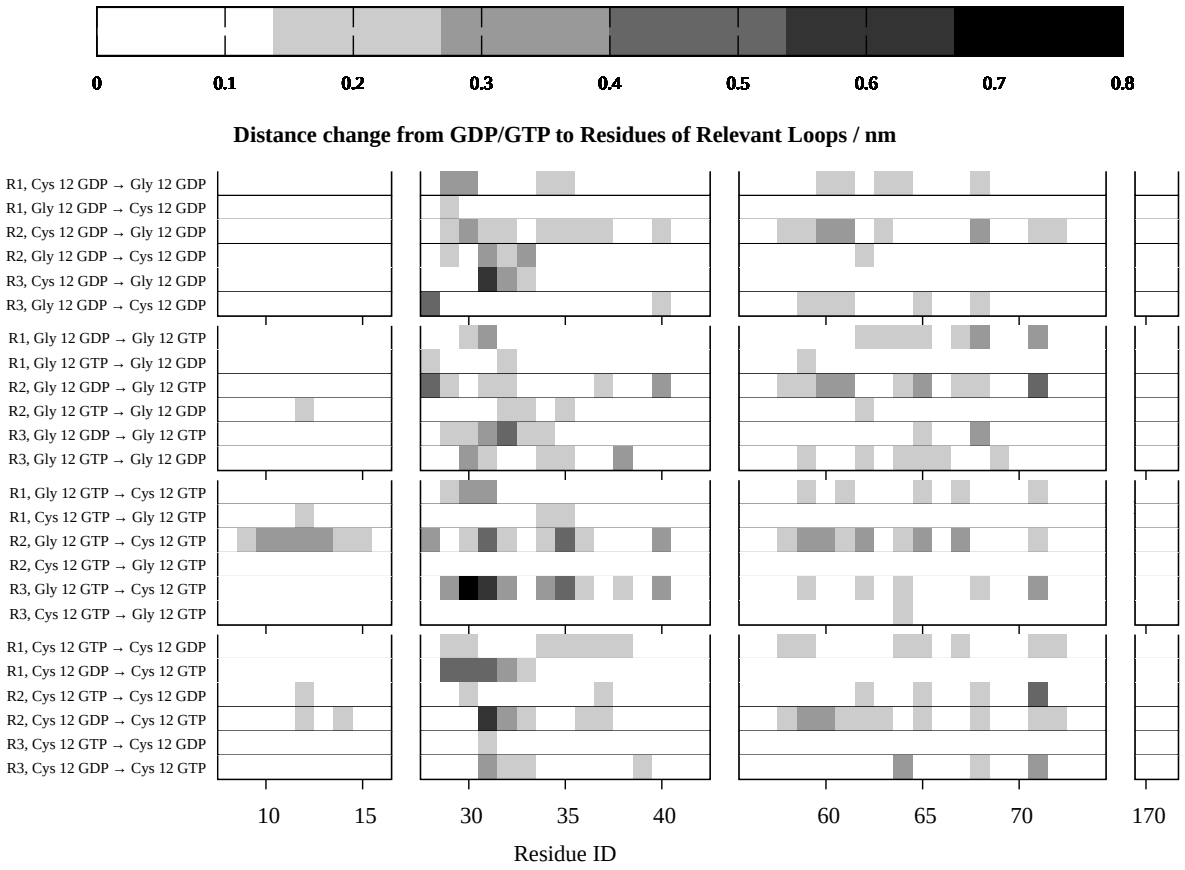

Figure 24: *Difference in starting and final position of GTP/GDP molecule.*

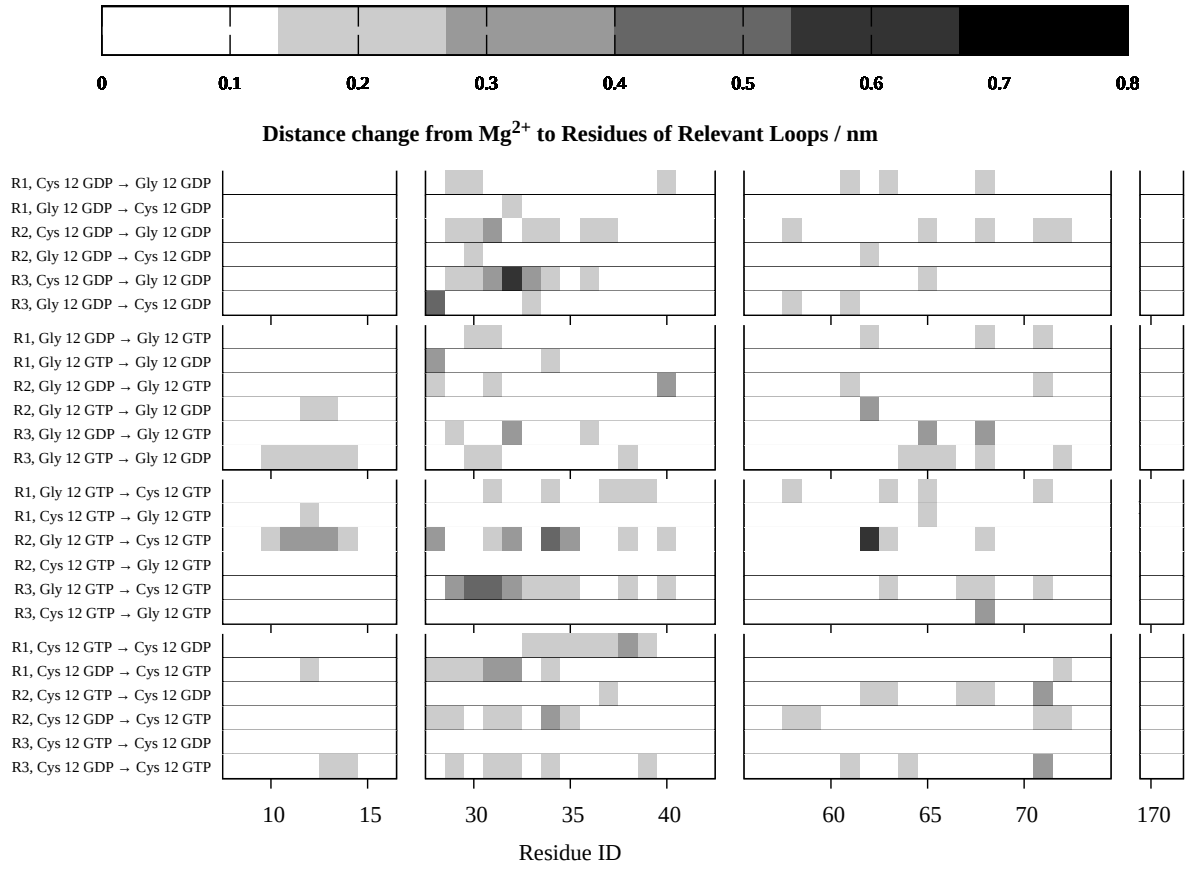

Figure 25: *Difference in starting and final position of magnesium ion.*

5 Conclusion

K-Ras protein is one of the significant players in cancer research as there are multiple mutations involved which show correlation with cancer development. For this reason, it was taken as the topic of the research presented in this thesis.

In the final analysis of the results obtained in researching the molecular dynamics and free energy binding of GTP/GDP molecule in K-Ras G12C mutation, a starting hypothesis was confirmed: Binding free energies showed the preference in binding of GTP molecule in the mutated type which goes together with the activity of mutated protein in MAPK pathway. This concludes that G12C mutation has a predisposition to cause cancer.

While performing simulations, there were obvious inconsistencies in results between replicas. Main reason for those turned out to be the lack of h-bond forming between sulfur on mutated cystein and Pγ oxygen of GTP molecule. For this reason, simulation replicas that do not form h-bonds are not considered in free energy calculations. These simulations are unstable and require higher simulation time to converge and produce relevant h-bond sampling. A reason that there is no forming of the h-bond in some replicas is not yet concluded.

Other problem that was encountered was a significant hysteresis between same system simulations going in different perturbation directions. RMSD and atom-atom distance analysis showed inconsistencies between those simulations in Switch-II loop.

There are two main ways for improving obtained results. First one would be prolonging simulations to get better sampling. This solution is not preferable, as it requires a lot of time and resources, and is not as significant as there are existing MD simulations done of this system. Another idea would be moving from the chosen apo structure of the protein to the holo structure, which might be much less flexible.

Either way, a direction to look into would also be to work on full automatization of extended TI simulations in a way that after each TI cycle analysis is performed and the system is set for the next cycle, repeating the proces until a condition is met. This will allow simulations to run smoothly without human intervention which would make the whole process faster.

6 Bibliography

[1] T. Pantsar, *The current understanding of KRAS protein structure and dynamics*, Computational and Structural Biotechnology Journal, vol. 18. Elsevier BV, pp. 189–198, **2020**. doi: 10.1016/j.csbj.2019.12.004.

[2] A. D. Cox and C. J. Der, *Ras history*, Small GTPases, vol. 1, no. 1. Informa UK Limited, pp. 2–27, Jul. **2010**. doi: 10.4161/sgtp.1.1.12178.

[3] Y. Pylayeva-Gupta, E. Grabocka, and D. Bar-Sagi, *RAS oncogenes: weaving a tumorigenic web*, Nature Reviews Cancer, vol. 11, no. 11. Springer Science and Business Media LLC, pp. 761–774, Oct. 13, **2011**. doi: 10.1038/nrc3106.

[4] D. K. Simanshu, D. V. Nissley, and F. McCormick, *RAS Proteins and Their Regulators in Human Disease*, Cell, vol. 170, no. 1. Elsevier BV, pp. 17–33, Jun. **2017**. doi: 10.1016/j.cell.2017.06.009.

[5] M. J. Whitley et al., *Comparative analysis of KRAS4a and KRAS4b splice variants reveals distinctive structural and functional properties*, Science Advances, vol. 10, no. 7. American Association for the Advancement of Science (AAAS), Feb. 16, **2024**. doi: 10.1126/sciadv.adj4137.

[6] M. Saraste, P. R. Sibbald, and A. Wittinghofer, *The P-loop — a common motif in ATP- and GTP-binding proteins*, Trends in Biochemical Sciences, vol. 15, no. 11. Elsevier BV, pp. 430–434, Nov. **1990**. doi: 10.1016/0968-0004(90)90281-f.

[7] [1] G. M. Cooper, *The Cell: A Molecular Approach*. New York: Sinauer Associates: Oxford University Press, **2019**.

[8] L. Schubert, M. L. Mariko, J. Clerc, O. Huillard, and L. Groussin, *MAPK Pathway Inhibitors in Thyroid Cancer: Preclinical and Clinical Data*, Cancers, vol. 15, no. 3. MDPI AG, p. 710, Jan. 24, **2023**. doi: 10.3390/cancers15030710.

[9] E. Santos, S. R. Tronick, S. A. Aaronson, S. Pulciani, and M. Barbacid, *T24 human bladder carcinoma oncogene is an activated form of the normal human homologue of BALB- and Harvey-MSV transforming genes*, Nature, vol. 298, no. 5872. Springer Science and Business Media LLC, pp. 343–347, Jul. **1982**. doi: 10.1038/298343a0.

[10] D. Gallwitz, C. Donath, and C. Sander, *A yeast gene encoding a protein homologous to the human c-has/bas proto-oncogene product*, Nature, vol. 306, no. 5944. Springer Science and Business Media LLC, pp. 704–707, Dec. 15, **1983**. doi: 10.1038/306704a0.

[11] C. Braicu et al., *A Comprehensive Review on MAPK: A Promising Therapeutic Target in Cancer*, Cancers, vol. 11, no. 10. MDPI AG, p. 1618, Oct. 22, **2019**. doi: 10.3390/cancers11101618.

[12] E. Cerami et al., *The cBio Cancer Genomics Portal: An Open Platform for Exploring Multidimensional Cancer Genomics Data*, Cancer Discovery, vol. 2, no. 5. American Association for Cancer Research (AACR), pp. 401–404, May 01, **2012**. doi: 10.1158/2159-8290.cd-12-0095.

[13] J. Gao et al., *Integrative Analysis of Complex Cancer Genomics and Clinical Profiles Using the cBioPortal*, Science Signaling, vol. 6, no. 269. American Association for the Advancement of Science (AAAS), Apr. 02, **2013**. doi: 10.1126/scisignal.2004088.

[14] I. de Bruijn et al., *Analysis and Visualization of Longitudinal Genomic and Clinical Data from the AACR Project GENIE Biopharma Collaborative in cBioPortal*, Cancer Research, vol. 83, no. 23. American Association for Cancer Research (AACR), pp. 3861–3867, Sep. 05, **2023**. doi: 10.1158/0008-5472.can-23-0816.

[15] S. A. Hollingsworth and R. O. Dror, *Molecular Dynamics Simulation for All*, Neuron, vol. 99, no. 6. Elsevier BV, pp. 1129–1143, Sep. **2018**. doi: 10.1016/j.neuron.2018.08.011.

[16] S. Sinha, B. Tam, and S. M. Wang, *Applications of Molecular Dynamics Simulation in Protein Study*, Membranes, vol. 12, no. 9. MDPI AG, p. 844, Aug. 29, **2022**. doi: 10.3390/membranes12090844.

[17] N. Metropolis and S. Ulam, *The Monte Carlo Method*, Journal of the American Statistical Association, vol. 44, no. 247. Informa UK Limited, pp. 335–341, Sep. **1949**. doi: 10.1080/01621459.1949.10483310.

[18] B. J. Alder and T. E. Wainwright, *Studies in Molecular Dynamics. I. General Method*, The Journal of Chemical Physics, vol. 31, no. 2. AIP Publishing, pp. 459–466, Aug. 01, **1959**. doi: 10.1063/1.1730376.

[19] A. Rahman and F. H. Stillinger, *Molecular Dynamics Study of Liquid Water*, The Journal of Chemical Physics, vol. 55, no. 7. AIP Publishing, pp. 3336–3359, Oct. 01, **1971**. doi: 10.1063/1.1676585.

[20] A. Warshel and M. Levitt, *Theoretical studies of enzymic reactions: Dielectric, electrostatic and steric stabilization of the carbonium ion in the reaction of lysozyme*, Journal of Molecular Biology, vol. 103, no. 2. Elsevier BV, pp. 227–249, May **1976**. doi: 10.1016/0022-2836(76)90311-9.

[21] J. A. McCammon, B. R. Gelin, and M. Karplus, *Dynamics of folded proteins*, Nature, vol. 267, no. 5612. Springer Science and Business Media LLC, pp. 585–590, Jun. **1977**. doi: 10.1038/267585a0.

[22] R. Car and M. Parrinello, *Unified Approach for Molecular Dynamics and Density-Functional Theory*, Physical Review Letters, vol. 55, no. 22. American Physical Society (APS), pp. 2471–2474, Nov. 25, **1985**. doi: 10.1103/physrevlett.55.2471.

[23] J. Meller, *Molecular Dynamics*, Encyclopedia of Life Sciences. Wiley, Apr. 19, **2001**. doi: 10.1038/npg.els.0003048.

[24] M. A. González, *Force fields and molecular dynamics simulations*, École thématique de la Société Française de la Neutronique, vol. 12. EDP Sciences, pp. 169–200, **2011**. doi: 10.1051/sfn/201112009.

[25] M. Christen et al., *The GROMOS software for biomolecular simulation: GROMOS05*, Journal of Computational Chemistry, vol. 26, no. 16. Wiley, pp. 1719–1751, Oct. 06, **2005**. doi: 10.1002/jcc.20303.

[26] X. Daura, A. E. Mark, and W. F. Van Gunsteren, *Parametrization of aliphatic CHn united atoms of GROMOS96 force field*, Journal of Computational Chemistry, vol. 19, no. 5. Wiley, pp. 535–547, Apr. 15, **1998**. doi: 10.1002/(sici)1096-987x(19980415)19:5<535::aid-jcc6>3.0.co;2-n.

[27] S. Riniker et al., *Calculation of Relative Free Energies for Ligand-Protein Binding, Solvation, and Conformational Transitions Using the GROMOS Software*, The Journal of Physical Chemistry B, vol. 115, no. 46. American Chemical Society (ACS), pp. 13570–13577, Nov. 01, **2011**. doi: 10.1021/jp204303a.

[28] C. D. Christ, A. E. Mark, and W. F. van Gunsteren, *Basic ingredients of free energy calculations: A review*, Journal of Computational Chemistry, vol. 31, no. 8. Wiley, pp. 1569–1582, Dec. 23, **2009**. doi: 10.1002/jcc.21450.

[29] M. Reinhardt and H. Grubmüller, *Small-sample limit of the Bennett acceptance ratio method and the variationally derived intermediates*, Physical Review E, vol. 104, no. 5. American Physical Society (APS), Nov. 24, **2021**. doi: 10.1103/physreve.104.054133.

[30] C. H. Bennett, *Efficient estimation of free energy differences from Monte Carlo data*, Journal of Computational Physics, vol. 22, no. 2. Elsevier BV, pp. 245–268, Oct. **1976**. doi: 10.1016/0021-9991(76)90078-4.

[31] Lindahl, , Abraham, Hess, and V. D. Spoel, *GROMACS 2021 Manual*, Jan. **2021**, doi: 10.5281/ZENODO.4457591.

[32] J. Boettcher and D. Kessler, *CRYSTAL STRUCTURE OF KRAS-G12C IN COMPLEX WITH COMPOUND 12*. Worldwide Protein Data Bank, Nov. 09, **2022**. doi: 10.2210/pdb8afc/pdb.

[33] Schrödinger, LLC, *The PyMOL Molecular Graphics Development Component*, Version 1.8, Aug. 19, **2010**.

[34] A. de Ruiter, D. Petrov, and C. Oostenbrink, *Optimization of Alchemical Pathways Using Extended Thermodynamic Integration*, Journal of Chemical Theory and Computation, vol. 17, no. 1. American Chemical Society (ACS), pp. 56–65, Dec. 22, **2020**. doi: 10.1021/acs.jctc.0c01170.

[35] D. Petrov, *Perturbation Free-Energy Toolkit: An Automated Alchemical Topology Builder*, Journal of Chemical Information and Modeling, vol. 61, no. 9. American Chemical Society (ACS), pp. 4382–4390, Aug. 20, **2021**. doi: 10.1021/acs.jcim.1c00428.

[36] M. M. H. Graf, M. Maurer, and C. Oostenbrink, *Free-energy calculations of residue mutations in a tripeptide using various methods to overcome inefficient sampling*, Journal of Computational Chemistry, vol. 37, no. 29. Wiley, pp. 2597–2605, Sep. 16, **2016**. doi: 10.1002/jcc.24488.

A Appendix: Frequency of K-Ras mutations in human cancers with fatalities - full data

Table 12: *Frequency of K-Ras mutations in human cancers, full table. Data were compiled from cBioPortal database for cancer genomics, TCGA PanCancer Atlas Studies (as of August 2nd 2024) [12, 13, 14].*

	Bladder c.	Breast c.	Cervical c.	Cholangiocarcinoma	Colorectal c.	Endometrial c.	Esophagogastric c.	Glioblastoma	Glioma	Head and neck c.	Hepatobiliary c.	Leukemia	Mature B-cell neoplasms	Melanoma	Non-small cell lung c.	Ovarian epithelial tumor	Pancreatic c.	Pleural mesothelioma	Prostate c.	Renal clear cell carcinoma	Renal non-clear cell carcinoma	Sarcoma	Sminoma	Thymic epithelial tumor	Thyroid cancer
E3K	-	-	-	-	-	-	-	-	-	-	-	-	-	-	1	-	-	-	-	-	-	-	-	-	-
K5E	-	-	-	-	-	-	-	-	1	-	-	-	-	-	-	-	-	-	-	-	-	-	-	-	-
G10dup	-	-	-	-	-	1	-	-	-	-	-	-	-	-	-	-	-	-	-	-	-	-	-	-	-
A11_G12dup	-	-	-	-	1	-	-	-	-	-	-	-	-	-	-	-	-	-	-	-	-	-	-	-	-
G12A	-	-	-	-	10	9	-	-	1	-	-	-	-	-	18	-	1	-	-	-	-	-	1	-	-
G12C	2	1	2	-	15	7	2	-	-	-	1	-	-	1	70	-	1	1	-	1	-	-	-	-	-
G12D	6	1	4	-	58	34	12	2	-	-	2	2	-	2	20	-	49	-	1	-	3	-	-	1	-
G12R	1	-	-	1	2	-	-	-	-	-	-	-	-	1	-	1	25	-	1	-	-	-	2	-	-
G12S	-	-	-	-	8	3	4	-	-	-	-	-	-	-	5	-	1	-	-	-	-	-	1	-	-
G12V	2	-	2	-	49	22	3	-	-	-	-	2	-	-	41	4	33	-	-	-	2	-	3	-	1
G13C	-	-	-	-	2	3	-	-	-	-	-	-	-	-	8	-	1	-	-	-	-	1	-	-	-
G13D	1	-	4	-	37	11	11	-	-	-	1	2	-	1	3	-	-	-	-	-	-	-	-	-	-
G13V	-	-	-	-	-	1	-	-	-	-	-	-	-	-	-	-	-	-	-	-	-	-	-	-	-
V14I	-	-	-	-	-	-	-	-	-	-	-	-	-	-	1	-	-	-	-	-	-	-	-	-	-
S17T	-	-	-	-	-	-	-	-	1	-	-	-	-	-	-	-	-	-	-	-	-	-	-	-	-
L19F	2	-	-	-	1	-	-	-	-	-	-	-	1	-	3	-	-	-	-	-	-	-	-	-	-
I21R	-	-	1	-	-	-	-	-	-	-	-	-	-	-	-	-	-	-	-	-	-	-	-	-	-
Q22K	-	-	-	-	1	-	-	-	-	-	-	-	1	-	-	-	-	-	-	-	-	-	-	-	-
I24N	-	-	-	-	-	1	-	-	-	-	-	-	-	-	-	-	-	-	-	-	-	-	-	-	-
D33E	-	-	-	-	-	-	-	-	-	-	-	-	-	-	1	-	-	-	-	-	-	-	-	-	-
P34L	-	-	-	-	1	-	-	-	-	-	-	-	-	-	-	-	-	-	-	-	-	-	-	-	-
I36M	-	-	-	-	-	-	-	-	-	-	-	1	-	-	-	-	-	-	-	-	-	-	-	-	-
D38Y	-	-	-	-	-	-	-	-	-	-	-	-	-	1	-	-	-	-	-	-	-	-	-	-	-
T58K	-	-	-	-	-	1	-	-	-	-	-	-	-	-	-	-	-	-	-	-	-	-	-	-	-
A59E	-	-	-	-	-	-	-	-	-	-	-	-	1	-	-	-	-	-	-	-	-	-	-	-	-
A59G	-	-	-	-	-	1	-	-	-	-	-	-	-	-	-	-	-	-	-	1	-	-	-	-	-
A59T	-	-	-	-	1	-	3	-	-	-	-	-	-	-	-	-	-	-	-	-	-	-	-	-	-
Q61E	-	-	-	-	1	-	-	-	-	-	-	-	-	-	-	-	-	-	-	-	-	-	-	-	-
Q61H	1	-	-	-	4	4	2	-	-	-	-	1	-	-	2	-	6	-	-	-	-	1	-	-	-
Q61K	-	-	-	1	3	-	-	-	-	-	-	-	-	1	-	-	-	-	-	-	-	-	-	-	2
Q61L	-	-	-	-	1	1	-	-	-	-	-	-	-	1	3	1	-	-	-	-	-	-	2	-	-
Q61P	-	-	-	-	1	-	-	-	-	-	-	-	-	-	-	-	-	-	-	-	-	-	-	-	-
Q61R	-	-	-	-	2	-	-	-	-	-	-	-	-	1	-	-	2	-	-	-	-	-	1	-	1
E62K	-	-	-	-	-	-	-	-	-	-	-	-	-	1	-	-	-	-	-	-	-	-	-	-	-
E63K	-	-	-	-	-	-	-	-	-	-	-	-	-	-	-	-	-	-	-	-	-	-	1	-	-
R68M	-	-	-	-	-	-	-	-	-	1	-	-	-	-	-	-	-	-	-	-	-	-	-	-	-
R68S	-	-	-	-	1	-	-	-	-	-	-	-	-	-	-	-	-	-	-	-	-	-	-	-	-
Y71C	-	-	-	-	1	-	-	-	-	-	-	-	-	-	-	-	-	-	-	-	-	-	-	-	-
K88*	-	-	-	-	-	-	-	-	-	-	-	-	-	-	1	-	-	-	-	-	-	-	-	-	-
D92Y	-	1	-	-	-	-	-	-	-	-	-	-	-	-	-	-	-	-	-	-	-	-	-	-	-
E98*	-	-	-	-	1	-	-	-	-	-	-	-	-	-	-	-	-	-	-	-	-	-	-	-	-
P110S	-	-	-	-	-	1	-	-	-	-	-	-	-	-	-	-	-	-	-	-	-	-	-	-	-
K117N	-	-	-	-	4	-	-	-	-	-	-	-	-	1	-	-	-	-	-	-	-	-	-	-	-
R123*	-	-	-	-	-	-	-	-	-	-	-	-	-	-	1	-	-	-	-	-	-	-	-	-	-
A130V	-	-	-	-	-	1	-	-	-	-	-	-	-	-	-	-	-	-	-	-	-	-	-	-	-
R135T	-	-	-	-	-	-	1	-	-	-	-	-	-	-	-	-	-	-	-	-	-	-	-	-	-
A146P	-	-	-	-	-	-	-	-	-	-	-	-	-	-	1	-	-	-	-	-	-	-	-	-	-
A146T	-	-	2	-	16	1	3	-	-	-	-	1	-	-	-	-	-	-	-	-	-	-	-	-	-
A146V	-	-	-	-	1	1	-	-	-	-	-	-	-	-	-	-	-	-	-	-	-	-	1	-	-
R151T	-	-	-	-	-	-	1	-	-	-	-	-	-	-	-	-	-	-	-	-	-	-	-	-	-
A155D	-	-	-	-	1	-	-	-	-	-	-	-	-	-	-	-	-	-	-	-	-	-	-	-	-
T158A	-	-	-	-	-	-	-	-	-	1	-	-	-	-	-	-	-	-	-	-	-	-	-	-	-
R164Q	-	-	-	-	-	2	-	-	-	-	-	-	-	-	-	-	-	-	-	-	-	-	-	-	-
I171Nfs*14	-	-	-	-	-	1	-	-	-	-	-	-	-	-	-	-	-	-	-	-	-	-	-	-	-
K176Q	-	-	-	-	-	1	-	-	-	-	-	-	-	-	-	-	-	-	-	-	-	-	-	-	-
?	-	-	-	-	-	1	-	-	-	-	-	-	-	-	-	-	-	-	-	-	-	-	-	-	-

Table 13: *Frequency of K-Ras mutation fatalities in human cancers, full table. Data were compiled from cBioPortal database for cancer genomics, TCGA PanCancer Atlas Studies (as of August 2nd 2024) [12, 13, 14].*

	Bladder c.	Breast c.	Cervical c.	Cholangiocarcinoma	Colorectal c.	Endometrial c.	Esophagogastric c.	Glioblastoma	Glioma	Head and neck c.	Hepatobiliary c.	Leukemia	Mature B-cell neoplasms	Melanoma	Non-small cell lung c.	Ovarian epithelial tumor	Pancreatic c.	Pleural mesothelioma	Prostate c.	Renal clear cell carcinoma	Renal non-clear cell carcinoma	Sarcoma	Sminoma	Thymic epithelial tumor	Thyroid cancer
E3K	-	-	-	-	-	-	-	-	-	-	-	-	-	-	1	-	-	-	-	-	-	-	-	-	-
K5E	-	-	-	-	-	-	-	-	-	-	-	-	-	-	-	-	-	-	-	-	-	-	-	-	-
G10dup	-	-	-	-	-	-	-	-	-	-	-	-	-	-	-	-	-	-	-	-	-	-	-	-	-
A11_G12dup	-	-	-	-	-	-	-	-	-	-	-	-	-	-	-	-	-	-	-	-	-	-	-	-	-
G12A	-	-	-	-	3	2	-	-	-	-	-	-	-	-	3	-	1	-	-	-	-	-	-	-	-
G12C	1	-	1	-	3	2	-	-	-	-	1	-	-	1	15	-	-	1	-	1	-	-	-	-	-
G12D	4	-	1	-	9	2	-	1	-	-	-	-	-	2	3	-	25	-	-	-	-	-	-	-	-
G12R	1	-	-	-	1	-	-	-	-	-	-	-	-	-	-	1	9	-	-	-	-	-	-	-	-
G12S	-	-	-	-	1	-	1	-	-	-	-	-	-	-	-	-	-	-	-	-	-	-	-	-	-
G12V	-	-	1	-	5	1	1	-	-	-	-	-	-	-	8	2	17	-	-	-	-	-	1	-	-
G13C	-	-	-	-	-	-	-	-	-	-	-	-	-	-	3	-	1	-	-	-	-	-	-	-	-
G13D	-	-	3	-	4	-	-	-	-	-	1	-	-	-	1	-	-	-	-	-	-	-	-	-	-
G13V	-	-	-	-	-	-	-	-	-	-	-	-	-	-	-	-	-	-	-	-	-	-	-	-	-
V14I	-	-	-	-	-	-	-	-	-	-	-	-	-	-	-	-	-	-	-	-	-	-	-	-	-
S17T	-	-	-	-	-	-	-	-	-	-	-	-	-	-	-	-	-	-	-	-	-	-	-	-	-
L19F	-	-	-	-	-	-	-	-	-	-	-	-	-	-	-	-	-	-	-	-	-	-	-	-	-
I21R	-	-	1	-	-	-	-	-	-	-	-	-	-	-	-	-	-	-	-	-	-	-	-	-	-
Q22K	-	-	-	-	1	-	-	-	-	-	-	-	-	-	-	-	-	-	-	-	-	-	-	-	-
I24N	-	-	-	-	-	-	-	-	-	-	-	-	-	-	-	-	-	-	-	-	-	-	-	-	-
D33E	-	-	-	-	-	-	-	-	-	-	-	-	-	-	-	-	-	-	-	-	-	-	-	-	-
P34L	-	-	-	-	-	-	-	-	-	-	-	-	-	-	-	-	-	-	-	-	-	-	-	-	-
I36M	-	-	-	-	-	-	-	-	-	-	-	-	-	-	-	-	-	-	-	-	-	-	-	-	-
D38Y	-	-	-	-	-	-	-	-	-	-	-	-	-	-	-	-	-	-	-	-	-	-	-	-	-
T58K	-	-	-	-	-	-	-	-	-	-	-	-	-	-	-	-	-	-	-	-	-	-	-	-	-
A59E	-	-	-	-	-	-	-	-	-	-	-	-	-	-	-	-	-	-	-	-	-	-	-	-	-
A59G	-	-	-	-	-	-	-	-	-	-	-	-	-	-	-	-	-	-	-	-	-	-	-	-	-
A59T	-	-	-	-	-	-	2	-	-	-	-	-	-	-	-	-	-	-	-	-	-	-	-	-	-
Q61E	-	-	-	-	-	-	-	-	-	-	-	-	-	-	-	-	-	-	-	-	-	-	-	-	-
Q61H	1	-	-	-	-	-	-	-	-	-	-	-	-	-	-	-	3	-	-	-	-	1	-	-	-
Q61K	-	-	-	1	-	-	-	-	-	-	-	-	-	-	-	-	-	-	-	-	-	-	-	-	-
Q61L	-	-	-	-	-	-	-	-	-	-	-	-	-	1	1	-	-	-	-	-	-	-	-	-	-
Q61P	-	-	-	-	-	-	-	-	-	-	-	-	-	-	-	-	-	-	-	-	-	-	-	-	-
Q61R	-	-	-	-	-	-	-	-	-	-	-	-	-	1	-	-	2	-	-	-	-	-	-	-	-
E62K	-	-	-	-	-	-	-	-	-	-	-	-	-	1	-	-	-	-	-	-	-	-	-	-	-
E63K	-	-	-	-	-	-	-	-	-	-	-	-	-	-	-	-	-	-	-	-	-	-	-	-	-
R68M	-	-	-	-	-	-	-	-	-	-	-	-	-	-	-	-	-	-	-	-	-	-	-	-	-
R68S	-	-	-	-	-	-	-	-	-	-	-	-	-	-	-	-	-	-	-	-	-	-	-	-	-
Y71C	-	-	-	-	-	-	-	-	-	-	-	-	-	-	-	-	-	-	-	-	-	-	-	-	-
K88*	-	-	-	-	-	-	-	-	-	-	-	-	-	-	-	-	-	-	-	-	-	-	-	-	-
D92Y	-	-	-	-	-	-	-	-	-	-	-	-	-	-	-	-	-	-	-	-	-	-	-	-	-
E98*	-	-	-	-	-	-	-	-	-	-	-	-	-	-	-	-	-	-	-	-	-	-	-	-	-
P110S	-	-	-	-	-	-	-	-	-	-	-	-	-	-	-	-	-	-	-	-	-	-	-	-	-
K117N	-	-	-	-	2	-	-	-	-	-	-	-	-	1	-	-	-	-	-	-	-	-	-	-	-
R123*	-	-	-	-	-	-	-	-	-	-	-	-	-	-	-	-	-	-	-	-	-	-	-	-	-
A130V	-	-	-	-	-	-	-	-	-	-	-	-	-	-	-	-	-	-	-	-	-	-	-	-	-
R135T	-	-	-	-	-	-	1	-	-	-	-	-	-	-	-	-	-	-	-	-	-	-	-	-	-
A146P	-	-	-	-	-	-	-	-	-	-	-	-	-	-	-	-	-	-	-	-	-	-	-	-	-
A146T	-	-	-	-	2	-	-	-	-	-	-	-	-	-	-	-	-	-	-	-	-	-	-	-	-
A146V	-	-	-	-	-	-	-	-	-	-	-	-	-	-	-	-	-	-	-	-	-	-	-	-	-
R151T	-	-	-	-	-	-	-	-	-	-	-	-	-	-	-	-	-	-	-	-	-	-	-	-	-
A155D	-	-	-	-	-	-	-	-	-	-	-	-	-	-	-	-	-	-	-	-	-	-	-	-	-
T158A	-	-	-	-	-	-	-	-	-	-	-	-	-	-	-	-	-	-	-	-	-	-	-	-	-
R164Q	-	-	-	-	-	-	-	-	-	-	-	-	-	-	-	-	-	-	-	-	-	-	-	-	-
I171Nfs*14	-	-	-	-	-	-	-	-	-	-	-	-	-	-	-	-	-	-	-	-	-	-	-	-	-
K176Q	-	-	-	-	-	-	-	-	-	-	-	-	-	-	-	-	-	-	-	-	-	-	-	-	-
?	-	-	-	-	-	-	-	-	-	-	-	-	-	-	-	-	-	-	-	-	-	-	-	-	-

Table 14: *Ratio of K-Ras mutation fatalities to comorbidities in human cancers, full table. Data were compiled from cBioPortal database for cancer genomics, TCGA PanCancer Atlas Studies (as of August 2nd 2024) [12, 13, 14].*

	Bladder c.	Breast c.	Cervical c.	Cholangiocarcinoma	Colorectal c.	Endometrial c.	Esophagogastric c.	Glioblastoma	Glioma	Head and neck c.	Hepatobiliary c.	Leukemia	Mature B-cell neoplasms	Melanoma	Non-small cell lung c.	Ovarian epithelial tumor	Pancreatic c.	Pleural mesothelioma	Prostate c.	Renal clear cell carcinoma	Renal non-clear cell carcinoma	Sarcoma	Sminoma	Thymic epithelial tumor	Thyroid cancer
E3K	-	-	-	-	-	-	-	-	-	-	-	-	-	-	1	-	-	-	-	-	-	-	-	-	-
K5E	-	-	-	-	-	-	-	-	1	-	-	-	-	-	-	-	-	-	-	-	-	-	-	-	-
G10dup	-	-	-	-	-	0	-	-	-	-	-	-	-	-	-	-	-	-	-	-	-	-	-	-	-
A11_G12dup	-	-	-	-	0	-	-	-	-	-	-	-	-	-	-	-	-	-	-	-	-	-	-	-	-
G12A	-	-	-	-	.3	.22	-	-	0	-	-	-	-	-	.17	-	1	-	-	-	-	-	0	-	-
G12C	.5	0	.5	-	.2	.29	0	-	-	-	0	-	-	1	.21	-	0	1	-	1	-	-	-	-	-
G12D	.67	0	.25	-	.16	.06	0	.5	-	-	0	0	-	1	.15	-	.51	-	0	-	0	-	-	0	-
G12R	1	-	-	0	.5	-	-	-	-	-	-	-	-	0	-	1	.36	-	0	-	-	-	0	-	-
G12S	-	-	-	-	.13	0	.25	-	-	-	-	-	-	-	0	-	0	-	-	-	-	-	0	-	-
G12V	0	-	.5	-	.1	.05	.33	-	-	-	-	0	-	-	.2	.5	.52	-	-	-	0	-	.33	-	0
G13C	-	-	-	-	0	0	-	-	-	-	-	-	-	-	.38	-	1	-	-	-	-	0	-	-	-
G13D	0	-	.75	-	.11	0	0	-	-	-	1	0	-	0	.33	-	-	-	-	-	-	-	-	-	-
G13V	-	-	-	-	-	0	-	-	-	-	-	-	-	-	-	-	-	-	-	-	-	-	-	-	-
V14I	-	-	-	-	-	-	-	-	-	-	-	-	-	-	0	-	-	-	-	-	-	-	-	-	-
S17T	-	-	-	-	-	-	-	-	0	-	-	-	-	-	-	-	-	-	-	-	-	-	-	-	-
L19F	0	-	-	-	0	-	-	-	-	-	-	-	0	-	0	-	-	-	-	-	-	-	-	-	-
I21R	-	-	1	-	-	-	-	-	-	-	-	-	-	-	-	-	-	-	-	-	-	-	-	-	-
Q22K	-	-	-	-	1	-	-	-	-	-	-	-	0	-	-	-	-	-	-	-	-	-	-	-	-
I24N	-	-	-	-	-	0	-	-	-	-	-	-	-	-	-	-	-	-	-	-	-	-	-	-	-
D33E	-	-	-	-	-	-	-	-	-	-	-	-	-	-	0	-	-	-	-	-	-	-	-	-	-
P34L	-	-	-	-	0	-	-	-	-	-	-	-	-	-	-	-	-	-	-	-	-	-	-	-	-
I36M	-	-	-	-	-	-	-	-	-	-	-	0	-	-	-	-	-	-	-	-	-	-	-	-	-
D38Y	-	-	-	-	-	-	-	-	-	-	-	-	-	0	-	-	-	-	-	-	-	-	-	-	-
T58K	-	-	-	-	-	0	-	-	-	-	-	-	0	-	-	-	-	-	-	-	-	-	-	-	-
A59E	-	-	-	-	-	-	-	-	-	-	-	-	0	-	-	-	-	-	-	-	-	-	-	-	-
A59G	-	-	-	-	-	0	-	-	-	-	-	-	-	-	-	-	-	-	-	0	-	-	-	-	-
A59T	-	-	-	-	0	-	.67	-	-	-	-	-	-	-	-	-	-	-	-	-	-	-	-	-	-
Q61E	-	-	-	-	0	-	-	-	-	-	-	-	-	-	-	-	-	-	-	-	-	-	-	-	-
Q61H	1	-	-	-	0	0	0	-	-	-	-	0	-	-	0	-	.5	-	-	-	-	1	-	-	-
Q61K	-	-	-	0	.33	-	-	-	-	-	-	-	-	0	-	-	-	-	-	-	-	-	-	-	0
Q61L	-	-	-	-	0	0	-	-	-	-	-	-	-	1	.33	0	-	-	-	-	-	-	0	-	-
Q61P	-	-	-	-	0	-	-	-	-	-	-	-	-	-	-	-	-	-	-	-	-	-	-	-	-
Q61R	-	-	-	-	0	-	-	-	-	-	-	-	-	1	-	-	1	-	-	-	-	-	0	-	0
E62K	-	-	-	-	-	-	-	-	-	-	-	-	-	1	-	-	-	-	-	-	-	-	-	-	-
E63K	-	-	-	-	-	-	-	-	-	-	-	-	-	-	-	-	-	-	-	-	-	-	0	-	-
R68M	-	-	-	-	-	-	-	-	-	0	-	-	-	-	-	-	-	-	-	-	-	-	-	-	-
R68S	-	-	-	-	0	-	-	-	-	-	-	-	-	-	-	-	-	-	-	-	-	-	-	-	-
Y71C	-	-	-	-	0	-	-	-	-	-	-	-	-	-	-	-	-	-	-	-	-	-	-	-	-
K88*	-	-	-	-	-	-	-	-	-	-	-	-	-	-	0	-	-	-	-	-	-	-	-	-	-
D92Y	-	0	-	-	-	-	-	-	-	-	-	-	-	-	-	-	-	-	-	-	-	-	-	-	-
E98*	-	-	-	-	0	-	-	-	-	-	-	-	-	-	-	-	-	-	-	-	-	-	-	-	-
P110S	-	-	-	-	-	0	-	-	-	-	-	-	-	-	-	-	-	-	-	-	-	-	-	-	-
K117N	-	-	-	-	.5	-	-	-	-	-	-	-	-	1	-	-	-	-	-	-	-	-	-	-	-
R123*	-	-	-	-	-	-	-	-	-	-	-	-	-	-	0	-	-	-	-	-	-	-	-	-	-
A130V	-	-	-	-	-	0	-	-	-	-	-	-	-	-	-	-	-	-	-	-	-	-	-	-	-
R135T	-	-	-	-	-	-	1	-	-	-	-	-	-	-	-	-	-	-	-	-	-	-	-	-	-
A146P	-	-	-	-	-	-	-	-	-	-	-	-	-	-	0	-	-	-	-	-	-	-	-	-	-
A146T	-	-	0	-	.13	0	0	-	-	-	-	0	-	-	-	-	-	-	-	-	-	-	-	-	-
A146V	-	-	-	-	0	0	-	-	-	-	-	-	-	-	-	-	-	-	-	-	-	-	0	-	-
R151T	-	-	-	-	-	-	0	-	-	-	-	-	-	-	-	-	-	-	-	-	-	-	-	-	-
A155D	-	-	-	-	0	-	-	-	-	-	-	-	-	-	-	-	-	-	-	-	-	-	-	-	-
T158A	-	-	-	-	-	-	-	-	-	0	-	-	-	-	-	-	-	-	-	-	-	-	-	-	-
R164Q	-	-	-	-	-	0	-	-	-	-	-	-	-	-	-	-	-	-	-	-	-	-	-	-	-
I171Nfs*14	-	-	-	-	-	0	-	-	-	-	-	-	-	-	-	-	-	-	-	-	-	-	-	-	-
K176Q	-	-	-	-	-	0	-	-	-	-	-	-	-	-	-	-	-	-	-	-	-	-	-	-	-
?	-	-	-	-	-	0	-	-	-	-	-	-	-	-	-	-	-	-	-	-	-	-	-	-	-

B Appendix: Free energy calculations file preparation code

```
import os
import shutil
import numpy as np
import SMArt
from SMArt.md import pipeline
from SMArt.md.data_st import MD_Parameters

SMArt.incl.set_print_warnings(False)

run_file_EQ_template = '''#!/bin/sh
#SBATCH --ntasks=1
#SBATCH --cpus-per-task=4
#SBATCH --gres=mps:33
#SBATCH --mem=4096
#SBATCH --partition NGN
#SBATCH --time=24:00:00

NAME='whoami'
PROGRAM={md_path}

export LD_LIBRARY_PATH=$LD_LIBRARY_PATH:/usr/lib:/usr/local/cuda/lib64:\
/usr/local/cuda/lib:/usr/lib/nvidia-current:\
/home/oostenbrink/programs/mmslogin/cukernellib_8

SYS_NAME={sys_name}
LAM_NAME={lam_name}
PREV_LAM={prev_lam}
NEXT_LAM={next_lam}
LAM_SYS_NAME=${{SYS_NAME}}_${{LAM_NAME}}_EQ
PREV_SYS_NAME=${{SYS_NAME}}_${{PREV_LAM}}_EQ

OLD={old}
FIRST={first}
LAST={last}
CNF_FILE={cnf_file}
OLD_CYCLE={old_cycle}

DIR={work_dir}
SIMULDIR=${{DIR}}${{LAM_NAME}}
PREV_DIR=${{DIR}}${{PREV_LAM}}
NEXT_DIR=${{DIR}}${{NEXT_LAM}}
if `test ${{OLD_CYCLE}} -eq 0`; then
        LAST_CONF=${{DIR}}/../${{SYS_NAME}}/${{LAM_NAME}}/${{SYS_NAME}}\
 _${{LAM_NAME}}.cnf
else
```

```
        LAST_CONF=${{DIR}}/../${{SYS_NAME}}_${{OLD_CYCLE}}_post_analysis/\
 ${{LAM_NAME}}/${{SYS_NAME}}_${{LAM_NAME}}.cnf
fi

#if there are no old eqs and tis performed for this lambda point do eq,
 ↪  else use last ti
if `test ${{OLD}} -eq 0`; then
    #create temporary directory;
    WORKDIR=/scratch/${{SLURM_JOBID}};
    mkdir -p ${{WORKDIR}};
    cd       ${{WORKDIR}};

    #input;
    TOPO={topo};
    PTTOPO={ptop};
    #if this is the first one, use original cnf (changed for later cycles)
    if `test ${{OLD_CYCLE}} -eq -1`; then
        if `test ${{FIRST}} -eq 1`; then
            INPUTCRD=${{CNF_FILE}};
        else
            INPUTCRD=${{PREV_DIR}}/${{PREV_SYS_NAME}}.cnf;
        fi
    else
        INPUTCRD=${{LAST_CONF}};
    fi
    IUNIT=${{SIMULDIR}}/EQ_ext_TI_${{LAM_NAME}}.imd;

    #output;
    OUTPUTCRD=${{LAM_SYS_NAME}}.cnf;
    OUTPUTTRX=${{LAM_SYS_NAME}}.trc;
    OUTPUTTRE=${{LAM_SYS_NAME}}.tre;
    OUTPUTTRG=${{LAM_SYS_NAME}}.trg;
    OUNIT=${{LAM_SYS_NAME}}.omd;

    export OMP_NUM_THREADS=${{SLURM_CPUS_PER_TASK}};

    MDOK=1;

    ${{PROGRAM}} \
        @topo   ${{TOPO}} \
        @conf   ${{INPUTCRD}} \
        @input  ${{IUNIT}} \
        @pttopo ${{PTTOPO}} \
        @fin    ${{OUTPUTCRD}} \
        @trc    ${{OUTPUTTRX}} \
        @tre    ${{OUTPUTTRE}} \
        @trg    ${{OUTPUTTRG}} \
```

```
92          >       ${{OUNIT}};
93      grep "finished successfully" ${{OUNIT}} > /dev/null || MDOK=0;
94
95      uname -a >> ${{OUNIT}};
96
97      #compress some files;
98      gzip ${{OUTPUTTRX}};
99      gzip ${{OUTPUTTRE}};
100     gzip ${{OUTPUTTRG}};
101
102     #copy files back;
103     OK=1;
104     cp ${{OUNIT}}           ${{SIMULDIR}} || OK=0;
105     cp ${{OUTPUTCRD}}       ${{SIMULDIR}} || OK=0;
106     cp ${{OUTPUTTRX}}.gz    ${{SIMULDIR}} || OK=0;
107     cp ${{OUTPUTTRE}}.gz    ${{SIMULDIR}} || OK=0;
108     cp ${{OUTPUTTRG}}.gz    ${{SIMULDIR}} || OK=0;
109
110     #clean up after successful run;
111     if `test ${{OK}} -eq 0`; then
112         uname -a > mess;
113         echo 'cp failed for EDSR_lig_bmax2_search, run 1' >> mess;
114         MAIL -s "ERROR" ${{NAME}} < mess:
115         cd ${{SIMULDIR}};
116     else
117         cd ${{SIMULDIR}};
118         rm ${{WORKDIR}}/*;
119         rmdir ${{WORKDIR}};
120     fi
121
122     #stop if MD was not successful
123     if `test ${{MDOK}} -eq 0`; then
124         exit
125     fi
126
127 else
128         cp ${{LAST_CONF}} ${{SIMULDIR}}/${{LAM_SYS_NAME}}.cnf;
129
130 fi
131
132 #perform last command (usually submit next job)
133
134 cd ${{SIMULDIR}}
```

```
sbatch --ntasks ${{SLURM_NTASKS}} --cpus-per-task ${{SLURM_CPUS_PER_TASK}} --gres=mps:$(scontrol show job ${{SLURM_JOB_ID}} | grep gres/mps | sed "s/^.*gres\/mps=//") --mem ${{SLURM_MEM_PER_NODE}} --partition ${{SLURM_JOB_PARTITION}} --time $(scontrol show job ${{SLURM_JOB_ID}} | grep TimeLimit | sed "s/^.*TimeLimit=//" | cut -d" " -f1) run_TI_${{LAM_NAME}}.run

if `test ${{LAST}} -eq 0`; then
    cd ${{NEXT_DIR}}/
    ./run_EQ_${{NEXT_LAM}}.run
fi

'''

run_file_TI_template = '''#!/bin/sh

NAME='whoami'
PROGRAM={md_path}

export LD_LIBRARY_PATH=$LD_LIBRARY_PATH:/usr/lib:/usr/local/cuda/lib64:\
/usr/local/cuda/lib:/usr/lib/nvidia-current:\
/home/oostenbrink/programs/mmslogin/cukernellib_8

SYS_NAME={sys_name}
LAM_NAME={lam_name}
LAM_SYS_NAME=${{SYS_NAME}}_${{LAM_NAME}}

DIR={work_dir}
SIMULDIR=${{DIR}}${{LAM_NAME}}

#create temporary directory
WORKDIR=/scratch/${{SLURM_JOBID}}
mkdir -p ${{WORKDIR}}
cd       ${{WORKDIR}}

#input
TOPO={topo}
INPUTCRD=${{SIMULDIR}}/${{SYS_NAME}}_${{LAM_NAME}}_EQ.cnf;
IUNIT=${{SIMULDIR}}/ext_TI_${{LAM_NAME}}.imd
PTTOPO={ptop}

#output
OUTPUTCRD=${{LAM_SYS_NAME}}.cnf
OUTPUTTRX=${{LAM_SYS_NAME}}.trc
OUTPUTTRE=${{LAM_SYS_NAME}}.tre
OUTPUTTRG=${{LAM_SYS_NAME}}.trg
OUNIT=${{LAM_SYS_NAME}}.omd
```

```
177
178 export OMP_NUM_THREADS=${{SLURM_CPUS_PER_TASK}}
179
180 MDOK=1
181
182 ${{PROGRAM}} \
183     @topo   ${{TOPO}} \
184     @conf   ${{INPUTCRD}} \
185     @input  ${{IUNIT}} \
186     @pttopo ${{PTTOPO}} \
187     @fin    ${{OUTPUTCRD}} \
188     @trc    ${{OUTPUTTRX}} \
189     @tre    ${{OUTPUTTRE}} \
190     @trg    ${{OUTPUTTRG}} \
191     >       ${{OUNIT}}
192 grep "finished successfully" ${{OUNIT}} > /dev/null || MDOK=0
193
194 uname -a >> ${{OUNIT}}
195
196 #compress some files
197 gzip ${{OUTPUTTRX}}
198 gzip ${{OUTPUTTRE}}
199 gzip ${{OUTPUTTRG}}
200
201 #copy files back
202 OK=1
203 cp ${{OUNIT}}           ${{SIMULDIR}} || OK=0
204 cp ${{OUTPUTCRD}}       ${{SIMULDIR}} || OK=0
205 cp ${{OUTPUTTRX}}.gz    ${{SIMULDIR}} || OK=0
206 cp ${{OUTPUTTRE}}.gz    ${{SIMULDIR}} || OK=0
207 cp ${{OUTPUTTRG}}.gz    ${{SIMULDIR}} || OK=0
208
209 #clean up after successful run
210 if `test ${{OK}} -eq 0`; then
211     uname -a > mess;
212     echo 'cp failed for EDSR_lig_bmax2_search, run 1' >> mess;
213     MAIL -s "ERROR" ${{NAME}} < mess:
214     cd ${{SIMULDIR}};
215 else
216     cd ${{SIMULDIR}};
217     rm ${{WORKDIR}}/*;
218     rmdir ${{WORKDIR}};
219 fi
220
221 #stop if MD was not successful
222 if `test ${{MDOK}} -eq 0`; then
223     exit
```

```
224 fi
225
226 '''
227
228 def make_imd_f_EQ(lp, lam_name, lam_work_dir, eq_time, eq_step_dt,
    ↪  traj_print_eq, en_print_eq):
229         imd.change_imd(dict(PERTURBATION={2:lp}))
230         imd.change_imd(dict(STEP={0:int(eq_time*1000/eq_step_dt)}))
231         imd.change_imd(dict(STEP={2:eq_step_dt}))
232         imd.change_imd(dict(PRINTOUT={0:traj_print_eq}))
233         imd.change_imd(dict(WRITETRAJ={0:traj_print_eq}))
234         imd.change_imd(dict(WRITETRAJ={4:en_print_eq}))
235         imd.change_imd(dict(WRITETRAJ={5:en_print_eq}))
236         imd_f_eq=os.path.join(lam_work_dir, 'EQ_ext_TI_'+lam_name+'.imd')
237         imd.write_imd(imd_f_eq)
238         pass
239
240 def make_imd_f_TI(lp, lam_name, lam_work_dir, prod_time, prod_step_dt,
    ↪  traj_print_ti, en_print_ti):
241         imd.change_imd(dict(PERTURBATION={2:lp}))
242         imd.change_imd(dict(STEP={0:int(prod_time*1000/prod_step_dt)}))
243         imd.change_imd(dict(STEP={2:prod_step_dt}))
244         imd.change_imd(dict(PRINTOUT={0:traj_print_ti}))
245         imd.change_imd(dict(WRITETRAJ={0:traj_print_ti}))
246         imd.change_imd(dict(WRITETRAJ={4:en_print_ti}))
247         imd.change_imd(dict(WRITETRAJ={5:en_print_ti}))
248         imd_f=os.path.join(lam_work_dir, 'ext_TI_'+lam_name+'.imd')
249         imd.write_imd(imd_f)
250         pass
251
252 def make_run_f_EQ(lam_name, md_path, sys_name, prev_lam, next_lam, old,
    ↪  first, last, cnf_file, old_cycle, work_dir, topo, ptop):
253         return run_file_EQ_template.format(lam_name = lam_name, md_path =
          ↪  md_path, sys_name = sys_name, prev_lam = prev_lam, next_lam =
          ↪  next_lam, old = old, first = first, last = last, cnf_file =
          ↪  cnf_file, old_cycle = old_cycle, work_dir = work_dir, topo =
          ↪  topo, ptop = ptop)
254
255 def make_run_f_TI(lam_name, md_path, sys_name, old_cycle, work_dir, topo,
    ↪  ptop):
256         return run_file_TI_template.format(lam_name = lam_name, md_path =
          ↪  md_path, sys_name = sys_name, old_cycle = old_cycle, work_dir =
          ↪  work_dir, topo = topo, ptop = ptop)
257
258 def check_for_old(cycle, sim_dir, sys_name, lam_name):
259         i = cycle - 1
260         while i >= 0:
```

```
261                 if (i == 0):
262                         old_dir = os.path.join(sim_dir,
                            ↪  sys_name+'/'+lam_name)
263                 else:
264                         old_dir =
                            ↪  os.path.join(sim_dir,sys_name+'_'+str(i)+'_post_analysis/'+l
265                 if os.path.isdir(old_dir):
266                         return i
267                 else:
268                         i-=1
269         return -1
270
271
272 if __name__ == '__main__':
273         import argparse
274         parser = argparse.ArgumentParser(fromfile_prefix_chars='@')
275         parser.convert_arg_line_to_args = lambda arg_line:arg_line.split()
276
277         #run file arguments
278         parser.add_argument('-c', '--cnf_file', help = 'path to
            ↪  configuration file of the system', type = str, required = True)
279         parser.add_argument('-md', '--md_path', help = 'path to md file
            ↪  version', type = str, required = True)
280         parser.add_argument('-d', '--sim_dir', help = 'simulation
            ↪  directory', type = str, required = True)
281         parser.add_argument('-i', '--imd_template', help = 'path to
            ↪  parameter input file', type = str, required = True)
282         parser.add_argument('-p', '--ptop', help = 'path to perturbation
            ↪  topology file', type = str, required = True)
283         parser.add_argument('-t', '--topo', help = 'path to topology file',
            ↪  type = str, required = True)
284         parser.add_argument('-s', '--sys_name', help = 'system name', type
            ↪  = str, required = True)
285         parser.add_argument('-n', '--sys_num', help = 'number of an
            ↪  additional cycle (0 for initial)', type = int, required = True)
286         #additional arguments
287         parser.add_argument('-eq_time', help='equilibration time in ns',
            ↪  type=float, default=0.2)
288         parser.add_argument('-prod_time', help='production time in ns',
            ↪  type=float, default=2.0)
289         parser.add_argument('-eq_step_dt', help='equilibration step time dt
            ↪  in ns', type=float, default=0.002)
290         parser.add_argument('-prod_step_dt', help='production step time dt
            ↪  in ns', type=float, default=0.002)
291         parser.add_argument('-traj_print_eq', help='equilibration
            ↪  trajectory printout', type=int, default=100000)
```

```
292         parser.add_argument('-en_print_eq', help='equilibration energy
            ↪  printout', type=int, default=100000)
293         parser.add_argument('-traj_print_ti', help='production trajectory
            ↪  printout', type=int, default=50000)
294         parser.add_argument('-en_print_ti', help='production energy
            ↪  printout', type=int, default=500)
295         parser.add_argument('-N_LPs', help='number of lambda points for the
            ↪  first cycle', type=int, default=21)
296
297         args = parser.parse_args()
298
299         cnf_file = args.cnf_file
300         md_path = args.md_path
301         sim_dir = args.sim_dir
302         imd_template = args.imd_template
303         ptop = args.ptop
304         topo = args.topo
305         sys_name = args.sys_name
306         sys_num = args.sys_num
307         eq_time = args.eq_time
308         prod_time = args.prod_time
309         eq_step_dt = args.eq_step_dt
310         prod_step_dt = args.prod_step_dt
311         traj_print_eq = args.traj_print_eq
312         en_print_eq = args.en_print_eq
313         traj_print_ti = args.traj_print_ti
314         en_print_ti = args.en_print_ti
315         N_LPs = args.N_LPs
316
317         imd = MD_Parameters(imd_template)
318
319         work_dir = os.path.join(sim_dir + sys_name + '/')
320         if (sys_num != 0):
321                 work_dir = os.path.join(sim_dir+sys_name + '_' +
                    ↪  str(sys_num) + '_post_analysis/')
322         if not os.path.isdir(work_dir):
323                 os.mkdir(work_dir)
324
325         #setting paths
326         if (sys_num == 0):
327                 new_lambda = 0
328                 new_times = 0
329         if (sys_num == 1):
330                 new_lambda = os.path.join(sim_dir + sys_name +
                    ↪  '/new_lambda.txt')
331                 new_times = os.path.join(sim_dir + sys_name +
                    ↪  '/new_times.txt')
```

```
332         else:
333                 new_lambda = os.path.join(sim_dir + sys_name + '_' +
                    ↪  str(sys_num-1) + '_post_analysis/new_lambda.txt')
334                 new_times = os.path.join(sim_dir + sys_name + '_' +
                    ↪  str(sys_num-1) +
                    ↪  '_post_analysis/new_times.txt')
335
336         #setting variables
337         first=1
338         last=0
339         old=0
340         cycle=0
341         old_cycle=-1
342         prev_lam='0'
343         next_lam='0'
344         LPs=[]
345         time=[]
346
347         #setting lambda points and times depending on the system number
348         if (sys_num == 0):
349                 LPs = SMArt.md.ana.incl.get_lset(np.linspace(0,1,N_LPs))
350         else:
351                 f = open(new_lambda)
352                 for line in f.readlines():
353                         LPs.append(float(line))
354                 f.close()
355                 f = open(new_times)
356                 for line in f.readlines():
357                         time.append(float(line))
358                 f.close()
359
360         #simulating through lambda points
361         for i, lp in enumerate(LPs):
362                 cycle = sys_num
363
364                 #making lambda point directories
365                 lam_name = 'l_{:.3f}'.format(lp)
366                 lam_work_dir = os.path.join(work_dir, lam_name)
367                 if not os.path.isdir(lam_work_dir):
368                         os.mkdir(lam_work_dir)
369                 f_EQ_run = os.path.join(lam_work_dir, 'run_EQ_' + lam_name
                    ↪  + '.run')
370                 f_TI_run = os.path.join(lam_work_dir, 'run_TI_' + lam_name
                    ↪  + '.run')
371
372                 #checking if last lambda
373                 if i == len(LPs)-1:
```

```
374                     last = 1
375             else:
376                     next_lam = 'l_{:.3f}'.format(LPs[i+1])
377
378             old=0 #resets for every lambda, checks if there is same
                ↪  lambda in old cycles
379             old_cycle=check_for_old(cycle, sim_dir, sys_name, lam_name)
380             if old_cycle != -1:
381                     old=1
382
383             if (sys_num != 0):
384                     prod_time = time[i]
385
386             #writing .imd and .run files
387             make_imd_f_EQ(lp, lam_name, lam_work_dir, eq_time,
                ↪  eq_step_dt, traj_print_eq, en_print_eq)
388             make_imd_f_TI(lp, lam_name, lam_work_dir, prod_time,
                ↪  prod_step_dt, traj_print_ti, en_print_ti)
389             f = open(f_EQ_run, 'w')
390             f.write(make_run_f_EQ(lam_name, md_path, sys_name,
                ↪  prev_lam, next_lam, old, first, last, cnf_file,
                ↪  old_cycle, work_dir, topo, ptop))
391             f.close()
392             os.system('chmod a+x '+f_EQ_run)
393             f = open(f_TI_run, 'w')
394             f.write(make_run_f_TI(lam_name, md_path, sys_name,
                ↪  old_cycle, work_dir, topo, ptop))
395             f.close()
396             os.system('chmod a+x '+f_TI_run)
397
398             first = 0
399             prev_lam = lam_name
400
```

C Appendix: H-bond occurrence tables

Res DONO	Res	ACC	Atom	D	A	OCCUR	%
13 GLY -	1	GDP	114	N	O3PA	2	0.32
13 GLY -	1	GDP	114	N	O1PB	1	0.16
13 GLY -	1	GDP	114	N	O3PB	340	54.4
14 VAL -	1	GDP	119	N	O1PB	111	17.76
15 GLY -	1	GDP	127	N	O1PA	5	0.8
15 GLY -	1	GDP	127	N	O3PA	80	12.8
15 GLY -	1	GDP	127	N	O1PB	419	67.04
16 LYSH -	1	GDP	132	N	O3PA	8	1.28
16 LYSH -	1	GDP	132	N	O1PB	612	97.92
16 LYSH -	1	GDP	139	NZ	O1PB	2	0.32
16 LYSH -	1	GDP	139	NZ	O1PB	5	0.8
16 LYSH -	1	GDP	139	NZ	O1PB	4	0.64
16 LYSH -	1	GDP	139	NZ	O3PB	2	0.32
17 SER -	1	GDP	145	N	O1PA	561	89.76
17 SER -	1	GDP	145	N	O3PA	6	0.96
17 SER -	1	GDP	145	N	O2PB	17	2.72
17 SER -	1	GDP	149	OG	O1PA	198	31.68
17 SER -	1	GDP	149	OG	O2PA	417	66.72
18 ALA -	1	GDP	153	N	O1PA	345	55.2
28 PHE -	1	GDP	262	CE1	N7	2	0.32
28 PHE -	1	GDP	264	CE1	O2*	6	0.96
28 PHE -	1	GDP	266	CZ	N3	2	0.32
28 PHE -	1	GDP	266	CZ	O6	1	0.16
28 PHE -	1	GDP	266	CZ	N7	6	0.96
28 PHE -	1	GDP	266	CZ	O2*	8	1.28
31 GLU -	1	GDP	287	N	O2*	1	0.16
32 TYR -	1	GDP	297	N	O2*	16	2.56
32 TYR -	1	GDP	297	N	O3*	8	1.28
32 TYR -	1	GDP	304	CD1	O5*	2	0.32
32 TYR -	1	GDP	304	CD1	O2PA	61	9.76
32 TYR -	1	GDP	308	CE1	O5*	1	0.16
32 TYR -	1	GDP	308	CE1	O1PA	2	0.32
32 TYR -	1	GDP	308	CE1	O2PA	12	1.92
60 GLY -	1	GDP	571	N	O3PB	4	0.64
116 ASN -	1	GDP	1172	ND2	N7	137	21.92
116 ASN -	1	GDP	1172	ND2	O4*	6	0.96
117 LYSH	1	GDP	1177	N	O6	1	0.16
117 LYSH	1	GDP	1184	NZ	O4*	2	0.32
117 LYSH	1	GDP	1184	NZ	N3	1	0.16
117 LYSH	1	GDP	1184	NZ	O4*	3	0.48
117 LYSH	1	GDP	1184	NZ	O4*	2	0.32
146 ALA -	1	GDP	1467	N	O6	118	18.88
146 ALA -	1	GDP	1467	N	N7	1	0.16
147 LYSH	1	GDP	1473	N	O6	467	74.72
147 LYSH	1	GDP	1473	N	N7	7	1.12
147 LYSH	1	GDP	1480	NZ	O2*	1	0.16
147 LYSH	1	GDP	1480	NZ	N3	2	0.32
147 LYSH	1	GDP	1480	NZ	N2	2	0.32
147 LYSH	1	GDP	1480	NZ	O2*	3	0.48
147 LYSH	1	GDP	1480	NZ	N3	1	0.16
147 LYSH	1	GDP	1480	NZ	O2*	1	0.16
148 THR -	1	GDP	1486	N	O6	2	0.32

Res DONO	Res	ACC	Atom	D	A	OCCUR	%
12 CYSH	1	GDP	110	SG	O1PB	2	0.29
13 GLY -	1	GDP	114	N	O1PA	2	0.29
13 GLY -	1	GDP	114	N	O3PA	34	5.01
13 GLY -	1	GDP	114	N	O1PB	56	8.25
13 GLY -	1	GDP	114	N	O3PB	455	67.01
14 VAL -	1	GDP	119	N	O1PA	24	3.53
14 VAL -	1	GDP	119	N	O1PB	84	12.37
15 GLY -	1	GDP	127	N	O5*	35	5.15
15 GLY -	1	GDP	127	N	O1PA	23	3.39
15 GLY -	1	GDP	127	N	O3PA	39	5.74
15 GLY -	1	GDP	127	N	O1PB	412	60.68
16 LYSH -	1	GDP	132	N	O1PA	88	12.96
16 LYSH -	1	GDP	132	N	O2PA	1	0.15
16 LYSH -	1	GDP	132	N	O3PA	8	1.18
16 LYSH -	1	GDP	132	N	O1PB	532	78.35
16 LYSH -	1	GDP	132	N	O2PB	9	1.33
16 LYSH -	1	GDP	139	NZ	O1PB	21	3.09
16 LYSH -	1	GDP	139	NZ	O2PB	1	0.15
16 LYSH -	1	GDP	139	NZ	O1PB	12	1.77
16 LYSH -	1	GDP	139	NZ	O3PB	4	0.59
16 LYSH -	1	GDP	139	NZ	O1PB	25	3.68
16 LYSH -	1	GDP	139	NZ	O2PB	1	0.15
16 LYSH -	1	GDP	139	NZ	O3PB	6	0.88
17 SER -	1	GDP	145	N	O1PA	489	72.02
17 SER -	1	GDP	145	N	O2PA	45	6.63
17 SER -	1	GDP	145	N	O3PA	7	1.03
17 SER -	1	GDP	145	N	O2PB	18	2.65
17 SER -	1	GDP	149	OG	O1PA	158	23.27
17 SER -	1	GDP	149	OG	O2PA	514	75.7
18 ALA -	1	GDP	153	N	O1PA	67	9.87
28 PHE -	1	GDP	262	CE1	O6	2	0.29
28 PHE -	1	GDP	262	CE1	N7	9	1.33
28 PHE -	1	GDP	264	CE1	N7	3	0.44
28 PHE -	1	GDP	264	CE1	O2*	3	0.44
28 PHE -	1	GDP	266	CZ	N3	1	0.15
28 PHE -	1	GDP	266	CZ	N7	1	0.15
28 PHE -	1	GDP	266	CZ	O2*	11	1.62
32 TYR -	1	GDP	297	N	O3*	2	0.29
32 TYR -	1	GDP	304	CD1	O2PA	48	7.07
32 TYR -	1	GDP	308	CE1	O1PA	1	0.15
32 TYR -	1	GDP	308	CE1	O2PA	1	0.15
60 GLY -	1	GDP	571	N	O1PB	13	1.91
60 GLY -	1	GDP	571	N	O3PB	5	0.74
116 ASN -	1	GDP	1172	ND2	N7	29	4.27
117 LYSH	1	GDP	1184	NZ	O4*	2	0.29
117 LYSH	1	GDP	1184	NZ	O4*	5	0.74
117 LYSH	1	GDP	1184	NZ	O3*	1	0.15
117 LYSH	1	GDP	1184	NZ	O4*	3	0.44
146 ALA -	1	GDP	1467	N	O6	116	17.08
147 LYSH	1	GDP	1473	N	O6	519	76.44
147 LYSH	1	GDP	1480	NZ	N3	2	0.29
147 LYSH	1	GDP	1480	NZ	N2	2	0.29
147 LYSH	1	GDP	1480	NZ	O2*	8	1.18
147 LYSH	1	GDP	1480	NZ	N3	1	0.15
147 LYSH	1	GDP	1480	NZ	N2	1	0.15
147 LYSH	1	GDP	1480	NZ	O2*	8	1.18
147 LYSH	1	GDP	1480	NZ	O2*	8	1.18

Res DONO	Res	ACC	Atom	D	A	OCCUR	%
12 CYSH	1	GDP	110	SG	O3PB	2	0.33
13 GLY -	1	GDP	114	N	O3PA	2	0.33
13 GLY -	1	GDP	114	N	O1PB	54	8.84
13 GLY -	1	GDP	114	N	O3PB	244	39.93
14 VAL -	1	GDP	119	N	O3PA	3	0.49
14 VAL -	1	GDP	119	N	O1PB	374	61.21
15 GLY -	1	GDP	127	N	O5*	2	0.33
15 GLY -	1	GDP	127	N	O1PA	2	0.33
15 GLY -	1	GDP	127	N	O3PA	86	14.08
15 GLY -	1	GDP	127	N	O1PB	137	22.42
16 LYSH -	1	GDP	132	N	O3PA	38	6.22
16 LYSH -	1	GDP	132	N	O1PB	192	31.42
16 LYSH -	1	GDP	139	NZ	O1PB	13	2.13
16 LYSH -	1	GDP	139	NZ	O3PB	1	0.16
16 LYSH -	1	GDP	139	NZ	O1PB	8	1.31
16 LYSH -	1	GDP	139	NZ	O1PB	16	2.62
16 LYSH -	1	GDP	139	NZ	O3PB	1	0.16
17 SER -	1	GDP	145	N	O1PA	358	58.59
17 SER -	1	GDP	145	N	O3PA	51	8.35
17 SER -	1	GDP	145	N	O2PB	46	7.53
17 SER -	1	GDP	149	OG	O1PA	13	2.13
17 SER -	1	GDP	149	OG	O2PA	579	94.76
18 ALA -	1	GDP	153	N	O1PA	519	84.94
28 PHE -	1	GDP	262	CE1	N7	2	0.33
28 PHE -	1	GDP	262	CE1	O2*	2	0.33
28 PHE -	1	GDP	264	CE1	N7	6	0.98
28 PHE -	1	GDP	266	CZ	O2*	31	5.07
28 PHE -	1	GDP	297	N	O2*	2	0.33
32 TYR -	1	GDP	304	CD1	O2PA	1	0.16
32 TYR -	1	GDP	571	N	O3PB	1	0.16
116 ASN -	1	GDP	1172	ND2	O6	6	0.98
116 ASN -	1	GDP	1172	ND2	N7	369	60.39
116 ASN -	1	GDP	1172	ND2	O4*	27	4.42
117 LYSH	1	GDP	1177	N	O6	5	0.82
117 LYSH	1	GDP	1184	NZ	O4*	3	0.49
117 LYSH	1	GDP	1184	NZ	N3	2	0.33
117 LYSH	1	GDP	1184	NZ	N2	1	0.16
117 LYSH	1	GDP	1184	NZ	O4*	1	0.16
117 LYSH	1	GDP	1184	NZ	N3	1	0.16
117 LYSH	1	GDP	1184	NZ	O4*	2	0.33
145 SER -	1	GDP	1463	OG	O6	1	0.16
146 ALA -	1	GDP	1467	N	O6	100	16.37
147 LYSH	1	GDP	1473	N	O6	476	77.91
147 LYSH	1	GDP	1473	N	N7	13	2.13
147 LYSH	1	GDP	1480	NZ	N2	3	0.49
147 LYSH	1	GDP	1480	NZ	O2*	1	0.16
147 LYSH	1	GDP	1480	NZ	N3	3	0.49
147 LYSH	1	GDP	1480	NZ	N2	1	0.16
147 LYSH	1	GDP	1480	NZ	O2*	1	0.16
148 THR -	1	GDP	1486	N	O6	8	1.31

Figure 26: *Occurrence of h-bonds in G12C-GDP→WT-GDP perturbation. Colored in yellow is P-loop, in red Switch-I loop, in blue Switch-II loop, and in orange the h-bond between sulfur in cysteine and Pγ/Pβ oxygen. Three colours represent three different replicas, numerated from left to right.*

Res	DONO	Res	ACC	Atom	D	A	OCCUR	%
13	GLY -	1	GDP	114	N	O3PB	113	28.9
14	VAL -	1	GDP	119	N	O1PB	36	9.21
15	GLY -	1	GDP	127	N	O3PA	12	3.07
15	GLY -	1	GDP	127	N	O1PB	303	77.49
16	LYSH -	1	GDP	132	N	O1PB	390	99.74
17	SER -	1	GDP	145	N	O1PA	248	63.43
17	SER -	1	GDP	145	N	O3PA	1	0.26
17	SER -	1	GDP	145	N	O1PB	1	0.26
17	SER -	1	GDP	145	N	O2PB	47	12.02
17	SER -	1	GDP	149	OG	O2PA	150	38.36
17	SER -	1	GDP	149	OG	O3PA	4	1.02
18	ALA -	1	GDP	153	N	O1PA	379	96.93
28	PHE -	1	GDP	262	CE	O3*	1	0.26
28	PHE -	1	GDP	262	CE	O5*	1	0.26
28	PHE -	1	GDP	264	CE2	O2*	2	0.51
28	PHE -	1	GDP	266	CZ	O6	1	0.26
28	PHE -	1	GDP	266	CZ	O3*	5	1.28
28	PHE -	1	GDP	266	CZ	O2PA	5	1.28
31	GLU -	1	GDP	287	N	O2*	4	1.02
32	TYR -	1	GDP	297	N	O3*	90	23.02
32	TYR -	1	GDP	297	N	O2PA	1	0.26
32	TYR -	1	GDP	304	CD2	O5*	2	0.51
32	TYR -	1	GDP	304	CD2	O2PA	22	5.63
116	ASN -	1	GDP	1172	ND2	N7	221	56.52
117	LYSH	1	GDP	1177	N	O6	6	1.53
117	LYSH	1	GDP	1184	NZ	O4*	1	0.26
117	LYSH	1	GDP	1184	NZ	O4*	3	0.77
117	LYSH	1	GDP	1184	NZ	O4*	1	0.26
146	ALA -	1	GDP	1467	N	O6	138	35.29
147	LYSH	1	GDP	1473	N	O6	27	6.91
147	LYSH	1	GDP	1480	NZ	N2	1	0.26

Res	DONO	Res	ACC	Atom	D	A	OCCUR	%
13	GLY -	1	GDP	114	N	O3PB	1	0.23
14	VAL -	1	GDP	119	N	O1PB	1	0.23
15	GLY -	1	GDP	127	N	O3PA	2	0.45
15	GLY -	1	GDP	127	N	O1PB	18	4.08
16	LYSH -	1	GDP	132	N	O1PA	17	3.85
16	LYSH -	1	GDP	132	N	O3PA	180	40.82
16	LYSH -	1	GDP	132	N	O1PB	107	24.26
16	LYSH -	1	GDP	132	N	O2PB	150	34.01
17	SER -	1	GDP	145	N	O1PA	394	89.34
17	SER -	1	GDP	145	N	O2PA	5	1.13
17	SER -	1	GDP	145	N	O3PA	1	0.23
17	SER -	1	GDP	145	N	O2PB	19	4.31
17	SER -	1	GDP	149	OG	O1PA	56	12.7
17	SER -	1	GDP	149	OG	O2PA	380	86.17
18	ALA -	1	GDP	153	N	O1PA	396	89.8
18	ALA -	1	GDP	153	N	O2PA	2	0.45
28	PHE -	1	GDP	266	CZ	O3*	6	1.36
117	LYSH	1	GDP	1184	NZ	O4*	1	0.23
145	SER -	1	GDP	1463	OG	O6	2	0.45
146	ALA -	1	GDP	1467	N	O6	12	2.72
146	ALA -	1	GDP	1467	N	N7	4	0.91
147	LYSH	1	GDP	1473	N	O6	355	80.5
147	LYSH	1	GDP	1473	N	N7	75	17.01
147	LYSH	1	GDP	1480	NZ	O2*	1	0.23
148	THR -	1	GDP	1486	N	O6	44	9.98

Res	DONO	Res	ACC	Atom	D	A	OCCUR	%
12	CYSH	1	GDP	110	SG	O3PB	2	0.3
13	GLY -	1	GDP	114	N	O3PA	2	0.3
13	GLY -	1	GDP	114	N	O1PB	13	1.95
13	GLY -	1	GDP	114	N	O3PB	538	80.54
14	VAL -	1	GDP	119	N	O1PB	103	15.42
15	GLY -	1	GDP	127	N	O5*	7	1.05
15	GLY -	1	GDP	127	N	O3PA	71	10.63
15	GLY -	1	GDP	127	N	O1PB	483	72.31
16	LYSH -	1	GDP	132	N	O1PA	2	0.3
16	LYSH -	1	GDP	132	N	O3PA	2	0.3
16	LYSH -	1	GDP	132	N	O1PB	660	98.8
16	LYSH -	1	GDP	139	NZ	O1PB	1	0.15
16	LYSH -	1	GDP	139	NZ	O3PB	2	0.3
16	LYSH -	1	GDP	139	NZ	O1PB	3	0.45
16	LYSH -	1	GDP	139	NZ	O3PB	3	0.45
16	LYSH -	1	GDP	139	NZ	O1PB	2	0.3
16	LYSH -	1	GDP	139	NZ	O3PB	2	0.3
17	SER -	1	GDP	145	N	O1PA	581	86.98
17	SER -	1	GDP	145	N	O3PA	4	0.6
17	SER -	1	GDP	145	N	O2PB	58	8.68
17	SER -	1	GDP	149	OG	O1PA	120	17.96
17	SER -	1	GDP	149	OG	O2PA	518	77.54
18	ALA -	1	GDP	153	N	O1PA	66	9.88
28	PHE -	1	GDP	262	CE	O2*	1	0.15
28	PHE -	1	GDP	264	CE2	O2*	1	0.15
28	PHE -	1	GDP	266	CZ	N7	3	0.45
28	PHE -	1	GDP	266	CZ	O2*	2	0.3
32	TYR -	1	GDP	297	N	O2PA	3	0.45
32	TYR -	1	GDP	304	CD2	O2PA	6	0.9
60	GLY -	1	GDP	571	N	O3PB	1	0.15
116	ASN -	1	GDP	1172	ND2	N7	185	27.69
116	ASN -	1	GDP	1172	ND2	O6	2	0.3
116	ASN -	1	GDP	1172	ND2	N7	23	3.44
117	LYSH	1	GDP	1177	N	O6	37	5.54
117	LYSH	1	GDP	1184	NZ	O4*	5	0.75
117	LYSH	1	GDP	1184	NZ	O4*	4	0.6
117	LYSH	1	GDP	1184	NZ	O4*	5	0.75
146	ALA -	1	GDP	1467	N	O6	236	35.33
147	LYSH	1	GDP	1473	N	O6	295	44.16
147	LYSH	1	GDP	1473	N	N7	1	0.15
147	LYSH	1	GDP	1480	NZ	O2*	4	0.6
147	LYSH	1	GDP	1480	NZ	O2*	2	0.3
147	LYSH	1	GDP	1480	NZ	O2*	4	0.6
148	THR -	1	GDP	1486	N	O6	1	0.15

Figure 27: *Occurrence of h-bonds in WT-GDP→G12C-GDP perturbation. Colored in yellow is P-loop, in red Switch-I loop, in blue Switch-II loop, and in orange the h-bond between sulfur in cysteine and Pγ/Pβ oxygen. Three colours represent three different replicas, numerated from left to right.*

Res	DONO	Res	ACC	Atom	D	A	OCCUR	%
13	GLY -	1	GTP	111	N	O1PB	6	1.14
13	GLY -	1	GTP	111	N	O3PB	138	26.19
13	GLY -	1	GTP	111	N	O1PG	108	20.49
13	GLY -	1	GTP	111	N	O2PG	38	7.21
13	GLY -	1	GTP	111	N	O3PG	79	14.99
14	VAL -	1	GTP	116	N	O1PB	50	9.49
14	VAL -	1	GTP	116	N	O1PG	5	0.95
14	VAL -	1	GTP	116	N	O3PG	1	0.19
15	GLY -	1	GTP	124	N	O1PA	1	0.19
15	GLY -	1	GTP	124	N	O3PA	61	11.57
15	GLY -	1	GTP	124	N	O1PB	394	74.76
15	GLY -	1	GTP	124	N	O2PG	1	0.19
16	LYSH -	1	GTP	129	N	O1PA	1	0.19
16	LYSH -	1	GTP	129	N	O3PA	12	2.28
16	LYSH -	1	GTP	129	N	O1PB	504	95.64
16	LYSH -	1	GTP	129	N	O2PB	3	0.57
16	LYSH -	1	GTP	136	NZ	O1PB	6	1.14
16	LYSH -	1	GTP	136	NZ	O3PB	4	0.76
16	LYSH -	1	GTP	136	NZ	O1PG	13	2.47
16	LYSH -	1	GTP	136	NZ	O2PG	1	0.19
16	LYSH -	1	GTP	136	NZ	O3PG	4	0.76
16	LYSH -	1	GTP	136	NZ	O1PB	4	0.76
16	LYSH -	1	GTP	136	NZ	O3PB	3	0.57
16	LYSH -	1	GTP	136	NZ	O1PG	13	2.47
16	LYSH -	1	GTP	136	NZ	O3PG	5	0.95
16	LYSH -	1	GTP	136	NZ	O1PB	5	0.95
16	LYSH -	1	GTP	136	NZ	O3PB	7	1.33
16	LYSH -	1	GTP	136	NZ	O1PG	10	1.9
16	LYSH -	1	GTP	136	NZ	O3PG	3	0.57
17	SER -	1	GTP	142	N	O1PA	478	90.7
17	SER -	1	GTP	142	N	O2PB	50	9.49
17	SER -	1	GTP	146	OC	O1PA	218	41.37
17	SER -	1	GTP	146	OC	O2PA	317	60.15
17	SER -	1	GTP	146	OC	O3PG	1	0.19
18	ALA -	1	GTP	150	N	O1PA	122	23.15
28	PHE -	1	GTP	259	CE	N7	1	0.19
28	PHE -	1	GTP	261	CE	O2*	1	0.19
28	PHE -	1	GTP	263	CZ	O2*	8	1.52
32	TYR -	1	GTP	305	CE	O5*	4	0.76
32	TYR -	1	GTP	305	CE	O2PA	1	0.19
32	TYR -	1	GTP	308	OH	O1PA	1	0.19
32	TYR -	1	GTP	308	OH	O2PA	21	3.98
58	THR -	1	GTP	557	OG	O1PG	1	0.19
60	GLY -	1	GTP	568	N	O1PG	10	1.9
60	GLY -	1	GTP	568	N	O2PG	2	0.38
60	GLY -	1	GTP	568	N	O3PG	29	5.5
116	ASN -	1	GTP	1169	ND	N9	1	0.19
116	ASN -	1	GTP	1169	ND	N7	47	8.92
116	ASN -	1	GTP	1169	ND	O4*	165	31.31
117	LYSH	1	GTP	1174	N	O6	8	1.52
117	LYSH	1	GTP	1181	NZ	O3*	2	0.38
145	SER -	1	GTP	1460	OC	O6	5	0.95
146	ALA -	1	GTP	1464	N	O6	8	1.52
146	ALA -	1	GTP	1464	N	N7	5	0.95
147	LYSH	1	GTP	1470	N	O6	355	67.36
147	LYSH	1	GTP	1470	N	N7	90	17.08
147	LYSH	1	GTP	1477	NZ	N3	4	0.76
147	LYSH	1	GTP	1477	NZ	N2	3	0.57
147	LYSH	1	GTP	1477	NZ	O2*	4	0.76
147	LYSH	1	GTP	1477	NZ	N3	2	0.38
147	LYSH	1	GTP	1477	NZ	O2*	3	0.57
147	LYSH	1	GTP	1477	NZ	N3	2	0.38
147	LYSH	1	GTP	1477	NZ	O2*	5	0.95
148	THR -	1	GTP	1483	N	O6	71	13.47

Res	DONO	Res	ACC	Atom	D	A	OCCUR	%
13	GLY -	1	GTP	111	N	O3PA	2	0.3
13	GLY -	1	GTP	111	N	O1PB	12	1.8
13	GLY -	1	GTP	111	N	O3PB	458	68.87
13	GLY -	1	GTP	111	N	O1PG	45	6.77
13	GLY -	1	GTP	111	N	O2PG	74	11.13
13	GLY -	1	GTP	111	N	O3PG	37	5.56
14	VAL -	1	GTP	116	N	O1PB	86	12.93
14	VAL -	1	GTP	116	N	O1PG	2	0.3
14	VAL -	1	GTP	116	N	O3PG	1	0.15
15	GLY -	1	GTP	124	N	O5*	1	0.15
15	GLY -	1	GTP	124	N	O1PA	1	0.15
15	GLY -	1	GTP	124	N	O3PA	60	9.02
15	GLY -	1	GTP	124	N	O1PG	1	0.15
15	GLY -	1	GTP	124	N	O3PA	1	0.15
16	LYSH -	1	GTP	129	N	O2PB	3	0.45
16	LYSH -	1	GTP	129	N	O1PB	663	99.7
16	LYSH -	1	GTP	136	NZ	O1PB	23	3.46
16	LYSH -	1	GTP	136	NZ	O2PB	1	0.15
16	LYSH -	1	GTP	136	NZ	O3PB	16	2.41
16	LYSH -	1	GTP	136	NZ	O1PG	11	1.65
16	LYSH -	1	GTP	136	NZ	O2PG	5	0.75
16	LYSH -	1	GTP	136	NZ	O3PG	23	3.46
16	LYSH -	1	GTP	136	NZ	O1PB	27	4.06
16	LYSH -	1	GTP	136	NZ	O3PB	23	3.46
16	LYSH -	1	GTP	136	NZ	O1PG	19	2.86
16	LYSH -	1	GTP	136	NZ	O2PG	2	0.3
16	LYSH -	1	GTP	136	NZ	O3PG	9	1.35
16	LYSH -	1	GTP	136	NZ	O1PB	36	5.41
16	LYSH -	1	GTP	136	NZ	O3PB	24	3.61
16	LYSH -	1	GTP	136	NZ	O1PG	14	2.11
16	LYSH -	1	GTP	136	NZ	O2PG	6	0.9
16	LYSH -	1	GTP	136	NZ	O3PG	21	3.16
17	SER -	1	GTP	142	N	O1PA	507	76.24
17	SER -	1	GTP	142	N	O2PB	69	10.38
17	SER -	1	GTP	146	OC	O1PA	376	56.54
17	SER -	1	GTP	146	OC	O2PA	339	50.98
17	SER -	1	GTP	146	OC	O3PA	1	0.15
18	ALA -	1	GTP	150	N	O1PA	68	10.23
28	PHE -	1	GTP	255	CD	O2*	1	0.15
28	PHE -	1	GTP	259	CE	N7	3	0.45
28	PHE -	1	GTP	259	CE	O2*	2	0.3
28	PHE -	1	GTP	261	CE	N7	7	1.05
28	PHE -	1	GTP	263	CZ	N7	4	0.6
28	PHE -	1	GTP	263	CZ	O2*	1	0.15
32	TYR -	1	GTP	294	N	O3*	2	0.3
32	TYR -	1	GTP	294	N	O5*	1	0.15
32	TYR -	1	GTP	294	N	O2PA	30	4.51
32	TYR -	1	GTP	299	CD	O5*	6	0.9
32	TYR -	1	GTP	299	CD	O2PA	29	4.36
32	TYR -	1	GTP	301	CD	O1PA	2	0.3
32	TYR -	1	GTP	301	CD	O2PA	32	4.81
60	GLY -	1	GTP	568	N	O2PG	2	0.3
60	GLY -	1	GTP	568	N	O3PG	3	0.45
116	ASN -	1	GTP	1169	ND	N7	114	17.14
117	LYSH	1	GTP	1181	NZ	O4*	2	0.3
117	LYSH	1	GTP	1181	NZ	O4*	1	0.15
117	LYSH	1	GTP	1181	NZ	O4*	3	0.45
146	ALA -	1	GTP	1464	N	O6	150	22.56
146	ALA -	1	GTP	1464	N	N7	1	0.15
147	LYSH	1	GTP	1470	N	O6	500	75.19
147	LYSH	1	GTP	1470	N	N7	16	2.41
147	LYSH	1	GTP	1477	NZ	N2	1	0.15
147	LYSH	1	GTP	1477	NZ	O2*	7	1.05
147	LYSH	1	GTP	1477	NZ	N3	3	0.45
147	LYSH	1	GTP	1477	NZ	O2*	3	0.45
147	LYSH	1	GTP	1477	NZ	N3	2	0.3
147	LYSH	1	GTP	1477	NZ	N2	1	0.15
147	LYSH	1	GTP	1477	NZ	O2*	2	0.3
148	THR -	1	GTP	1483	N	O6	8	1.2

Res	DONO	Res	ACC	Atom	D	A	OCCUR	%
13	GLY -	1	GTP	111	N	O3PA	4	0.76
13	GLY -	1	GTP	111	N	O1PB	367	69.38
13	GLY -	1	GTP	111	N	O3PB	153	28.92
13	GLY -	1	GTP	111	N	O1PG	2	0.38
13	GLY -	1	GTP	111	N	O3PG	8	1.51
14	VAL -	1	GTP	116	N	O3PA	2	0.38
14	VAL -	1	GTP	116	N	O1PB	52	9.83
14	VAL -	1	GTP	124	N	O2*	2	0.38
15	GLY -	1	GTP	124	N	O3*	75	14.18
16	LYSH -	1	GTP	129	N	O1PB	1	0.19
16	LYSH -	1	GTP	136	NZ	O1PB	130	24.57
16	LYSH -	1	GTP	136	NZ	O1PB	116	21.93
16	LYSH -	1	GTP	136	NZ	O2PB	2	0.38
16	LYSH -	1	GTP	136	NZ	O1PB	119	22.5
16	LYSH -	1	GTP	136	NZ	O2PB	1	0.19
16	LYSH -	1	GTP	136	NZ	O3PB	1	0.19
17	SER -	1	GTP	142	N	O5*	479	90.55
17	SER -	1	GTP	142	N	O1PA	153	28.92
17	SER -	1	GTP	146	OC	O5*	73	13.8
17	SER -	1	GTP	146	OC	O1PA	106	20.04
17	SER -	1	GTP	146	OC	O2PA	272	51.42
18	ALA -	1	GTP	150	N	O4*	4	0.76
28	PHE -	1	GTP	259	CE	O6	1	0.19
28	PHE -	1	GTP	259	CE	N7	4	0.76
28	PHE -	1	GTP	261	CE	O6	2	0.38
28	PHE -	1	GTP	261	CE	N7	1	0.19
28	PHE -	1	GTP	263	CZ	N7	18	3.4
32	TYR -	1	GTP	294	N	N7	1	0.19
58	THR -	1	GTP	557	OG	O1PB	2	0.38
58	THR -	1	GTP	557	OG	O2PB	52	9.83
58	THR -	1	GTP	557	OG	O1PG	9	1.7
58	THR -	1	GTP	557	OG	O2PG	7	1.32
60	GLY -	1	GTP	568	N	O1PB	2	0.38
60	GLY -	1	GTP	568	N	O2PB	1	0.19
60	GLY -	1	GTP	568	N	O3PB	268	50.66
60	GLY -	1	GTP	568	N	O1PG	63	11.91
60	GLY -	1	GTP	568	N	O2PG	102	19.28
60	GLY -	1	GTP	568	N	O3PG	3	0.57
61	GLN -	1	GTP	573	N	O1PG	8	1.51
61	GLN -	1	GTP	573	N	O2PG	2	0.38
116	ASN -	1	GTP	1169	ND	N3	428	80.91
116	ASN -	1	GTP	1169	ND	O2*	3	0.57
116	ASN -	1	GTP	1169	ND	O3*	5	0.95
117	LYSH	1	GTP	1181	NZ	O2*	20	3.78
117	LYSH	1	GTP	1181	NZ	N3	1	0.19
117	LYSH	1	GTP	1181	NZ	O2*	8	1.51
117	LYSH	1	GTP	1181	NZ	O2*	9	1.7
146	ALA -	1	GTP	1464	N	N2	106	20.04
146	ALA -	1	GTP	1464	N	N1	5	0.95
147	LYSH	1	GTP	1470	N	O6	22	4.16
147	LYSH	1	GTP	1477	NZ	O6	15	2.84
147	LYSH	1	GTP	1477	NZ	O6	15	2.84
147	LYSH	1	GTP	1477	NZ	O6	23	4.35

Figure 28: *Occurrence of h-bonds in WT-GDP→WT-GTP perturbation. Colored in yellow is P-loop, in red Switch-I loop, in blue Switch-II loop, and in orange the h-bond between sulfur in cysteine and Pγ/Pβ oxygen. Three colours represent three different replicas, numerated from left to right.*

Res	DONO	Res	ACC	Atom	D	A	OCCUR	%	Res	DONO	Res	ACC	Atom	D	A	OCCUR	%	Res	DONO	Res	ACC	Atom	D	A	OCCUR	%
13	GLY -	1	GTP	111	N	O1PB	4	0.65	13	GLY -	1	GTP	111	N	O3PA	1	0.16	13	GLY -	1	GTP	111	N	O3PA	1	0.17
13	GLY -	1	GTP	111	N	O3PB	504	81.95	13	GLY -	1	GTP	111	N	O1PB	62	10.21	13	GLY -	1	GTP	111	N	O1PB	1	0.17
13	GLY -	1	GTP	111	N	O1PG	88	14.31	13	GLY -	1	GTP	111	N	O3PB	10	1.65	13	GLY -	1	GTP	111	N	O3PB	100	17.3
13	GLY -	1	GTP	111	N	O2PG	9	1.46	13	GLY -	1	GTP	111	N	O1PG	19	3.13	13	GLY -	1	GTP	111	N	O1PG	5	0.87
13	GLY -	1	GTP	111	N	O3PG	31	5.04	13	GLY -	1	GTP	111	N	O2PG	1	0.16	13	GLY -	1	GTP	111	N	O2PG	129	22.32
14	VAL -	1	GTP	116	N	O1PB	248	40.33	13	GLY -	1	GTP	111	N	O3PG	2	0.33	13	GLY -	1	GTP	111	N	O3PG	46	7.96
14	VAL -	1	GTP	116	N	O1PG	5	0.81	14	VAL -	1	GTP	116	N	O1PB	3	0.49	14	VAL -	1	GTP	116	N	O1PB	24	4.15
14	VAL -	1	GTP	116	N	O2PG	2	0.33	15	GLY -	1	GTP	124	N	O1PB	24	3.95	14	VAL -	1	GTP	116	N	O1PG	48	8.3
14	VAL -	1	GTP	116	N	O3PG	5	0.81	15	GLY -	1	GTP	124	N	O2PG	1	0.16	14	VAL -	1	GTP	116	N	O2PG	12	2.08
15	GLY -	1	GTP	124	N	O5*	3	0.49	15	GLY -	1	GTP	124	N	O3PG	1	0.16	14	VAL -	1	GTP	116	N	O3PG	14	2.42
15	GLY -	1	GTP	124	N	O1PA	18	2.93	16	LYSH -	1	GTP	129	N	O1PA	34	5.6	15	GLY -	1	GTP	124	N	O5*	2	0.35
15	GLY -	1	GTP	124	N	O3PA	50	8.13	16	LYSH -	1	GTP	129	N	O3PA	329	54.2	15	GLY -	1	GTP	124	N	O1PB	98	16.96
15	GLY -	1	GTP	124	N	O1PB	496	80.65	16	LYSH -	1	GTP	129	N	O1PB	188	30.97	15	GLY -	1	GTP	124	N	O1PG	237	41
16	LYSH -	1	GTP	129	N	O1PB	603	98.05	16	LYSH -	1	GTP	129	N	O2PB	39	6.43	15	GLY -	1	GTP	124	N	O2PG	10	1.73
16	LYSH -	1	GTP	129	N	O2PB	8	1.3	16	LYSH -	1	GTP	129	N	O2PG	1	0.16	15	GLY -	1	GTP	124	N	O3PG	9	1.56
16	LYSH -	1	GTP	136	NZ	O1PB	28	4.55	16	LYSH -	1	GTP	129	N	O3PG	1	0.16	16	LYSH -	1	GTP	129	N	O1PA	1	0.17
16	LYSH -	1	GTP	136	NZ	O3PB	10	1.63	16	LYSH -	1	GTP	136	NZ	O1PG	1	0.16	16	LYSH -	1	GTP	129	N	O1PB	413	71.45
16	LYSH -	1	GTP	136	NZ	O1PG	6	0.98	16	LYSH -	1	GTP	136	NZ	O1PG	3	0.49	16	LYSH -	1	GTP	129	N	O3PB	13	2.25
16	LYSH -	1	GTP	136	NZ	O2PG	7	1.14	16	LYSH -	1	GTP	136	NZ	O2PG	3	0.49	16	LYSH -	1	GTP	129	N	O1PG	151	26.12
16	LYSH -	1	GTP	136	NZ	O1PB	17	2.76	16	LYSH -	1	GTP	136	NZ	O1PG	2	0.33	16	LYSH -	1	GTP	129	N	O2PG	3	0.52
16	LYSH -	1	GTP	136	NZ	O3PB	9	1.46	17	SER -	1	GTP	142	N	O1PA	484	79.74	16	LYSH -	1	GTP	136	NZ	O1PB	1	0.17
16	LYSH -	1	GTP	136	NZ	O1PG	2	0.33	17	SER -	1	GTP	142	N	O2PA	45	7.41	16	LYSH -	1	GTP	136	NZ	O1PG	6	1.04
16	LYSH -	1	GTP	136	NZ	O2PG	5	0.81	17	SER -	1	GTP	142	N	O3PA	17	2.8	16	LYSH -	1	GTP	136	NZ	O2PG	2	0.35
16	LYSH -	1	GTP	136	NZ	O1PB	9	1.46	17	SER -	1	GTP	142	N	O1PB	1	0.16	16	LYSH -	1	GTP	136	NZ	O1PB	1	0.17
16	LYSH -	1	GTP	136	NZ	O2PB	1	0.16	17	SER -	1	GTP	142	N	O2PB	42	6.92	16	LYSH -	1	GTP	136	NZ	O3PB	3	0.52
16	LYSH -	1	GTP	136	NZ	O3PB	3	0.49	17	SER -	1	GTP	146	OG	O1PA	47	7.74	16	LYSH -	1	GTP	136	NZ	O1PG	4	0.69
16	LYSH -	1	GTP	136	NZ	O1PG	6	0.98	17	SER -	1	GTP	146	OG	O2PA	554	91.27	16	LYSH -	1	GTP	136	NZ	O2PG	4	0.69
16	LYSH -	1	GTP	136	NZ	O2PG	4	0.65	17	SER -	1	GTP	146	OG	O1PG	6	0.99	16	LYSH -	1	GTP	136	NZ	O3PG	1	0.17
17	SER -	1	GTP	142	N	O1PA	293	47.64	18	ALA -	1	GTP	150	N	O1PA	570	93.9	16	LYSH -	1	GTP	136	NZ	O1PB	1	0.17
17	SER -	1	GTP	142	N	O3PA	1	0.16	18	ALA -	1	GTP	150	N	O2PA	7	1.15	16	LYSH -	1	GTP	136	NZ	O3PB	2	0.35
17	SER -	1	GTP	142	N	O1PB	2	0.33	28	PHE -	1	GTP	261	CE2	N7	1	0.16	16	LYSH -	1	GTP	136	NZ	O1PG	15	2.6
17	SER -	1	GTP	142	N	O2PB	191	31.06	28	PHE -	1	GTP	263	CZ	O2*	2	0.33	16	LYSH -	1	GTP	136	NZ	O2PG	8	1.38
17	SER -	1	GTP	146	OG	O1PA	25	4.07	28	PHE -	1	GTP	263	CZ	O3*	4	0.66	16	LYSH -	1	GTP	136	NZ	O3PG	1	0.17
17	SER -	1	GTP	146	OG	O2PA	138	22.44	60	GLY -	1	GTP	568	N	O2PG	4	0.66	17	SER -	1	GTP	142	N	O1PA	144	24.91
17	SER -	1	GTP	146	OG	O3PA	7	1.14	60	GLY -	1	GTP	568	N	O3PG	5	0.82	17	SER -	1	GTP	142	N	O1PB	422	73.01
17	SER -	1	GTP	146	OG	O2PB	47	7.64	116	ASN -	1	GTP	1169	ND2	O4*	1	0.16	17	SER -	1	GTP	142	N	O2PB	1	0.17
18	ALA -	1	GTP	150	N	O1PA	580	94.31	117	LYSH	1	GTP	1181	NZ	O4*	1	0.16	17	SER -	1	GTP	146	OG	O1PA	448	77.51
28	PHE -	1	GTP	259	CE2	O2*	3	0.49	117	LYSH	1	GTP	1181	NZ	N3	1	0.16	17	SER -	1	GTP	146	OG	O2PA	133	23.01
28	PHE -	1	GTP	261	CE2	N7	4	0.65	145	SER -	1	GTP	1460	OG	O6	6	0.99	17	SER -	1	GTP	146	OG	O1PB	2	0.35
28	PHE -	1	GTP	263	CZ	N7	1	0.16	146	ALA -	1	GTP	1464	N	O6	3	0.49	28	PHE -	1	GTP	261	CE2	N7	1	0.17
28	PHE -	1	GTP	263	CZ	O2*	8	1.3	146	ALA -	1	GTP	1464	N	N7	4	0.66	28	PHE -	1	GTP	261	CE2	O2*	2	0.35
28	PHE -	1	GTP	263	CZ	O3*	1	0.16	147	LYSH	1	GTP	1470	N	O6	561	92.42	28	PHE -	1	GTP	263	CZ	N7	1	0.17
32	TYR -	1	GTP	294	N	O3*	13	2.11	147	LYSH	1	GTP	1470	N	N7	43	7.08	28	PHE -	1	GTP	263	CZ	O2*	19	3.29
32	TYR -	1	GTP	301	CD2	O1PA	1	0.16	147	LYSH	1	GTP	1477	NZ	N3	1	0.16	31	GLU -	1	GTP	284	N	O2*	2	0.35
32	TYR -	1	GTP	301	CD2	O2PA	42	6.83	147	LYSH	1	GTP	1477	NZ	O2*	5	0.82	32	TYR -	1	GTP	301	CD2	O1PA	2	0.35
32	TYR -	1	GTP	305	CE2	O2PA	2	0.33	147	LYSH	1	GTP	1477	NZ	N3	1	0.16	32	TYR -	1	GTP	301	CD2	O2PA	9	1.56
60	GLY -	1	GTP	568	N	O1PG	63	10.24	147	LYSH	1	GTP	1477	NZ	O2*	5	0.82	32	TYR -	1	GTP	305	CE2	O1PA	2	0.35
60	GLY -	1	GTP	568	N	O2PG	5	0.81	147	LYSH	1	GTP	1477	NZ	N3	1	0.16	58	THR -	1	GTP	557	OG	O2PB	49	8.48
60	GLY -	1	GTP	568	N	O3PG	5	0.81	147	LYSH	1	GTP	1477	NZ	O2*	3	0.49	58	THR -	1	GTP	557	OG	O3PB	6	1.04
116	ASN -	1	GTP	1169	ND2	N7	30	4.88	148	THR -	1	GTP	1483	N	O6	34	5.6	61	GLN -	1	GTP	573	N	O2PG	2	0.35
116	ASN -	1	GTP	1169	ND2	O4*	71	11.54										116	ASN -	1	GTP	1169	ND2	O6	4	0.69
117	LYSH	1	GTP	1181	NZ	O4*	1	0.16										116	ASN -	1	GTP	1169	ND2	N7	498	86.16
117	LYSH	1	GTP	1181	NZ	N3	2	0.33										117	LYSH	1	GTP	1174	N	O6	4	0.69
117	LYSH	1	GTP	1181	NZ	O4*	3	0.49										117	LYSH	1	GTP	1181	NZ	N3	1	0.17
117	LYSH	1	GTP	1181	NZ	O4*	3	0.49										117	LYSH	1	GTP	1181	NZ	N2	1	0.17
117	LYSH	1	GTP	1181	NZ	O3*	1	0.16										117	LYSH	1	GTP	1181	NZ	O4*	1	0.17
146	ALA -	1	GTP	1464	N	O6	171	27.8										146	ALA -	1	GTP	1464	N	O6	405	70.07
146	ALA -	1	GTP	1464	N	N7	2	0.33										147	LYSH	1	GTP	1470	N	O6	204	35.29
147	LYSH	1	GTP	1470	N	O6	425	69.11										147	LYSH	1	GTP	1477	NZ	N3	2	0.35
147	LYSH	1	GTP	1470	N	N7	40	6.5										147	LYSH	1	GTP	1477	NZ	N2	1	0.17
147	LYSH	1	GTP	1477	NZ	N2	2	0.33										147	LYSH	1	GTP	1477	NZ	O2*	1	0.17
147	LYSH	1	GTP	1477	NZ	O2*	1	0.16										147	LYSH	1	GTP	1477	NZ	N3	4	0.69
147	LYSH	1	GTP	1477	NZ	N3	1	0.16										147	LYSH	1	GTP	1477	NZ	O2*	3	0.52
147	LYSH	1	GTP	1477	NZ	N2	1	0.16										147	LYSH	1	GTP	1477	NZ	N3	2	0.35
147	LYSH	1	GTP	1477	NZ	O2*	2	0.33										147	LYSH	1	GTP	1477	NZ	N2	1	0.17
147	LYSH	1	GTP	1477	NZ	N2	1	0.16										147	LYSH	1	GTP	1477	NZ	O2*	3	0.52
147	LYSH	1	GTP	1477	NZ	O2*	3	0.49																		
148	THR -	1	GTP	1483	N	O6	45	7.32																		

Figure 29: *Occurrence of h-bonds in WT-GTP→WT-GDP perturbation. Colored in yellow is P-loop, in red Switch-I loop, in blue Switch-II loop, and in orange the h-bond between sulfur in cysteine and Pγ/Pβ oxygen. Three colours represent three different replicas, numerated from left to right.*

Res	DONO	Res	ACC	Atom	D	A	OCCUR	%	Res	DONO	Res	ACC	Atom	D	A	OCCUR	%	Res	DONO	Res	ACC	Atom	D	A	OCCUR	%
12	CYS -	1	GTP	110	SG	O1PG	56	5.73	12	CYS -	1	GTP	110	SG	O1PG	53	9.12	12	CYS -	1	GTP	110	SG	O1PB	2	0.44
13	GLY -	1	GTP	114	N	O3PA	1	0.1	12	CYS -	1	GTP	110	SG	O2PG	74	12.74	12	CYS -	1	GTP	110	SG	O3PB	1	0.22
13	GLY -	1	GTP	114	N	O1PB	8	0.82	13	GLY -	1	GTP	114	N	O3PA	2	0.34	12	CYS -	1	GTP	110	SG	O1PG	2	0.44
13	GLY -	1	GTP	114	N	O3PB	290	29.68	13	GLY -	1	GTP	114	N	O3PB	266	45.78	13	GLY -	1	GTP	114	N	O3PA	9	2
13	GLY -	1	GTP	114	N	O1PG	542	55.48	13	GLY -	1	GTP	114	N	O1PG	115	19.79	13	GLY -	1	GTP	114	N	O1PB	367	81.37
14	VAL -	1	GTP	119	N	O1PB	291	29.79	13	GLY -	1	GTP	114	N	O2PG	195	33.56	13	GLY -	1	GTP	114	N	O3PB	38	8.43
15	GLY -	1	GTP	127	N	O1PA	1	0.1	13	GLY -	1	GTP	114	N	O3PG	40	6.88	14	VAL -	1	GTP	119	N	O1PB	10	2.22
15	GLY -	1	GTP	127	N	O3PA	306	31.32	14	VAL -	1	GTP	119	N	O1PB	51	8.78	15	GLY -	1	GTP	127	N	O3*	60	13.3
15	GLY -	1	GTP	127	N	O1PB	707	72.36	15	GLY -	1	GTP	127	N	O5*	1	0.17	16	LYSH -	1	GTP	139	NZ	O1PB	60	13.3
16	LYSH -	1	GTP	132	N	O3PA	3	0.31	15	GLY -	1	GTP	127	N	O3PA	36	6.2	16	LYSH -	1	GTP	139	NZ	O2PB	3	0.67
16	LYSH -	1	GTP	132	N	O1PB	970	99.28	15	GLY -	1	GTP	127	N	O1PB	417	71.77	16	LYSH -	1	GTP	139	NZ	O1PB	77	17.07
16	LYSH -	1	GTP	132	N	O2PB	37	3.79	16	LYSH -	1	GTP	132	N	O1PA	2	0.34	16	LYSH -	1	GTP	139	NZ	O2PB	3	0.67
16	LYSH -	1	GTP	139	NZ	O1PB	37	3.79	16	LYSH -	1	GTP	132	N	O1PB	578	99.48	16	LYSH -	1	GTP	139	NZ	O1PB	66	14.63
16	LYSH -	1	GTP	139	NZ	O3PB	1	0.1	16	LYSH -	1	GTP	132	N	O2PB	4	0.69	17	SER -	1	GTP	145	N	O5*	440	97.56
16	LYSH -	1	GTP	139	NZ	O1PG	151	15.46	16	LYSH -	1	GTP	139	NZ	O1PB	24	4.13	17	SER -	1	GTP	145	N	O1PA	63	13.97
16	LYSH -	1	GTP	139	NZ	O2PG	1	0.1	16	LYSH -	1	GTP	139	NZ	O3PB	4	0.69	17	SER -	1	GTP	149	OG	O5*	25	5.54
16	LYSH -	1	GTP	139	NZ	O1PB	38	3.89	16	LYSH -	1	GTP	139	NZ	O1PG	5	0.86	17	SER -	1	GTP	149	OG	O1PA	85	18.85
16	LYSH -	1	GTP	139	NZ	O3PB	6	0.61	16	LYSH -	1	GTP	139	NZ	O2PG	8	1.38	17	SER -	1	GTP	149	OG	O2PA	313	69.4
16	LYSH -	1	GTP	139	NZ	O1PG	139	14.23	16	LYSH -	1	GTP	139	NZ	O3PG	33	5.68	18	ALA -	1	GTP	153	N	O4*	2	0.44
16	LYSH -	1	GTP	139	NZ	O1PB	41	4.2	16	LYSH -	1	GTP	139	NZ	O1PB	23	3.96	28	PHE -	1	GTP	262	CE	N7	1	0.22
16	LYSH -	1	GTP	139	NZ	O3PB	7	0.72	16	LYSH -	1	GTP	139	NZ	O3PB	10	1.72	28	PHE -	1	GTP	264	CE	O6	1	0.22
16	LYSH -	1	GTP	139	NZ	O1PG	144	14.74	16	LYSH -	1	GTP	139	NZ	O1PG	2	0.34	28	PHE -	1	GTP	264	CE	N7	3	0.67
16	LYSH -	1	GTP	139	NZ	O2PG	1	0.1	16	LYSH -	1	GTP	139	NZ	O2PG	16	2.75	28	PHE -	1	GTP	266	CZ	N7	2	0.44
17	SER -	1	GTP	145	N	O1PA	615	62.95	16	LYSH -	1	GTP	139	NZ	O3PG	31	5.34	58	THR -	1	GTP	560	OG	O1PB	11	2.44
17	SER -	1	GTP	145	N	O2PB	353	36.13	16	LYSH -	1	GTP	139	NZ	O1PB	20	3.44	58	THR -	1	GTP	560	OG	O2PB	214	47.45
17	SER -	1	GTP	149	OG	O1PA	104	10.64	16	LYSH -	1	GTP	139	NZ	O3PB	2	0.34	60	GLY -	1	GTP	571	N	O3PB	1	0.22
17	SER -	1	GTP	149	OG	O2PA	82	8.39	16	LYSH -	1	GTP	139	NZ	O1PG	2	0.34	60	GLY -	1	GTP	571	N	O1PG	51	11.31
18	ALA -	1	GTP	153	N	O1PA	848	86.8	16	LYSH -	1	GTP	139	NZ	O2PG	14	2.41	60	GLY -	1	GTP	571	N	O2PG	180	39.91
28	PHE -	1	GTP	262	CE	N7	1	0.1	16	LYSH -	1	GTP	139	NZ	O3PG	34	5.85	61	GLN -	1	GTP	576	N	O1PG	1	0.22
28	PHE -	1	GTP	262	CE	O2*	1	0.1	17	SER -	1	GTP	145	N	O1PA	533	91.74	61	GLN -	1	GTP	583	NE	O3PB	19	4.21
28	PHE -	1	GTP	266	CZ	O2*	3	0.31	17	SER -	1	GTP	145	N	O2PB	1	0.17	61	GLN -	1	GTP	583	NE	O1PG	26	5.76
32	TYR -	1	GTP	304	CD	O2*	1	0.1	17	SER -	1	GTP	149	OG	O1PA	179	30.81	61	GLN -	1	GTP	583	NE	O3PG	13	2.88
32	TYR -	1	GTP	308	CE	O5*	364	37.26	17	SER -	1	GTP	149	OG	O2PA	451	77.62	62	GLU -	1	GTP	588	N	O3PB	1	0.22
32	TYR -	1	GTP	308	CE	O2PA	46	4.71	28	PHE -	1	GTP	262	CE	O2*	1	0.17	62	GLU -	1	GTP	588	N	O1PG	15	3.33
32	TYR -	1	GTP	311	OH	O5*	2	0.2	28	PHE -	1	GTP	266	CZ	O2*	7	1.2	116	ASN -	1	GTP	1172	ND	N3	371	82.26
32	TYR -	1	GTP	311	OH	O1PA	20	2.05	28	PHE -	1	GTP	266	CZ	O1PA	5	0.86	116	ASN -	1	GTP	1172	ND	O2*	5	1.11
32	TYR -	1	GTP	311	OH	O2PA	958	98.06	60	GLY -	1	GTP	571	N	O1PG	49	8.43	116	ASN -	1	GTP	1172	ND	O3*	2	0.44
60	GLY -	1	GTP	571	N	O1PG	182	18.63	60	GLY -	1	GTP	571	N	O2PG	33	5.68	117	LYSH	1	GTP	1184	NZ	O2*	7	1.55
60	GLY -	1	GTP	571	N	O3PG	443	45.34	60	GLY -	1	GTP	571	N	O3PG	15	2.58	117	LYSH	1	GTP	1184	NZ	O2*	12	2.66
116	ASN -	1	GTP	1172	ND	O4*	486	49.74	61	GLN -	1	GTP	576	N	O1PG	7	1.2	117	LYSH	1	GTP	1184	NZ	O2*	7	1.55
117	LYSH	1	GTP	1184	NZ	O4*	1	0.1	61	GLN -	1	GTP	583	NE	O1PG	1	0.17	146	ALA -	1	GTP	1467	N	N2	44	9.76
117	LYSH	1	GTP	1184	NZ	O3*	1	0.1	116	ASN -	1	GTP	1172	ND	N7	113	19.45	146	ALA -	1	GTP	1467	N	N1	7	1.55
117	LYSH	1	GTP	1184	NZ	O4*	1	0.1	117	LYSH	1	GTP	1177	N	O6	3	0.52	147	LYSH	1	GTP	1473	N	O6	44	9.76
117	LYSH	1	GTP	1184	NZ	N3	1	0.1	117	LYSH	1	GTP	1184	NZ	O4*	1	0.17	147	LYSH	1	GTP	1480	NZ	O6	24	5.32
117	LYSH	1	GTP	1184	NZ	O4*	1	0.1	117	LYSH	1	GTP	1184	NZ	O4*	1	0.17	147	LYSH	1	GTP	1480	NZ	O6	30	6.65
145	SER -	1	GTP	1463	OG	O6	16	1.64	145	SER -	1	GTP	1463	OG	O6	2	0.34	147	LYSH	1	GTP	1480	NZ	N7	1	0.22
146	ALA -	1	GTP	1467	N	O6	40	4.09	146	ALA -	1	GTP	1467	N	O6	158	27.19	147	LYSH	1	GTP	1480	NZ	O6	20	4.43
146	ALA -	1	GTP	1467	N	N7	12	1.23	146	ALA -	1	GTP	1467	N	N7	10	1.72									
147	LYSH	1	GTP	1473	N	O6	618	63.25	147	LYSH	1	GTP	1473	N	O6	457	78.66									
147	LYSH	1	GTP	1473	N	N7	310	31.73	147	LYSH	1	GTP	1473	N	N7	18	3.1									
147	LYSH	1	GTP	1480	NZ	N3	1	0.1	147	LYSH	1	GTP	1480	NZ	N3	1	0.17									
147	LYSH	1	GTP	1480	NZ	O2*	8	0.82	147	LYSH	1	GTP	1480	NZ	O2*	3	0.52									
147	LYSH	1	GTP	1480	NZ	N3	1	0.1	147	LYSH	1	GTP	1480	NZ	N3	1	0.17									
147	LYSH	1	GTP	1480	NZ	N2	4	0.41	147	LYSH	1	GTP	1480	NZ	O2*	6	1.03									
147	LYSH	1	GTP	1480	NZ	O2*	6	0.61	147	LYSH	1	GTP	1480	NZ	N3	1	0.17									
147	LYSH	1	GTP	1480	NZ	O2*	8	0.82	147	LYSH	1	GTP	1480	NZ	O2*	6	1.03									
148	THR -	1	GTP	1486	N	O6	239	24.46	148	THR -	1	GTP	1486	N	O6	4	0.69									

Figure 30: *Occurrence of h-bonds in WT-GTP→G12C-GTP perturbation. Colored in yellow is P-loop, in red Switch-I loop, in blue Switch-II loop, and in orange the h-bond between sulfur in cysteine and Pγ/Pβ oxygen. Three colours represent three different replicas, numerated from left to right.*

Res	DONO	Res	ACC	Atom	D	A	OCCUR	%
12	CYS -	1	GTP	110	SG	O3PB	2	0.54
12	CYS -	1	GTP	110	SG	O1PG	74	19.95
13	GLY -	1	GTP	114	N	O3PA	14	3.77
13	GLY -	1	GTP	114	N	O1PB	11	2.96
13	GLY -	1	GTP	114	N	O3PB	241	64.96
14	VAL -	1	GTP	119	N	O3PA	3	0.81
14	VAL -	1	GTP	119	N	O1PB	168	45.28
15	GLY -	1	GTP	127	N	O3PA	68	18.33
15	GLY -	1	GTP	127	N	O1PB	309	83.29
16	LYSH -	1	GTP	132	N	O1PB	329	88.68
16	LYSH -	1	GTP	132	N	O2PB	67	18.06
16	LYSH -	1	GTP	139	NZ	O1PB	78	21.02
16	LYSH -	1	GTP	139	NZ	O2PB	1	0.27
16	LYSH -	1	GTP	139	NZ	O3PB	4	1.08
16	LYSH -	1	GTP	139	NZ	O2PG	1	0.27
16	LYSH -	1	GTP	139	NZ	O1PB	47	12.67
16	LYSH -	1	GTP	139	NZ	O3PB	4	1.08
16	LYSH -	1	GTP	139	NZ	O1PG	1	0.27
16	LYSH -	1	GTP	139	NZ	O1PB	60	16.17
16	LYSH -	1	GTP	139	NZ	O2PB	1	0.27
16	LYSH -	1	GTP	139	NZ	O3PB	4	1.08
16	LYSH -	1	GTP	139	NZ	O2PG	1	0.27
17	SER -	1	GTP	145	N	O1PA	12	3.23
17	SER -	1	GTP	145	N	O2PB	360	97.04
17	SER -	1	GTP	149	OG	O1PA	1	0.27
17	SER -	1	GTP	149	OG	O2PA	113	30.46
17	SER -	1	GTP	149	OG	O2PB	221	59.57
18	ALA -	1	GTP	153	N	O1PA	371	100
28	PHE -	1	GTP	264	CE1	N7	1	0.27
28	PHE -	1	GTP	266	CZ	O2*	15	4.04
60	GLY -	1	GTP	571	N	O1PG	306	82.48
116	ASN -	1	GTP	1172	ND2	N7	2	0.54
117	LYSH	1	GTP	1184	NZ	O4*	3	0.81
117	LYSH	1	GTP	1184	NZ	O4*	5	1.35
117	LYSH	1	GTP	1184	NZ	O3*	1	0.27
145	SER -	1	GTP	1463	OG	O6	1	0.27
146	ALA -	1	GTP	1467	N	O6	19	5.12
147	LYSH	1	GTP	1473	N	O6	348	93.8
147	LYSH	1	GTP	1473	N	N7	8	2.16
147	LYSH	1	GTP	1480	NZ	N3	1	0.27
147	LYSH	1	GTP	1480	NZ	O2*	3	0.81
147	LYSH	1	GTP	1480	NZ	N3	2	0.54
147	LYSH	1	GTP	1480	NZ	O2*	4	1.08
147	LYSH	1	GTP	1480	NZ	N3	1	0.27
147	LYSH	1	GTP	1480	NZ	N2	1	0.27
147	LYSH	1	GTP	1480	NZ	O2*	6	1.62

Res	DONO	Res	ACC	Atom	D	A	OCCUR	%
12	CYS -	1	GTP	110	SG	O1PB	4	0.63
12	CYS -	1	GTP	110	SG	O3PB	1	0.16
13	GLY -	1	GTP	114	N	O3PA	22	3.49
13	GLY -	1	GTP	114	N	O1PB	389	61.65
13	GLY -	1	GTP	114	N	O3PB	40	6.34
15	GLY -	1	GTP	127	N	O1PA	4	0.63
16	LYSH -	1	GTP	132	N	O1PA	149	23.61
16	LYSH -	1	GTP	132	N	O3PA	220	34.87
16	LYSH -	1	GTP	132	N	O1PB	25	3.96
16	LYSH -	1	GTP	132	N	O2PB	3	0.48
16	LYSH -	1	GTP	139	NZ	O1PB	1	0.16
17	SER -	1	GTP	145	N	O1PA	278	44.06
17	SER -	1	GTP	145	N	O2PA	30	4.75
17	SER -	1	GTP	145	N	O3PA	1	0.16
17	SER -	1	GTP	145	N	O2PB	234	37.08
17	SER -	1	GTP	149	OG	O2PA	629	99.68
18	ALA -	1	GTP	153	N	O1PA	418	66.24
18	ALA -	1	GTP	153	N	O2PA	20	3.17
28	PHE -	1	GTP	262	CE2	O2*	2	0.32
28	PHE -	1	GTP	266	CZ	N7	1	0.16
28	PHE -	1	GTP	266	CZ	O2*	3	0.48
117	LYSH	1	GTP	1184	NZ	N3	1	0.16
117	LYSH	1	GTP	1184	NZ	O4*	3	0.48
117	LYSH	1	GTP	1184	NZ	O4*	2	0.32
117	LYSH	1	GTP	1184	NZ	N3	2	0.32
145	SER -	1	GTP	1463	OG	O6	2	0.32
146	ALA -	1	GTP	1467	N	O6	21	3.33
146	ALA -	1	GTP	1467	N	N7	1	0.16
147	LYSH	1	GTP	1473	N	O6	577	91.44
147	LYSH	1	GTP	1473	N	N7	45	7.13
147	LYSH	1	GTP	1480	NZ	N3	1	0.16
147	LYSH	1	GTP	1480	NZ	O2*	13	2.06
147	LYSH	1	GTP	1480	NZ	N3	1	0.16
147	LYSH	1	GTP	1480	NZ	O2*	11	1.74
147	LYSH	1	GTP	1480	NZ	N3	3	0.48
147	LYSH	1	GTP	1480	NZ	O2*	8	1.27
148	THR -	1	GTP	1486	N	O6	37	5.86

Res	DONO	Res	ACC	Atom	D	A	OCCUR	%
12	CYS -	1	GTP	110	SG	O2PG	3	0.45
13	GLY -	1	GTP	114	N	O2PG	651	96.88
13	GLY -	1	GTP	114	N	O3PG	12	1.79
14	VAL -	1	GTP	119	N	O1PG	311	46.28
14	VAL -	1	GTP	119	N	O2PG	2	0.3
15	GLY -	1	GTP	127	N	O1PG	648	96.43
15	GLY -	1	GTP	127	N	O3PG	25	3.72
16	LYSH -	1	GTP	132	N	O1PB	127	18.9
16	LYSH -	1	GTP	132	N	O3PB	2	0.3
16	LYSH -	1	GTP	132	N	O1PG	529	78.72
16	LYSH -	1	GTP	139	NZ	O3PB	16	2.38
16	LYSH -	1	GTP	139	NZ	O1PG	55	8.18
16	LYSH -	1	GTP	139	NZ	O2PG	73	10.86
16	LYSH -	1	GTP	139	NZ	O3PB	19	2.83
16	LYSH -	1	GTP	139	NZ	O1PG	76	11.31
16	LYSH -	1	GTP	139	NZ	O2PG	74	11.01
16	LYSH -	1	GTP	139	NZ	O3PB	17	2.53
16	LYSH -	1	GTP	139	NZ	O1PG	74	11.01
16	LYSH -	1	GTP	139	NZ	O2PG	77	11.46
17	SER -	1	GTP	145	N	O1PB	666	99.11
17	SER -	1	GTP	145	N	O2PB	1	0.15
17	SER -	1	GTP	149	OG	O1PA	655	97.47
17	SER -	1	GTP	149	OG	O3PA	1	0.15
17	SER -	1	GTP	149	OG	O1PB	1	0.15
28	PHE -	1	GTP	266	CZ	N9	2	0.3
28	PHE -	1	GTP	266	CZ	N7	1	0.15
28	PHE -	1	GTP	266	CZ	O2*	20	2.98
32	TYR -	1	GTP	297	N	O2*	1	0.15
32	TYR -	1	GTP	297	N	O3*	2	0.3
32	TYR -	1	GTP	304	CD1	O1PA	13	1.93
32	TYR -	1	GTP	304	CD1	O2PA	50	7.44
32	TYR -	1	GTP	308	CE1	O1PA	11	1.64
32	TYR -	1	GTP	308	CE1	O2PA	7	1.04
32	TYR -	1	GTP	311	OH	O1PA	10	1.49
32	TYR -	1	GTP	311	OH	O2PA	4	0.6
58	THR -	1	GTP	560	OG	O2PB	5	0.74
60	GLY -	1	GTP	571	N	O3PA	3	0.45
60	GLY -	1	GTP	571	N	O3PB	8	1.19
116	ASN -	1	GTP	1172	ND2	O6	3	0.45
116	ASN -	1	GTP	1172	ND2	N7	597	88.84
117	LYSH	1	GTP	1177	N	O6	7	1.04
146	ALA -	1	GTP	1467	N	O6	471	70.09
147	LYSH	1	GTP	1473	N	O6	208	30.95
147	LYSH	1	GTP	1480	NZ	N3	3	0.45
147	LYSH	1	GTP	1480	NZ	N2	3	0.45
147	LYSH	1	GTP	1480	NZ	O2*	5	0.74
147	LYSH	1	GTP	1480	NZ	N3	4	0.6
147	LYSH	1	GTP	1480	NZ	N2	3	0.45
147	LYSH	1	GTP	1480	NZ	O2*	3	0.45
147	LYSH	1	GTP	1480	NZ	N3	2	0.3
147	LYSH	1	GTP	1480	NZ	N2	5	0.74
147	LYSH	1	GTP	1480	NZ	O2*	5	0.74

Figure 31: *Occurrence of h-bonds in G12C-GTP→WT-GTP perturbation. Colored in yellow is P-loop, in red Switch-I loop, in blue Switch-II loop, and in orange the h-bond between sulfur in cysteine and Pγ/Pβ oxygen. Three colours represent three different replicas, numerated from left to right.*

Res DONO	Res	ACC	Atom	D	A	OCCUR	%	Res DONO	Res	ACC	Atom	D	A	OCCUR	%	Res DONO	Res	ACC	Atom	D	A	OCCUR	%
12 CYSH -	1	GTP	110	SG	O1PG	72	13.46	12 CYSH -	1	GTP	110	SG	O1PG	52	8.51	12 CYSH -	1	GTP	110	SG	O1PB	32	5.32
12 CYSH -	1	GTP	110	SG	O3PG	6	1.12	12 CYSH -	1	GTP	110	SG	O2PG	39	6.38	12 CYSH -	1	GTP	110	SG	O3PB	1	0.17
13 GLY -	1	GTP	114	N	O3PA	2	0.37	13 GLY -	1	GTP	114	N	O3PA	15	2.45	12 CYSH -	1	GTP	110	SG	O1PG	15	2.5
13 GLY -	1	GTP	114	N	O1PB	29	5.42	13 GLY -	1	GTP	114	N	O1PB	3	0.49	13 GLY -	1	GTP	114	N	O3PA	20	3.33
13 GLY -	1	GTP	114	N	O3PB	279	52.15	13 GLY -	1	GTP	114	N	O3PB	396	64.81	13 GLY -	1	GTP	114	N	O1PB	456	75.87
13 GLY -	1	GTP	114	N	O1PG	41	7.66	13 GLY -	1	GTP	114	N	O1PG	36	5.89	13 GLY -	1	GTP	114	N	O3PB	69	11.48
13 GLY -	1	GTP	114	N	O2PG	5	0.93	13 GLY -	1	GTP	114	N	O2PG	46	7.53	13 GLY -	1	GTP	114	N	O1PG	6	1
13 GLY -	1	GTP	114	N	O3PG	25	4.67	13 GLY -	1	GTP	114	N	O3PG	34	5.56	13 GLY -	1	GTP	114	N	O2PG	3	0.5
14 VAL -	1	GTP	119	N	O3PA	1	0.19	14 VAL -	1	GTP	119	N	O1PB	107	17.51	14 VAL -	1	GTP	119	N	O1PB	44	7.32
14 VAL -	1	GTP	119	N	O1PB	231	43.18	14 VAL -	1	GTP	119	N	O1PG	8	1.31	15 GLY -	1	GTP	127	N	O2*	3	0.5
14 VAL -	1	GTP	119	N	O1PG	1	0.19	14 VAL -	1	GTP	119	N	O2PG	2	0.33	15 GLY -	1	GTP	127	N	O3*	57	9.48
15 GLY -	1	GTP	127	N	O4*	1	0.19	14 VAL -	1	GTP	119	N	O3PG	1	0.16	16 LYSH -	1	GTP	132	N	O1PB	1	0.17
15 GLY -	1	GTP	127	N	O5*	12	2.24	15 GLY -	1	GTP	127	N	O1PA	1	0.16	16 LYSH -	1	GTP	139	NZ	O1PB	77	12.81
15 GLY -	1	GTP	127	N	O1PA	8	1.5	15 GLY -	1	GTP	127	N	O3PA	30	4.91	16 LYSH -	1	GTP	139	NZ	O2PB	7	1.16
15 GLY -	1	GTP	127	N	O3PA	54	10.09	15 GLY -	1	GTP	127	N	O1PB	428	70.05	16 LYSH -	1	GTP	139	NZ	O2PG	1	0.17
15 GLY -	1	GTP	127	N	O1PB	187	34.95	16 LYSH -	1	GTP	132	N	O3PA	1	0.16	16 LYSH -	1	GTP	139	NZ	O1PB	88	14.64
16 LYSH -	1	GTP	132	N	O3PA	8	1.5	16 LYSH -	1	GTP	132	N	O1PB	610	99.84	16 LYSH -	1	GTP	139	NZ	O2PB	3	0.5
16 LYSH -	1	GTP	132	N	O1PB	487	91.03	16 LYSH -	1	GTP	139	NZ	O1PB	61	9.98	16 LYSH -	1	GTP	139	NZ	O1PB	93	15.47
16 LYSH -	1	GTP	132	N	O2PB	1	0.19	16 LYSH -	1	GTP	139	NZ	O3PB	49	8.02	16 LYSH -	1	GTP	139	NZ	O2PB	1	0.17
16 LYSH -	1	GTP	139	NZ	O1PB	12	2.24	16 LYSH -	1	GTP	139	NZ	O1PG	10	1.64	17 SER -	1	GTP	145	N	O5*	590	98.17
16 LYSH -	1	GTP	139	NZ	O3PB	15	2.8	16 LYSH -	1	GTP	139	NZ	O2PG	5	0.82	17 SER -	1	GTP	145	N	O1PA	93	15.47
16 LYSH -	1	GTP	139	NZ	O1PG	47	8.79	16 LYSH -	1	GTP	139	NZ	O3PG	9	1.47	17 SER -	1	GTP	149	OG	O5*	35	5.82
16 LYSH -	1	GTP	139	NZ	O2PG	4	0.75	16 LYSH -	1	GTP	139	NZ	O1PB	60	9.82	17 SER -	1	GTP	149	OG	O1PA	85	14.14
16 LYSH -	1	GTP	139	NZ	O3PG	1	0.19	16 LYSH -	1	GTP	139	NZ	O2PB	1	0.16	17 SER -	1	GTP	149	OG	O2PA	470	78.2
16 LYSH -	1	GTP	139	NZ	O1PB	14	2.62	16 LYSH -	1	GTP	139	NZ	O3PB	61	9.98	17 SER -	1	GTP	149	OG	O1PG	1	0.17
16 LYSH -	1	GTP	139	NZ	O2PB	1	0.19	16 LYSH -	1	GTP	139	NZ	O1PG	6	0.98	18 ALA -	1	GTP	153	N	O4*	4	0.67
16 LYSH -	1	GTP	139	NZ	O3PB	12	2.24	16 LYSH -	1	GTP	139	NZ	O2PG	11	1.8	28 PHE -	1	GTP	262	CE	O6	1	0.17
16 LYSH -	1	GTP	139	NZ	O1PG	59	11.03	16 LYSH -	1	GTP	139	NZ	O3PG	10	1.64	28 PHE -	1	GTP	262	CE	N7	1	0.17
16 LYSH -	1	GTP	139	NZ	O3PG	1	0.19	16 LYSH -	1	GTP	139	NZ	O1PB	50	8.18	28 PHE -	1	GTP	264	CE	O6	2	0.33
16 LYSH -	1	GTP	139	NZ	O1PB	32	5.98	16 LYSH -	1	GTP	139	NZ	O3PB	48	7.86	28 PHE -	1	GTP	264	CE	N7	5	0.83
16 LYSH -	1	GTP	139	NZ	O2PB	1	0.19	16 LYSH -	1	GTP	139	NZ	O1PG	10	1.64	28 PHE -	1	GTP	266	CZ	N7	12	2
16 LYSH -	1	GTP	139	NZ	O3PB	11	2.06	16 LYSH -	1	GTP	139	NZ	O2PG	5	0.82	58 THR -	1	GTP	560	OG	O1PB	38	6.32
16 LYSH -	1	GTP	139	NZ	O1PG	51	9.53	16 LYSH -	1	GTP	139	NZ	O3PG	12	1.96	58 THR -	1	GTP	560	OG	O2PB	395	65.72
16 LYSH -	1	GTP	139	NZ	O2PG	2	0.37	17 SER -	1	GTP	145	N	O1PA	543	88.87	58 THR -	1	GTP	560	OG	O1PG	13	2.16
17 SER -	1	GTP	145	N	O1PA	325	60.75	17 SER -	1	GTP	145	N	O2PB	10	1.64	58 THR -	1	GTP	560	OG	O2PG	35	5.82
17 SER -	1	GTP	145	N	O2PB	147	27.48	17 SER -	1	GTP	149	OG	O1PA	151	24.71	58 THR -	1	GTP	560	OG	O3PG	3	0.5
17 SER -	1	GTP	149	OG	O1PA	11	2.06	17 SER -	1	GTP	149	OG	O2PA	470	76.92	60 GLY -	1	GTP	571	N	O1PB	1	0.17
17 SER -	1	GTP	149	OG	O2PA	78	14.58	18 ALA -	1	GTP	153	N	O1PA	7	1.15	60 GLY -	1	GTP	571	N	O3PB	51	8.49
17 SER -	1	GTP	149	OG	O2PB	11	2.06	28 PHE -	1	GTP	266	CZ	O2*	13	2.13	60 GLY -	1	GTP	571	N	O1PG	20	3.33
18 ALA -	1	GTP	153	N	O1PA	525	98.13	28 PHE -	1	GTP	266	CZ	O1PA	9	1.47	60 GLY -	1	GTP	571	N	O2PG	77	12.81
28 PHE -	1	GTP	262	CE	O2*	1	0.19	32 TYR -	1	GTP	304	CD	O2*	1	0.16	60 GLY -	1	GTP	571	N	O3PG	12	2
28 PHE -	1	GTP	264	CE	O2*	1	0.19	60 GLY -	1	GTP	571	N	O1PG	3	0.49	61 GLN -	1	GTP	576	N	O1PG	5	0.83
28 PHE -	1	GTP	266	CZ	O2*	7	1.31	60 GLY -	1	GTP	571	N	O2PG	6	0.98	61 GLN -	1	GTP	576	N	O2PG	3	0.5
32 TYR -	1	GTP	304	CD	O3*	4	0.75	61 GLN -	1	GTP	576	N	O2PG	1	0.16	63 GLU -	1	GTP	598	N	O1PG	1	0.17
32 TYR -	1	GTP	308	CE	O5*	169	31.59	116 ASN -	1	GTP	1172	ND	N7	391	63.99	63 GLU -	1	GTP	598	N	O2PG	1	0.17
32 TYR -	1	GTP	308	CE	O1PA	6	1.12	117 LYSH -	1	GTP	1177	N	O6	3	0.49	116 ASN -	1	GTP	1172	ND	N3	504	83.86
32 TYR -	1	GTP	308	CE	O2PA	30	5.61	117 LYSH -	1	GTP	1184	NZ	O4*	4	0.65	116 ASN -	1	GTP	1172	ND	O2*	3	0.5
32 TYR -	1	GTP	308	CE	O3PG	1	0.19	117 LYSH -	1	GTP	1184	NZ	O4*	5	0.82	116 ASN -	1	GTP	1172	ND	O3*	2	0.33
32 TYR -	1	GTP	311	OH	O1PA	2	0.37	117 LYSH -	1	GTP	1184	NZ	O4*	2	0.33	117 LYSH	1	GTP	1184	NZ	O2*	18	3
32 TYR -	1	GTP	311	OH	O2PA	526	98.32	145 SER -	1	GTP	1463	OG	O6	1	0.16	117 LYSH	1	GTP	1184	NZ	O2*	13	2.16
60 GLY -	1	GTP	571	N	O1PG	15	2.8	146 ALA -	1	GTP	1467	N	O6	184	30.11	117 LYSH	1	GTP	1184	NZ	O2*	7	1.16
60 GLY -	1	GTP	571	N	O2PG	5	0.93	147 LYSH -	1	GTP	1473	N	O6	378	61.87	146 ALA -	1	GTP	1467	N	N2	48	7.99
60 GLY -	1	GTP	571	N	O3PG	28	5.23	147 LYSH -	1	GTP	1473	N	N7	6	0.98	146 ALA -	1	GTP	1467	N	N1	8	1.33
117 LYSH	1	GTP	1184	NZ	O4*	1	0.19	147 LYSH -	1	GTP	1480	NZ	N3	1	0.16	146 ALA -	1	GTP	1467	N	O6	1	0.17
145 SER -	1	GTP	1463	OG	O6	8	1.5	147 LYSH -	1	GTP	1480	NZ	O2*	7	1.15	147 LYSH	1	GTP	1473	N	O6	37	6.16
146 ALA -	1	GTP	1467	N	O6	5	0.93	147 LYSH -	1	GTP	1480	NZ	O2*	7	1.15	147 LYSH	1	GTP	1480	NZ	O6	37	6.16
147 LYSH -	1	GTP	1473	N	O6	476	88.97	147 LYSH -	1	GTP	1480	NZ	N3	2	0.33	147 LYSH	1	GTP	1480	NZ	O6	21	3.49
147 LYSH -	1	GTP	1473	N	N7	53	9.91	147 LYSH -	1	GTP	1480	NZ	O2*	8	1.31	147 LYSH	1	GTP	1480	NZ	O6	18	3
147 LYSH -	1	GTP	1480	NZ	N3	2	0.37																
147 LYSH -	1	GTP	1480	NZ	N2	1	0.19																
147 LYSH -	1	GTP	1480	NZ	O2*	3	0.56																
147 LYSH -	1	GTP	1480	NZ	N3	3	0.56																
147 LYSH -	1	GTP	1480	NZ	N2	1	0.19																
147 LYSH -	1	GTP	1480	NZ	O2*	3	0.56																
147 LYSH -	1	GTP	1480	NZ	N3	1	0.19																
147 LYSH -	1	GTP	1480	NZ	O2*	4	0.75																
148 THR -	1	GTP	1486	N	O6	23	4.3																

Figure 32: *Occurrence of h-bonds in G12C-GTP→G12C-GDP perturbation. Colored in yellow is P-loop, in red Switch-I loop, in blue Switch-II loop, and in orange the h-bond between sulfur in cysteine and Pγ/Pβ oxygen. Three colours represent three different replicas, numerated from left to right.*

Res	DONO	Res	ACC	Atom	D	A	OCCUR	%	Res	DONO	Res	ACC	Atom	D	A	OCCUR	%	Res	DONO	Res	ACC	Atom	D	A	OCCUR	%
12	CYSH	1	GTP	110	SG	O3PB	1	0.09	12	CYSH	1	GTP	110	SG	O1PB	36	6.81	12	CYSH	1	GTP	110	SG	O1PG	1	0.19
12	CYSH	1	GTP	110	SG	O1PG	220	20.39	12	CYSH	1	GTP	110	SG	O1PG	14	2.65	12	CYSH	1	GTP	110	SG	O2PG	6	1.13
12	CYSH	1	GTP	110	SG	O3PG	2	0.19	12	CYSH	1	GTP	110	SG	O2PG	3	0.57	12	CYSH	1	GTP	110	SG	O3PG	1	0.19
13	GLY	1	GTP	114	N	O3PA	10	0.93	12	CYSH	1	GTP	110	SG	O3PG	4	0.76	13	GLY	1	GTP	114	N	O3PB	41	7.72
13	GLY	1	GTP	114	N	O1PB	34	3.15	13	GLY	1	GTP	114	N	O1PA	3	0.57	13	GLY	1	GTP	114	N	O1PG	26	4.9
13	GLY	1	GTP	114	N	O3PB	459	42.54	13	GLY	1	GTP	114	N	O3PA	20	3.78	13	GLY	1	GTP	114	N	O2PG	152	28.63
13	GLY	1	GTP	114	N	O1PG	146	13.53	13	GLY	1	GTP	114	N	O1PB	179	33.84	13	GLY	1	GTP	114	N	O3PG	168	31.64
13	GLY	1	GTP	114	N	O2PG	74	6.86	13	GLY	1	GTP	114	N	O3PB	14	2.65	14	VAL	1	GTP	119	N	O1PB	12	2.26
13	GLY	1	GTP	114	N	O3PG	172	15.94	13	GLY	1	GTP	114	N	O1PG	23	4.35	14	VAL	1	GTP	119	N	O1PG	141	26.55
14	VAL	1	GTP	119	N	O1PB	112	10.38	13	GLY	1	GTP	114	N	O2PG	21	3.97	14	VAL	1	GTP	119	N	O2PG	6	1.13
14	VAL	1	GTP	119	N	O1PG	20	1.85	13	GLY	1	GTP	114	N	O3PG	11	2.08	14	VAL	1	GTP	119	N	O3PG	2	0.38
14	VAL	1	GTP	119	N	O2PG	9	0.83	14	VAL	1	GTP	119	N	O1PA	15	2.84	15	GLY	1	GTP	127	N	O3PA	15	2.82
14	VAL	1	GTP	119	N	O3PG	12	1.11	14	VAL	1	GTP	119	N	O2PA	1	0.19	15	GLY	1	GTP	127	N	O1PB	240	45.2
15	GLY	1	GTP	127	N	O1PA	3	0.28	14	VAL	1	GTP	119	N	O1PB	4	0.76	15	GLY	1	GTP	127	N	O1PG	136	25.61
15	GLY	1	GTP	127	N	O3PA	78	7.23	14	VAL	1	GTP	119	N	O3PG	2	0.38	15	GLY	1	GTP	127	N	O3PG	7	1.32
15	GLY	1	GTP	127	N	O1PB	810	75.07	15	GLY	1	GTP	127	N	O5*	29	5.48	16	LYSH	1	GTP	132	N	O3PA	4	0.75
16	LYSH	1	GTP	132	N	O1PA	2	0.19	15	GLY	1	GTP	127	N	O1PA	17	3.21	16	LYSH	1	GTP	132	N	O1PB	444	83.62
16	LYSH	1	GTP	132	N	O3PA	10	0.93	15	GLY	1	GTP	127	N	O2PA	17	3.21	16	LYSH	1	GTP	132	N	O3PB	2	0.38
16	LYSH	1	GTP	132	N	O1PB	1049	97.22	15	GLY	1	GTP	127	N	O3PA	4	0.76	16	LYSH	1	GTP	132	N	O1PG	76	14.31
16	LYSH	1	GTP	132	N	O2PB	23	2.13	15	GLY	1	GTP	127	N	O1PB	34	6.43	16	LYSH	1	GTP	139	NZ	O1PB	7	1.32
16	LYSH	1	GTP	139	NZ	O1PB	17	1.58	15	GLY	1	GTP	127	N	O1PG	1	0.19	16	LYSH	1	GTP	139	NZ	O3PB	3	0.56
16	LYSH	1	GTP	139	NZ	O3PB	1	0.09	16	LYSH	1	GTP	132	N	O5*	3	0.57	16	LYSH	1	GTP	139	NZ	O1PG	27	5.08
16	LYSH	1	GTP	139	NZ	O1PG	6	0.56	16	LYSH	1	GTP	132	N	O1PA	129	24.39	16	LYSH	1	GTP	139	NZ	O2PG	23	4.33
16	LYSH	1	GTP	139	NZ	O2PG	12	1.11	16	LYSH	1	GTP	132	N	O2PA	19	3.59	16	LYSH	1	GTP	139	NZ	O3PG	1	0.19
16	LYSH	1	GTP	139	NZ	O1PB	11	1.02	16	LYSH	1	GTP	132	N	O3PA	131	24.76	16	LYSH	1	GTP	139	NZ	O1PB	5	0.94
16	LYSH	1	GTP	139	NZ	O3PB	1	0.09	16	LYSH	1	GTP	132	N	O1PB	124	23.44	16	LYSH	1	GTP	139	NZ	O3PB	4	0.75
16	LYSH	1	GTP	139	NZ	O1PG	7	0.65	16	LYSH	1	GTP	132	N	O2PB	1	0.19	16	LYSH	1	GTP	139	NZ	O1PG	20	3.77
16	LYSH	1	GTP	139	NZ	O2PG	4	0.37	16	LYSH	1	GTP	139	NZ	O1PB	10	1.89	16	LYSH	1	GTP	139	NZ	O2PG	18	3.39
16	LYSH	1	GTP	139	NZ	O3PG	1	0.09	16	LYSH	1	GTP	139	NZ	O3PB	1	0.19	16	LYSH	1	GTP	139	NZ	O3PG	2	0.38
16	LYSH	1	GTP	139	NZ	O1PB	24	2.22	16	LYSH	1	GTP	139	NZ	O1PG	6	1.13	16	LYSH	1	GTP	139	NZ	O3PB	6	1.13
16	LYSH	1	GTP	139	NZ	O3PB	5	0.46	16	LYSH	1	GTP	139	NZ	O2PG	3	0.57	16	LYSH	1	GTP	139	NZ	O1PG	17	3.2
16	LYSH	1	GTP	139	NZ	O1PG	4	0.37	16	LYSH	1	GTP	139	NZ	O1PA	3	0.57	16	LYSH	1	GTP	139	NZ	O2PG	30	5.65
16	LYSH	1	GTP	139	NZ	O3PG	3	0.28	16	LYSH	1	GTP	139	NZ	O1PB	10	1.89	16	LYSH	1	GTP	139	NZ	O3PG	1	0.19
17	SER	1	GTP	145	N	O1PA	730	67.66	16	LYSH	1	GTP	139	NZ	O1PG	4	0.76	17	SER	1	GTP	145	N	O1PA	351	66.1
17	SER	1	GTP	145	N	O3PA	44	4.08	16	LYSH	1	GTP	139	NZ	O2PG	2	0.38	17	SER	1	GTP	145	N	O1PB	148	27.87
17	SER	1	GTP	145	N	O2PB	205	19	16	LYSH	1	GTP	139	NZ	O3PG	2	0.38	17	SER	1	GTP	145	N	O2PB	3	0.56
17	SER	1	GTP	149	OG	O1PA	158	14.64	16	LYSH	1	GTP	139	NZ	O1PB	4	0.76	17	SER	1	GTP	149	OG	O1PA	253	47.65
17	SER	1	GTP	149	OG	O2PA	870	80.63	16	LYSH	1	GTP	139	NZ	O1PG	3	0.57	17	SER	1	GTP	149	OG	O2PA	283	53.3
17	SER	1	GTP	149	OG	O3PA	1	0.09	16	LYSH	1	GTP	139	NZ	O2PG	1	0.19	17	SER	1	GTP	149	OG	O1PB	1	0.19
17	SER	1	GTP	149	OG	O2PB	61	5.65	16	LYSH	1	GTP	139	NZ	O3PG	2	0.38	18	ALA	1	GTP	153	N	O1PA	7	1.32
18	ALA	1	GTP	153	N	O1PA	451	41.8	17	SER	1	GTP	145	N	O1PA	294	55.58	28	PHE	1	GTP	262	CE	O6	1	0.19
28	PHE	1	GTP	262	CE	N7	3	0.28	17	SER	1	GTP	145	N	O2PA	70	13.23	28	PHE	1	GTP	262	CE	N7	2	0.38
28	PHE	1	GTP	264	CE	O2*	7	0.65	17	SER	1	GTP	145	N	O3PA	43	8.13	28	PHE	1	GTP	264	CE	O2*	1	0.19
28	PHE	1	GTP	266	CZ	N3	8	0.74	17	SER	1	GTP	145	N	O2PB	7	1.32	28	PHE	1	GTP	266	CZ	N9	1	0.19
28	PHE	1	GTP	266	CZ	N7	6	0.56	17	SER	1	GTP	149	OG	O1PA	176	33.27	28	PHE	1	GTP	266	CZ	O2*	18	3.39
28	PHE	1	GTP	266	CZ	O2*	49	4.54	17	SER	1	GTP	149	OG	O2PA	301	56.9	32	TYR	1	GTP	297	N	O2*	10	1.88
28	PHE	1	GTP	266	CZ	O3*	1	0.09	17	SER	1	GTP	149	OG	O1PG	2	0.38	32	TYR	1	GTP	297	N	O3*	4	0.75
32	TYR	1	GTP	297	N	O2*	5	0.46	17	SER	1	GTP	149	OG	O3PG	2	0.38	32	TYR	1	GTP	304	CD	O1PA	4	0.75
32	TYR	1	GTP	304	CD	O5*	3	0.28	18	ALA	1	GTP	153	N	O1PA	38	7.18	32	TYR	1	GTP	304	CD	O2PA	72	13.56
32	TYR	1	GTP	304	CD	O2PA	18	1.67	18	ALA	1	GTP	153	N	O2PA	1	0.19	58	THR	1	GTP	560	OG	O2PB	10	1.88
32	TYR	1	GTP	304	CD	O3PG	1	0.09	28	PHE	1	GTP	262	CE	O6	1	0.19	60	GLY	1	GTP	571	N	O2PA	5	0.94
32	TYR	1	GTP	308	CE	O2PA	4	0.37	28	PHE	1	GTP	262	CE	N7	5	0.95	60	GLY	1	GTP	571	N	O3PB	5	0.94
60	GLY	1	GTP	571	N	O1PG	167	15.48	28	PHE	1	GTP	264	CE	N7	1	0.19	60	GLY	1	GTP	571	N	O1PG	7	1.32
60	GLY	1	GTP	571	N	O2PG	22	2.04	28	PHE	1	GTP	266	CZ	O2*	6	1.13	60	GLY	1	GTP	571	N	O2PG	1	0.19
60	GLY	1	GTP	571	N	O3PG	11	1.02	32	TYR	1	GTP	297	N	O3*	1	0.19	60	GLY	1	GTP	571	N	O3PG	2	0.38
116	ASN	1	GTP	1172	ND	O6	29	2.69	32	TYR	1	GTP	304	CD	O1PA	5	0.95	116	ASN	1	GTP	1172	ND	O6	1	0.19
116	ASN	1	GTP	1172	ND	N7	280	25.95	32	TYR	1	GTP	304	CD	O2PA	1	0.19	116	ASN	1	GTP	1172	ND	N7	333	62.71
117	LYSH	1	GTP	1177	N	O6	12	1.11	32	TYR	1	GTP	304	CD	O3PG	1	0.19	116	ASN	1	GTP	1172	ND	O4*	10	1.88
117	LYSH	1	GTP	1184	NZ	O4*	8	0.74	58	THR	1	GTP	560	OG	O1PB	15	2.84	117	LYSH	1	GTP	1177	N	O6	4	0.75
117	LYSH	1	GTP	1184	NZ	N3	1	0.09	60	GLY	1	GTP	571	N	O3PB	3	0.57	117	LYSH	1	GTP	1184	NZ	O4*	1	0.19
117	LYSH	1	GTP	1184	NZ	O4*	5	0.46	60	GLY	1	GTP	571	N	O1PG	19	3.59	117	LYSH	1	GTP	1184	NZ	O4*	2	0.38
117	LYSH	1	GTP	1184	NZ	O4*	9	0.83	60	GLY	1	GTP	571	N	O2PG	6	1.13	117	LYSH	1	GTP	1184	NZ	O4*	2	0.38
146	ALA	1	GTP	1467	N	O6	263	24.37	60	GLY	1	GTP	571	N	O3PG	4	0.76	145	SER	1	GTP	1463	OG	O6	1	0.19
147	LYSH	1	GTP	1473	N	O6	678	62.84	116	ASN	1	GTP	1172	ND	N7	87	16.45	146	ALA	1	GTP	1467	N	O6	368	69.3
147	LYSH	1	GTP	1473	N	N7	7	0.65	116	ASN	1	GTP	1172	ND	O4*	1	0.19	146	ALA	1	GTP	1467	N	N7	3	0.56
147	LYSH	1	GTP	1480	NZ	N3	4	0.37	117	LYSH	1	GTP	1177	N	O6	14	2.65	147	LYSH	1	GTP	1473	N	O6	196	36.91
147	LYSH	1	GTP	1480	NZ	N2	1	0.09	146	ALA	1	GTP	1467	N	O6	61	11.53	147	LYSH	1	GTP	1480	NZ	N2	1	0.19
147	LYSH	1	GTP	1480	NZ	O2*	1	0.09	147	LYSH	1	GTP	1473	N	O6	353	66.73	147	LYSH	1	GTP	1480	NZ	O2*	5	0.94
147	LYSH	1	GTP	1480	NZ	N3	1	0.09	147	LYSH	1	GTP	1480	NZ	N2	2	0.38	147	LYSH	1	GTP	1480	NZ	O2*	1	0.19
147	LYSH	1	GTP	1480	NZ	N2	1	0.09	147	LYSH	1	GTP	1480	NZ	N7	1	0.19	147	LYSH	1	GTP	1480	NZ	N3	1	0.19
147	LYSH	1	GTP	1480	NZ	N3	2	0.19	147	LYSH	1	GTP	1480	NZ	O2*	3	0.57	148	THR	1	GTP	1486	N	O6	1	0.19
147	LYSH	1	GTP	1480	NZ	N2	2	0.19	147	LYSH	1	GTP	1480	NZ	O2*	1	0.19									
147	LYSH	1	GTP	1480	NZ	O2*	5	0.46	147	LYSH	1	GTP	1480	NZ	N3	1	0.19									
									147	LYSH	1	GTP	1480	NZ	O2*	2	0.38									

Figure 33: *Occurrence of h-bonds in G12C-GDP→G12C-GTP perturbation. Colored in yellow is P-loop, in red Switch-I loop, in blue Switch-II loop, and in orange the h-bond between sulfur in cysteine and Pγ/Pβ oxygen. Three colours represent three different replicas, numerated from left to right.*